




University of  
Stavanger

**Faculty of Science and Technology**

## MASTER'S THESIS

Study program/Specialization: Petroleum Geosciences Engineering	Spring, 2019 Open
Writer: Cicilie Trede	 _____ (Writer's signature)
Faculty supervisor: Dora Luz Marin Restrepo	
Title of thesis: 3D seismic analysis of the Basement to Early Cretaceous in the Selje High, Slørebotn Sub-basin and Måløy Slope, southern Norwegian Sea.	
Credits (ECTS): 30	
Keywords: <i>Agat Formation</i> <i>Selje High</i> <i>Slørebotn Sub-basin</i> <i>Måløy Slope</i> <i>Jurassic – Cretaceous rifting</i> <i>Source area</i> <i>Spectral decomposition</i>	Pages: 126  Stavanger, 15 <sup>th</sup> June, 2019

Copyright

by

Cicilie Trede

2019

**3D seismic analysis of the Basement to Early Cretaceous in the Selje High, Slørebotn  
Sub-basin and Måløy Slope, southern Norwegian Sea.**

**by**

**Cicilie Trede**

**Msc Thesis**

Presented to the Faculty of Science and Technology

The University of Stavanger

Norway

**The University of Stavanger**

**2019**

## **Acknowledgements**

Firstly, I would like to thank my supervisor Dora Marin for her continuous support and motivation throughout this project.

I would also like to thank Wiktor Weibull and Alejandro Escalona for valuable feedback on this thesis. Additionally, I am grateful to Jennifer Cunningham for the technical support with the GeoTeric software.

Thanks to my family and friends for the continued encouragement and support throughout my Master's degree.

Finally, I would like to thank my helpful classmates.

## **Abstract**

### **3D seismic analysis of the Basement to Early Cretaceous in the Selje High, Slørebotn Sub-basin and Måløy Slope, southern Norwegian Sea.**

Cicilie Trede

The University of Stavanger, 2019

Supervisors: Dora Luz Marin Restrepo

Several coarse-grained sedimentary rocks have been reported in the Upper Jurassic and the Cretaceous succession in the southern Norwegian Sea and the northern North Sea. The Jurassic interval has been interpreted as syn-rift deposits while the Cretaceous succession is considered post-rift strata. However, the timing of the fault activity in the Early Cretaceous has been debated. In addition, the coarse-grained sandstones of the Early Cretaceous Agat Formation are still poorly understood, and few studies are related to this interval in the Selje High area. Furthermore, the basement in the northern North Sea in the Utsira High has proven to bear potential as a reservoir in fractured basement rocks, nevertheless, further studies are needed on this in the northern North Sea. This study aims to improve the understanding of the fault activity in the Late Jurassic to Early Cretaceous and the lateral distribution of the coarse-grained formations of Early Cretaceous, thus improve the paleogeographic understanding in the area surrounding Selje High. A further purpose is to improve the understanding of the Pre-Devonian basement.

This is accomplished by using a dataset containing 3D and 2D reflection seismic and six wells. In addition to traditional seismic interpretation, spectral decomposition was used to highlight the Basement and the Agat Formation.

Main findings comprise of three fault families of Late Jurassic age exposed to rotation which uplifted basement highs. These were later reactivated during the late Early Cretaceous.

However, a second theory is suggested favoring thermal subsidence in the Early Cretaceous. The main controlling factor on the lateral extent of the coarse-grained Agat Formation is the rifting bathymetry from the Late Jurassic and eustatic sea level changes. The Agat Formation

is sourced as slumps from the Selje High and submarine fans from the eastern platform area through submarine canyons of Late Jurassic age. These submarine canyons are found in the basement of structural highs and are present up until the Base Cretaceous Unconformity. Lastly, the basement proved to have minor faulting or fractures in the Selje High, thus possibly bearing the potential as a reservoir.

# TABLE OF CONTENT

1. INTRODUCTION .....	1
1.1 Objectives .....	2
1.2 Previous work .....	4
1.2.1 Seismic expression of active rift basins .....	4
1.2.2 Rifting events in the Late Jurassic and Early Cretaceous and its influence on sedimentation .....	5
1.2.3 Depositional model of the Agat Formation .....	6
2. GEOLOGICAL SETTING .....	8
2.1 Tectonic setting .....	10
2.1.1 Jurassic .....	10
2.1.2 Cretaceous .....	11
2.2 Stratigraphy .....	13
2.2.1 Pre-Devonian .....	15
2.2.2 Pre-Jurassic .....	16
2.2.3 Jurassic .....	16
2.2.4 Cretaceous .....	16
2.2.5 Post-Cretaceous .....	19
3. DATA AND METHODOLOGY .....	20
3.1 Data .....	20
3.2 Methodology .....	22
3.2.1 Well correlation .....	22
3.2.2 Seismic interpretation .....	22
3.2.3 Spectral decomposition .....	25
4. OBSERVATIONS AND RESULTS .....	27
4.1 Structural well correlation .....	27
4.2 Seismic interpretation of the main intervals .....	31
4.2.1 Basement .....	31
4.2.2 Pre-BCU .....	56
4.2.3 Agat Formation .....	70
5. DISCUSSION .....	88
5.1 Tectonic evolution .....	88
5.1.1 Late Jurassic .....	88
5.1.2 Early Cretaceous .....	91
5.2 Basement structure and implications for exploration .....	97

5.3	Paleogeography .....	99
5.3.1	Late Jurassic .....	99
5.3.2	Early Cretaceous Agat Formation .....	101
6.	CONCLUSIONS.....	105
6.1	Future work.....	106



## TABLE OF FIGURES

<b>Figure 1:</b> Study area (red square) and the structural elements of the northern North Sea and the southern Norwegian Sea. Gn H = Gnausen High, Go H = Gossa High, Gi H = Giske High, M H = Makrell Horst, and S H = Selje High. Modified from (Blystad et al., 1995). .....	3
<b>Figure 2:</b> An idealized section of an active rift basin with a description of seismic characteristics for the four tectonic systems tracts. 1) Rift initiation, 2) Rift climax, 3) Immediate post-rift, and 4) Late post-rift. (Prosser, 1993) .....	4
<b>Figure 3:</b> Idealized section to illustrate Cretaceous infilling of half-grabens typical for the Cretaceous sedimentary succession in the Norwegian Sea. The Cretaceous infill has been interpreted as the post-rift infilling of hanging wall sub-basins following Jurassic faulting and extensions (Færseth & Lien, 2002). .....	5
<b>Figure 4:</b> Regional seismic line crossing from West to East, from the Slørebotn Sub-basin through the Selje High to the Måløy Slope and the platform area. A) Uninterpreted seismic line. B) Interpreted seismic line. The interpretation in the west close to the platform area is uncertain. ....	9
<b>Figure 5:</b> Regional line showing from the NW to the SSE from the Slørebotn sub-basin, Måløy Terrace and Selje High. This regional line is along the same line as interpreted in Figure 4. Modified by (Brekke, 2000). .....	12
<b>Figure 6:</b> Lithostratigraphic chart of the Northern North Sea from the Tampen Spur and Horda Platform. The lithostratigraphy in the study area is believed to be similar. Modified from (NPD, 2014). .....	14
<b>Figure 7:</b> Cores from well 6204/10-2R showing the Åsgard Formation from 1951m to 1961m. The cores show dark fine-grained sediments. Collected from NPD fact pages (NPD, 2019).....	18
<b>Figure 8:</b> Chronostratigraphic chart for the Cretaceous from the Sogn Graben, Måløy Terrace, and Selje High. (Modified from (Vergara, Brunstad, Nordlie, Chranock, & Gradstein, 2006).....	19
<b>Figure 9:</b> An overview of the dataset from the study area. Blue lines are 2D seismic lines, while the black box show the seismic 3D cube. Black circles are the wells. The Norwegian mainland are located to the east. ....	21

<b>Figure 10:</b> A close-up of the seabed highlighting the polarity of the seismic cube. ....	22
<b>Figure 11:</b> Seismic displayed with the synthetic seismogram to highlight the good correlation between the synthetic and the seismic. ....	22
<b>Figure 12:</b> Seismic well-tie for well 6204/10-1. The following well logs displayed are: GR, sonic, density, acoustic impedance, and reflection coefficient. The top of present formations are marked. ....	23
<b>Figure 13:</b> Seismic well-tie for well 6204/11-2. The following well logs displayed are: GR, sonic, density, acoustic impedance, and reflection coefficient. The top of present formations are marked. ....	23
<b>Figure 14:</b> Structural well correlation between all wells in the study area going from southwest to northeast (yellow line in map), through the Selje High, Måløy Slope, and Slørebotn Sub-basin. The correlation is from Basement until the top of Upper Cretaceous. ...	30
<b>Figure 15:</b> Structural map of the basement with all the faults divided into three fault families. Fault family 1 (FF1) in yellow, Fault family 2 (FF2) in green and Fault family 3 (FF3) in blue. ....	32
<b>Figure 16:</b> Seismic line displaying faults from fault family 1. Uninterpreted seismic line. ...	34
<b>Figure 17:</b> Seismic line displaying faults from fault family 1. Interpreted seismic line showing the Selje High and the main characteristics of fault family 1. Red arrows indicates lap relationships. Two major faults bounding the .....	35
<b>Figure 18:</b> Seismic line displaying faults from fault family 2. Uninterpreted seismic line. ...	37
<b>Figure 19:</b> Seismic line displaying faults from fault family 2. Interpreted seismic line showing the Selje High and the main characteristics of fault family 2. ....	38
<b>Figure 20:</b> Seismic line displaying faults from fault family 3. Uninterpreted seismic line. ...	40
<b>Figure 21:</b> Seismic line displaying faults from fault family 3. Interpreted seismic line showing the faults in the north and the main characteristics of fault family 3. ....	41
<b>Figure 22:</b> Basement map. a) Surface map of the basement in time (ms). b) Structural map of the basement in time (ms) with faults active during the period. Contour interval: 300ms. Elevated basement areas are marked as the Selje High and the Platform area. ....	43

**Figure 23:** Seismic inline crossing along the platform area to highlight the basement incisions observed in the structural map. The seismic line is along the yellow line in the structural basement map. Uninterpreted section. .... 45

**Figure 24:** Seismic inline crossing along the platform area to highlight the basement incisions observed in the structural map. The seismic line is along the yellow line in the structural basement map. The top basement (blue) and BCU (red) are marked in the seismic line, along with onlap within the submarine canyons. Folding is also observed. .... 46

**Figure 25:** Basement horizon seen from above with constant bandwidth frequency decomposition in GeoTeric. The result of a frequency decomposition with an RGB color blend (17Hz - 24Hz - 31Hz) displayed on the basement surface. Submarine canyons/gullies, incisions and the elevated basement areas are marked. .... 50

**Figure 26:** Basement horizon seen from above with constant high definition frequency decomposition in GeoTeric. The result of a frequency decomposition using with an RGB color blend (15Hz - 30Hz - 45Hz) displayed on the basement surface. Submarine canyons/gullies, incisions and the elevated basement areas are marked..... 51

**Figure 27:** Basement horizon with constant bandwidth frequency decomposition in GeoTeric. The result of a frequency decomposition with an RGB color blend (17Hz - 24Hz - 31Hz) displayed on the basement surface and seen from the NW to highlight the submarine canyons along the fault plane of the platform area. .... 52

**Figure 28:** Basement horizon with HD frequency decomposition in GeoTeric. The result of a frequency decomposition with an RGB color blend (15Hz - 30Hz - 45Hz) displayed on the basement surface and seen from the NW to highlight the submarine canyons along the fault plane of the platform area..... 53

**Figure 29:** Close-up of the highest part of the Selje High, marking the possible slump scarps in the basement with a stippled red line. .... 54

**Figure 30:** Close-up of the top of Selje High seen from above, highlighting the possible faults or fractures oriented N-S. .... 55

**Figure 31:** Maps of the Base Cretaceous Unconformity (BCU). A) Surface map of the BCU in time (ms) B) Structural map of the BCU in time (ms) with faults active during the period. Contour interval: 200ms. Elevated basement areas are marked as the Selje High and the Platform area. .... 59

<b>Figure 32:</b> Time thickness map between the BCU and the Basement with thickness in time (ms). The elevated basement areas have lowest thickness (red) and the structural lows have varying thickness of 100-400 ms. ....	60
<b>Figure 33:</b> Seismic XL 300 highlighting the Pre-BCU wedges and the Agat Formation. Onlaps are marked for the Agat Formation. Seismic line going from A to A' as marked in the structural map. ....	63
<b>Figure 34:</b> Seismic XL 404 highlighting the Pre-BCU wedges and the Agat Formation. Downlap is observed of the Agat Formation on the BCU. Seismic line going from B to B' as marked in the structural map. ....	64
<b>Figure 35:</b> Seismic XL 1073 highlighting the Pre-BCU wedges and the Agat Formation. Two wedges are defined in this seismic line. Onlap in the hanging wall is observed for the Agat Formation in both wedges. Seismic line going from C to C' as marked in the structural map. ....	65
<b>Figure 36:</b> Seismic XL 1125 highlighting the Pre-BCU wedges and the Agat Formation. The same two wedges as observed in Figure 36 have now merged to one large wedge with a minor fault in between. Onlap in the hanging wall is observed for the Agat Formation on both sides of the minor fault. Seismic line going from D to D' as marked in the structural map.....	66
<b>Figure 37:</b> Seismic XL 1550 highlighting the Pre-BCU wedges and the Agat Formation. The entire wedge is not observed in seismic, however, the Pre-BCU succession is likely pinching out in the east. A Pre-BCU wedge is also observed on the west of Selje High thickening towards the Sogn-Graben. Seismic line going from E to E' as marked in the structural map. 67	67
<b>Figure 38:</b> A map with the structural elements highlighting the location of the Pre-Cretaceous wedges in the area. As explained above. These are located in relation to the faults.....	68
<b>Figure 39:</b> Structural maps of the Agat Formation. a) Top Agat b) Base Agat Maps of the Base Cretaceous Unconformity (BCU). a) Surface map of the BCU in time (ms) b) Structural map of the BCU in time (ms) with faults active during the period. Contour interval: 200ms. Elevated basement areas are marked as the Selje High and the Platform area. ....	73
<b>Figure 40:</b> Time thickness map for the Agat Formation A) Time thickness map between the BCU and Top Agat Formation and B) Time thickness map between the Base Agat Formation and the Top Agat Formation. The faults are displayed in the figure to highlight that these are marking the lateral extent of the Agat Formation. ....	74

**Figure 41:** Seismic X-line 404 highlighting the Agat Formation with a yellow stippled line. The Agat Formation is downlapping the BCU in the west marked with red arrows. .... 77

**Figure 42:** Seismic X-line 1125 highlighting the Agat Formation with a yellow stippled line. The Agat Formation is onlapping the BCU in the west marked with red arrows. A mound or a fold is observed in the hanging wall of Selje High. .... 78

**Figure 43:** Uninterpreted random seismic line between well 6204/11-1 and 6204/11-2. .... 81

**Figure 44:** Interpreted random seismic line between well 6204/11-1 and 6204/11-2. Agat Formation is onlapping the BCU and a GWC are defined in the anticlinal shape of well 6204/11-1. .... 82

**Figure 45:** Top Agat Formation with a constant bandwidth spectral decomposition with an RGB color blend (17Hz – 30Hz – 42Hz). Circular and linear geometries are observed in the south and in the north, respectively. .... 84

**Figure 46:** Iso-proportional slicing between top and base of Agat Formation. Constant Bandwidth Spectral decomposition with a RGB color blend (17Hz – 30Hz – 42Hz). a) Top Agat b) Upper Bound c) Bound 1. The same geometries as observed in Figure 46 are observed here. Marked in a). .... 85

**Figure 47:** Iso-proportional slicing between Top and Base of Agat Formation. Constant Bandwidth Spectral decomposition with a RGB color blend (17Hz – 30Hz – 42Hz). d) Bound 2, e) Lower Bound, f) Base Agat. The same geometries as observed in Figure 46 are less evident in these three slices, where the color has dimmed significantly. .... 86

**Figure 48:** Structural model of the Late Jurassic highlighting the fault activity and rotation of the Selje High. The Jurassic or older interval are dominated by deep marine shales. Erosion in the foot wall is marked along with possible gravity flows in the hanging wall. The Jurassic or older onlaps the Basement in the hanging wall. .... 90

**Figure 49:** Structural model of the Early Cretaceous theory 1 highlighting the tectonic quiescence period around Selje High. Erosion in the foot wall is marked along with possible gravity flows in the hanging wall. The Agat Formation onlaps the Basement, while the Åsgard Formation is truncated. Åsgard Formation partially deposited on the Selje High. .... 93

**Figure 50:** Structural model of the Early Cretaceous alternative theory highlighting the reactivation of the fault activity around Selje High. Erosion in the foot wall is marked along with possible gravity flows in the hanging wall. The Agat Formation onlaps the Basement,

while the Åsgard Formation is truncated. Åsgard Formation partially deposited on the Selje High. Wedge geometries in the Åsgard and Agat Formation are observed. .... 96

**Figure 51:** Submarine canyons observed downslope of the Equatorial Guinean seafloor. The figure displays to different canyons types. Type 1 favors submarine fans, while type 2 are more mud-rich and less carved into the slope (Jobe, Lowe, & Uchytíl, 2011). .... 98

**Figure 52:** Conceptual sketch of the Late Jurassic. The Selje High is present during this period, and all the major faults in the study area are present in the Late Jurassic. Some sandy gravity flows are drawn in the northern area to imply that Sognefjord and Heather Sandstone Formation were also deposited during this period. .... 100

**Figure 53:** Drainage systems and source areas in a rotated fault block. A general illustration suggested by Faleide, Bjørlykke, and Gabrielsen (2010), which suits the deposition of the Agat Formation well. .... 102

**Figure 54:** Conceptual sketch of the Early Cretaceous Theory 1. The Selje High is still a prominent structural high during this period, and for this theory none of the faults interpreted in the study area is present. Submarine fans are deposited in the northern area and possibly at the western flank of Selje High. Slump deposits are deposited on the eastern flank of the Selje High. .... 103

**Figure 55:** Conceptual sketch of the Early Cretaceous alternative theory. The Selje High is still a prominent structural high during this period, and for this theory the faults have been reactivated. Submarine fans are deposited in the northern area and possibly at the western flank of Selje High. Slump deposits are deposited on the eastern flank of the Selje High. .. 104

## LIST OF TABLES

<b>Table 1:</b> Information about target, results, and lithology for the two wells 6204/10-1 and 6204/10-2R, which have drilled the basement. All information in the table is extracted from well reports for the two wells from NPD fact pages (NPD, 2019). .....	15
<b>Table 2:</b> List of wells in the seismic cube with additional information regarding check shots, side-tracks, target, and discoveries. Information is collected from the completion reports found on NPD fact pages (NPD, 2019).....	20
<b>Table 3:</b> List of the seismic horizons interpreted in the study area and which wells have the well picks for the given horizons. ....	24
<b>Table 4:</b> Information about the three different spectral decomposition methods that are available and are used in this thesis. Information extracted and modified from a GeoTeric video tutorial online (GeoTeric, 2017b, 2017a).....	26

# 1. INTRODUCTION

The first acquired exploration seismic on the Norwegian Continental shelf was in 1969, and the first license awarded in the Norwegian Sea in 1980 (Brekke, 2000). Since then, the understanding of the Norwegian margin has continuously improved; however, there are still some time periods and areas that need further investigation. For the Norwegian Sea margin, the initial focus was the late Palaeozoic and Mesozoic on the shallow shelf areas (Brekke & Riis, 1987; Brekke, 2000). In later years, the deep-water sandstone deposits of Cretaceous and Palaeogene age in outer areas of the continental margin became of more interest (Brekke, 2000). These sandstone intervals are commonly interpreted as formed due to turbidite currents, and some as debris flows and seafloor currents transported from the mainland or from local structural highs (Brekke, 2000; Martinsen, Lien, & Jackson, 2005). Thus, the lateral extent of these reservoir rocks can be difficult to predict, and may show variation in reservoir quality (Martinsen et al., 2005).

The study area (Figure 1) is situated on the border between the northern North Sea and the southern Norwegian Sea at approximately 62°N. The main structural feature in the area is the basement high called the Selje Horst or Selje High. The study area is bounded by the Sogn Graben in the southwest, the Måløy Terrace in the south, the shallow platform area to the east and the Slørebotn Sub-basin to the northwest. All these structures are important in understanding the distribution of the sandstones in the area.

There are few studies related to the Lower Cretaceous and the Upper Jurassic intervals in the study area. The Lower Cretaceous Agat Formation has proven to be a potential hydrocarbon bearing sandstone reservoir (Gulbrandsen & Nyborkken, 1991). The Agat Formation was first defined after the discovery of the Agat field in the northern North Sea and has later been identified in two wells in the study area in the southern Norwegian Sea (wells 6204/10-1 and 6204/11-2) (NPD, 2019). The distribution of this important sandstone formation in the Norwegian Sea is still poorly understood and the formation needs further investigation to better understand the thickness, depositional model and the lateral extent of which this formation is distributed. In addition to the finding of the Agat formation in well 6204/10-1, an interval of unexpected conglomerates was discovered within the same group, the Cromer Knoll Group (NPD, 2019). The origin of these conglomerates is poorly understood but is initially thought to be eroded basement highs which are in close proximity to the area of deposition (NPD, 2019).



Only a few of the many wells at the Norwegian continental shelf have drilled pre-Devonian age, which has been defined as basement (Basset, 2003). Most of them are drilled on structural highs where depth to the basement is noticeably less than in the basinal areas. The basement contains various rock types and has been exposed to different degrees of metamorphose, fracturing and deformation (NPD, 2019). Furthermore, some of the wells show evidence of weathered rock materials, often conglomerates, creating a zone between the basement and the overlying sediments (NPD, 2019). A study on the basement can reveal if the basement is suitable as a reservoir, and how it influences the sedimentation of younger strata.

## **1.1 Objectives**

The main purpose of this paper is to improve the understanding of the tectonostratigraphic evolution from Pre-Devonian Basement to Early Cretaceous in the area surrounding the Selje High. Special attention has been given to the Lower Cretaceous Agat sandstone Formation and its distribution and source area.

The following objectives are defined for the purpose of fulfilling the aim of this study:

- To establish the timing of major faults in the area and to define the syn-rift and post-rift stages to further understand the lateral distribution and origin of the sandstone formations in the area;
- To study the lateral distribution and origin of the coarse-grained sandstone intervals of the Agat Formation;
- To study the origin of unexpected conglomerates discovered in the Cretaceous Cromer Knoll Group in well 6204/10-1;
- To improve the paleogeographic understanding of the area; and
- To improve the understanding of the basement and its implications for exploration.

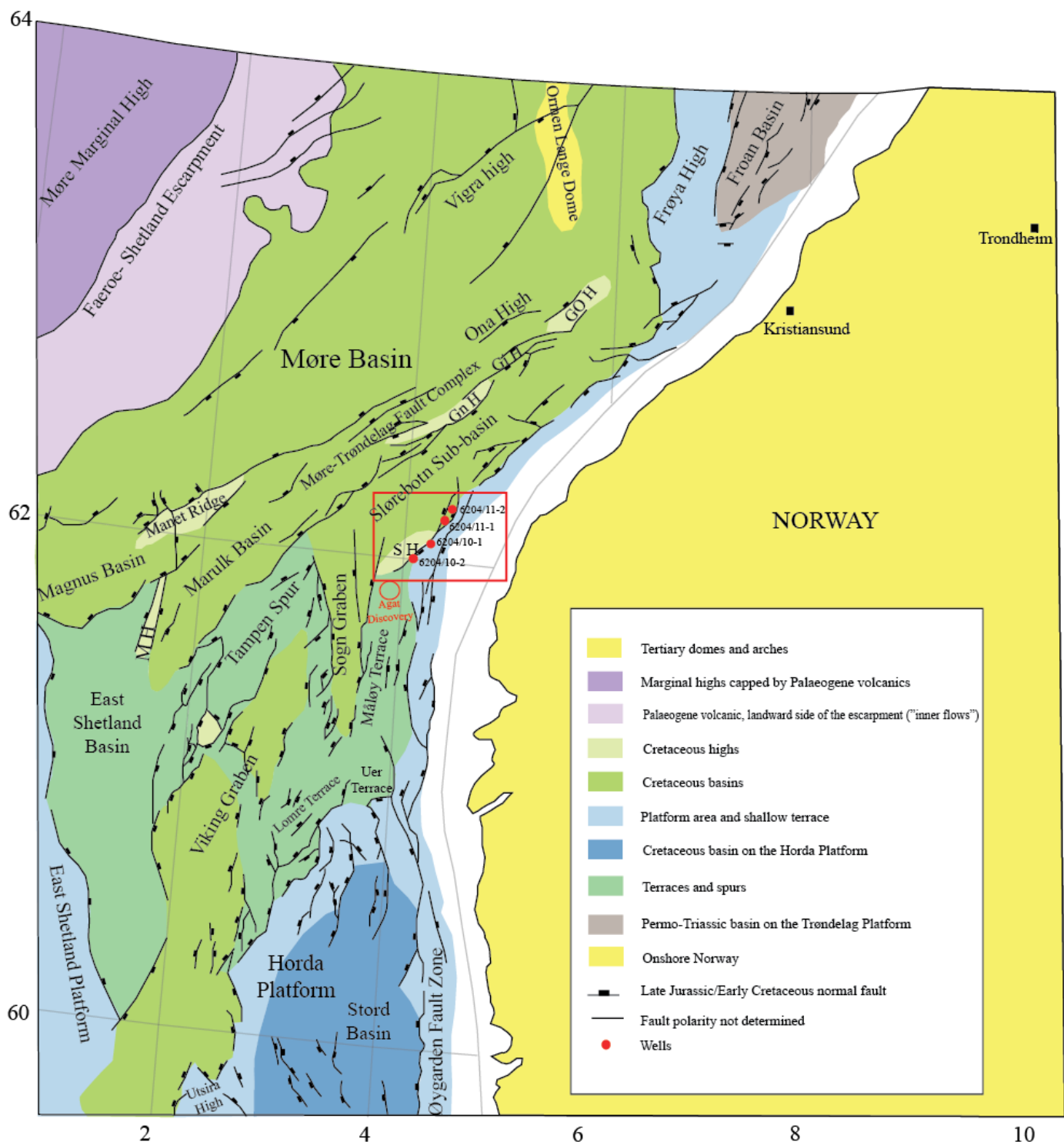


**Figure 1:** Study area (red square) and the structural elements of the northern North Sea and the southern Norwegian Sea. Gn H = Gnausen High, Go H = Gosså High, Gi H = Giske High, M H = Makrell Horst, and S H = Selje High. Modified from (Blystad et al., 1995).

## 1.2 Previous work

### 1.2.1 Seismic expression of active rift basins

Prosser (1993) did a detailed study on depositional systems and their seismic expressions in active rift basins where four tectonic system tracts were defined; 1) rift initiation, 2) rift climax, 3) immediate post-rift, and 4) late post-rift. Figure 2 displays an idealized example of a basin with descriptions of the seismic characteristics one can possibly find in the given tectonic system tract.

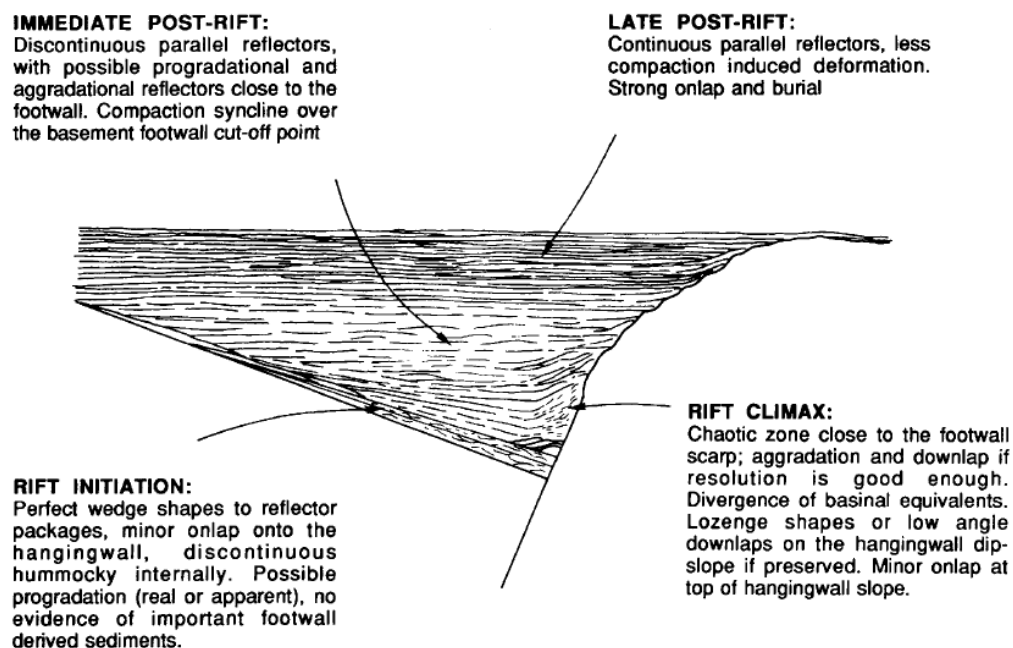


**Figure 2:** An idealized section of an active rift basin with a description of seismic characteristics for the four tectonic systems tracts. 1) Rift initiation, 2) Rift climax, 3) Immediate post-rift, and 4) Late post-rift. (Prosser, 1993)

Færseth and Lien (2002) highlighted five elements that are commonly used to identify tectonic activity:

- 1) Onlap surfaces
- 2) Thickness variations across faults
- 3) Wedge-shaped sedimentary bodies
- 4) Variations in sedimentation rate
- 5) Influx of coarse clastics

### 1.2.2 Rifting events in the Late Jurassic and Early Cretaceous and its influence on sedimentation

The tectonic evolution during Mesozoic times have been debated, and especially if the Jurassic rifting continued into the Cretaceous or not. The understanding of the tectonic activity during Jurassic is highly relevant for the further understanding of the deposition of the Cretaceous interval.

Lundin and Dore (1997) suggested that the Early Cretaceous was tectonically active based on a series of observations. 1) Variation in thickness of the Lower Cretaceous succession, 2) wedge-shapes, and 3) offset of the base Cretaceous unconformity because of major faults. These observations have also been made in the northern North Sea, which is better known than the Norwegian Sea, however, these have by other authors been considered as thermal subsidence and infilling of the topography caused by the Jurassic rifting event (Figure 3) (Bertram & Milton, 1988; Gabrielsen, Kyrkjæbo, Faleide, Fjeldskaar, & Kjennerud, 2001; Færseth & Lien, 2002).

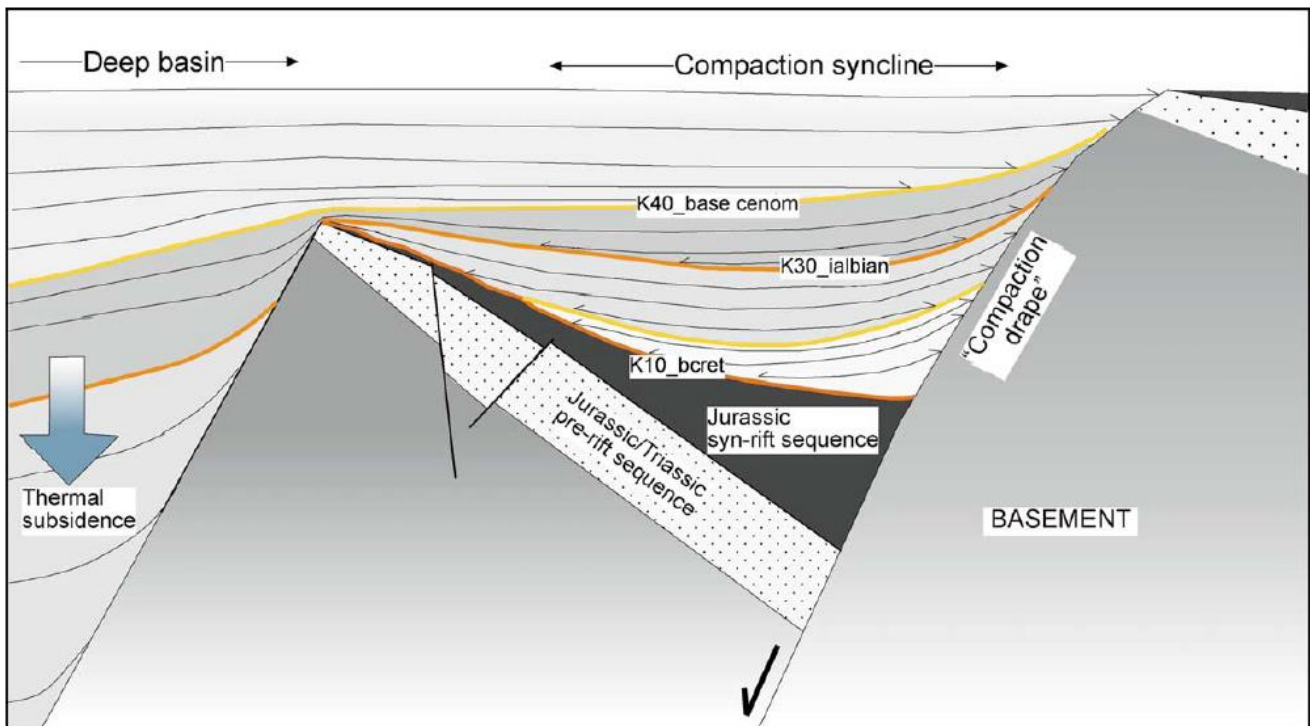


**Figure 3:** Idealized section to illustrate Cretaceous infilling of half-grabens typical for the Cretaceous sedimentary succession in the Norwegian Sea. The Cretaceous infill has been interpreted as the post-rift infilling of hanging wall sub-basins following Jurassic faulting and extensions (Færseth & Lien, 2002).

Extensions in the Early Cretaceous have been considered part of the Jurassic rifting event in several papers (Blystad et al., 1995; McCann, Shannon, & Moore, 1995). However, Doré et al. (1999), proposed the rifting of Early Cretaceous to be a separate extensional event from the Jurassic, as the transition between the two events highlights the change of stress direction from E-W to NW-SE.

Færseth and Lien (2002) did a detailed interpretation of Cretaceous sedimentation in the Norwegian Sea with respect to the Jurassic rifting event until the Campanian rifting. The conclusion was that the deposition of the Cretaceous sediments was highly dependent on the tectonic configuration from the Jurassic rifting, but that the Early Cretaceous was a period of tectonic quiescence.

Figure 3 illustrates an idealized section of the Cretaceous infilling of the Jurassic rifts, where the Jurassic succession marks the syn-rift event and the Cretaceous succession is the post-rift event. This illustration substantiates the model described above for the northern North Sea.

### **1.2.3 Depositional model of the Agat Formation**

The Agat field was found in the north-eastern part of the North Sea approximately 50 km off the Norwegian coastline and initiated the interest for the Agat Formation (Figure 1) (Gulbrandsen & Nyborkken, 1991). This was the first field discovered offshore Norway in the Lower Cretaceous interval containing hydrocarbons. The Agat field is located between the mainland of Norway and the Sogn Graben. The sandstones of the Agat Formation is found mainly around the Måløy Terrace towards the Sogn Graben and is believed to be sourced from the narrow shelf area (Martinsen et al., 2005). The Agat Formation is of Aptian to Albian age (Gulbrandsen & Nyborkken, 1991; NPD, 2019).

After the discovery of the Agat field, the depositional environment of the Agat Formation has been debated, and several different models have been suggested.

Gulbrandsen (1987) suggested the first depositional model for the Agat Formation. The depositional model was based on the sands being sourced from multiple point sources on the shelf break in the east as submarine fans. Shanmugam et al. (1994) and Skibeli, Barnes, Straume, Syvertsen, and Shanmugam (1995) investigated several drilled wells in the Agat field looking at core data and proposing another depositional model comparing to Gulbrandsen (1987). Based on the cores, they suggested a depositional model favoring slumps

and debris flows in an upper slope setting as the gravity processes causing the deposition of the Agat Formation.

In 1999, Nystuen published a new proposal for a model of the depositional environment of the Agat Formation, with more similar features to the Gulbrandsen (1987) model. Nystuen (1999) suggested that the dominated process for the Agat deposits was turbidity currents that were probably located within a channel system. Bugge, Tveiten, and Bäckström (2001) suggested a model also based on turbidity currents, however in their model the accommodation space was created in the slide scarps from slumping were sands accumulated as individual bodies. A general interpretation of the wells in the Agat field area shows turbidite deposition with occasional debris flows (Bugge et al., 2001).

## 2. GEOLOGICAL SETTING

The study area is situated on the North-Atlantic continental margin which is a passive margin that has been exposed to multiple rift events before reaching its maximum when the continental separation in the Norwegian Greenland Sea started in 53 Ma (Ziegler, 1975; Blystad et al., 1995; Brekke, 2000; Vergara, Wreglesworth, Trayfoot, & Richardsen, 2001; Osmundsen, Sommaruga, Skilbrei, & Olesen, 2002; Nasuti, Pascal, & Ebbing, 2012).

The study area is located on the boundary between the southern Norwegian Sea and the northern North Sea, where the NE – SW trending Møre-Trøndelag Fault Complex intersects with the structural trends of the northern North Sea (N – S and NNW – SSW) (Brekke, 2000). The Møre-Trøndelag Fault Complex is marking the eastern boundary of the Møre Basin and is separating the deeper basin from the shallower minor basin areas (Figure 1). The highs and ridges in this complex are controlled by faults in the area and have NE – SW to ENE – WSW trends (Figure 1). (Brekke, 2000).

The Selje high, which is a horst structure, is the most prominent structure in the study area and is part of the Møre-Trøndelag Fault Complex. This structural high is a result of Jurassic-Early Cretaceous(?) faulting and is an uplifted footwall basement block. This block is part of a half-graben and has been rotated. The Selje High is located in the northern part of the Måløy Terrace (trending in a N – S direction), with the Sogn Graben (trending in a N – S direction) to the southwest and the Slørebotn sub-basin (trending in ENE – WSW direction) in the northwest (Figure 1) (Blystad et al., 1995). A regional seismic line in an E-W direction is presented in Figure 4, highlighting the geology in the study area.

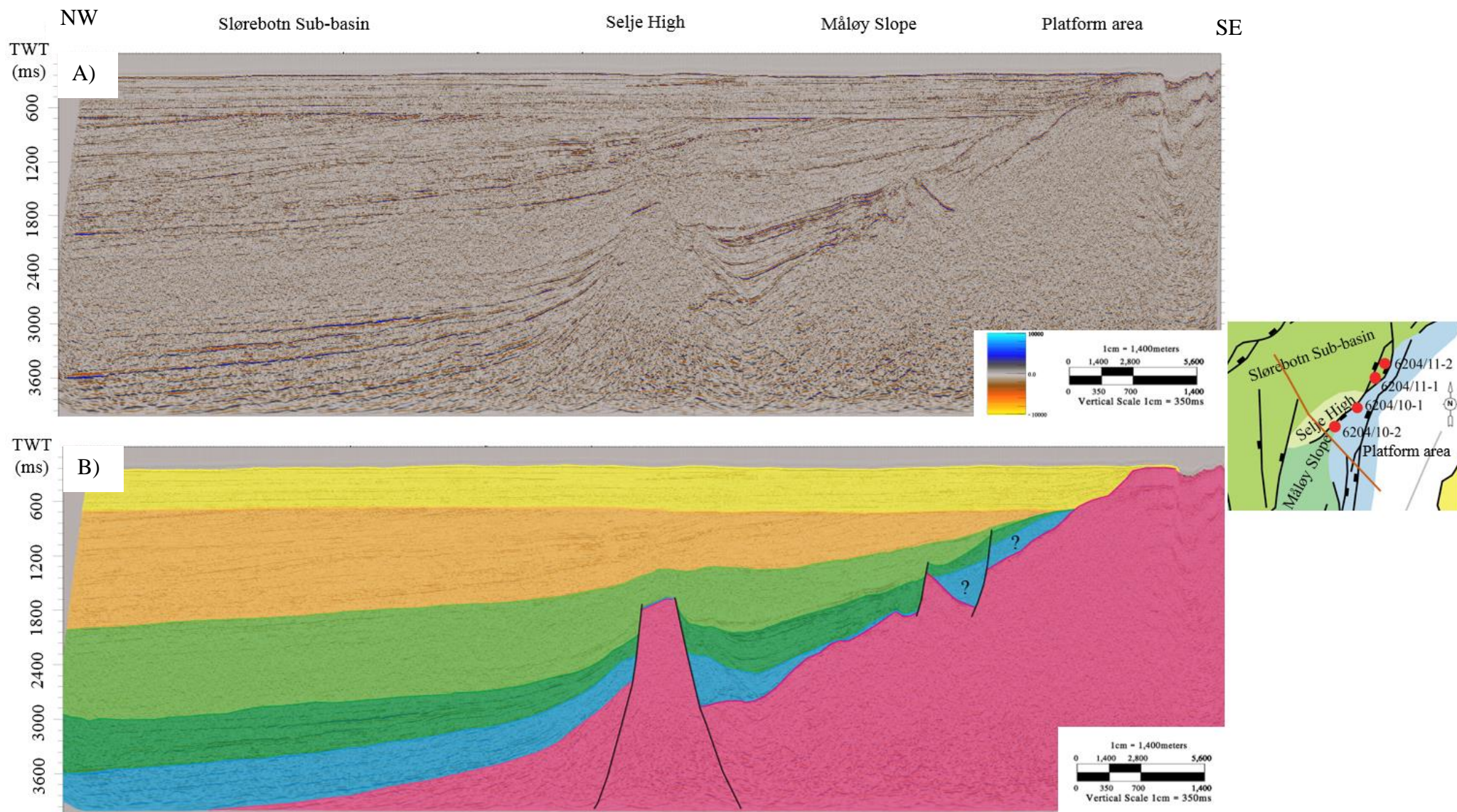


**Figure 4:** Regional seismic line crossing from West to East, from the Slørebotn Sub-basin through the Selje High to the Måløy Slope and the platform area. A) Uninterpreted seismic line. B) Interpreted seismic line. The interpretation in the west close to the platform area is uncertain.



## **2.1 Tectonic setting**

The Northeast Atlantic margin was tectonically active from Carboniferous to late Pliocene time (Brekke, 2000). Three main tectonic episodes formed the present tectonic architecture of the North Sea and the Norwegian Sea; 1) Permo-Triassic rifting; 2) Late Jurassic – Early Cretaceous(?) rifting; 3) Late Cretaceous rifting and subsequent drift and seafloor spreading (Brekke & Riis, 1987; Blystad et al., 1995; Brekke, 2000; Osmundsen et al., 2002; Martinsen et al., 2005).

The Iapetus Ocean closed during the pre-Late Devonian period and the Caledonian Orogeny (Brekke & Riis, 1987; Brekke, 2000). In the Devonian, a long event of rifting affected the eastern part of the North-Atlantic margin and a new period of several rifting events succeeded from Permian to Early Cretaceous with periods of tectonic quiescence in between (Blystad et al., 1995). These rifting events were a result of extensional tectonics (Brekke, 2000). In the Late Cretaceous to Tertiary the last rifting event occurred, however, this rifting event was a result of relative movements along plate boundaries in relevance to the beginning of the continental break up and sea-floor spreading of the North Atlantic margin separating the continents Eurasia and Greenland (Brekke & Riis, 1987; Blystad et al., 1995; Brekke, 2000). The trends dominating the Northeast Atlantic margin are NE – SW, N – S and NW – SE faults, which also were subjected to reactivation during several rift phases (Osmundsen et al., 2002).

To further highlight the intervals of interest in this study, a more detailed explanation of the tectonic evolution of Jurassic and Cretaceous is given below.

### **2.1.1 Jurassic**

In the Jurassic, a series of rifting events occurred with the most intense phase in the Middle to Late Jurassic (Vollset & Doré, 1984). These rifts were influenced by the structural framework created in the Triassic.

In the Late Jurassic significant changes in the geology followed which resulted in the development of new landscapes (Nøttvedt & Johannessen, 2008). A series of rifting events influenced the North Sea and resulted in the creation of the Viking and Central Graben (Ziegler, 1975). Fault blocks were rotated due to normal faulting along the Viking Graben (Faleide et al., 2010). The first period of rifting began in the North Sea in the south and moved all the way to the Barents Sea in the north (Vollset & Doré, 1984; Nøttvedt &

Johannessen, 2008). The rifting in Jurassic has different interpretations, however, Faleide et al. (2010) suggested that the rifting period lasted only to the end of Jurassic for the northern North Sea, while the rifting in the Norwegian Sea ended in the Early Cretaceous. The Late Jurassic rifting was different from the previous rifting period of Permian to Triassic, as the Late Jurassic rift thinned the crust severely and the whole rift submerged into the sea. Most of the faults of Jurassic age were terminated before reaching the end of Jurassic, but a few faults are evident in younger strata (Faleide et al., 2010).

### **2.1.2 Cretaceous**

Faleide et al. (2010) suggested that the rifting from Jurassic died out in the Cretaceous, and that the entire Cretaceous succession is post-rift strata. The ending of rifting resulted in the crust cooling and subsidence of the Cretaceous basins occurred (Faleide et al., 2010).

Furthermore, Færseth and Lien (2002) also explained that the Cretaceous period was dominated by tectonic quiescence and thermal subsidence.

However, several other authors claimed that the Early Cretaceous showed evidences of active rifting. Lundin and Dore (1997) explained the tectonic of Early Cretaceous in this sense. The North Sea rift from Jurassic age got extinct in the Kimmeridgian and subsidence occurred as explained by Færseth and Lien (2002) and Faleide et al. (2010). However, sea floor spreading in the Atlantic were moving northwards to the Møre Basin in the Early Aptian leading to NW-SE extensions, which were different from the Late Jurassic trends. Thus, the conclusion was that the Late Jurassic and the Early Cretaceous were two separate events, but the time in between the events was not necessarily large (Lundin & Dore, 1997).

A regional geological line highlighting the Selje High, Slørebotn Sub-basin and Måløy Terrace is presented in Figure 5.

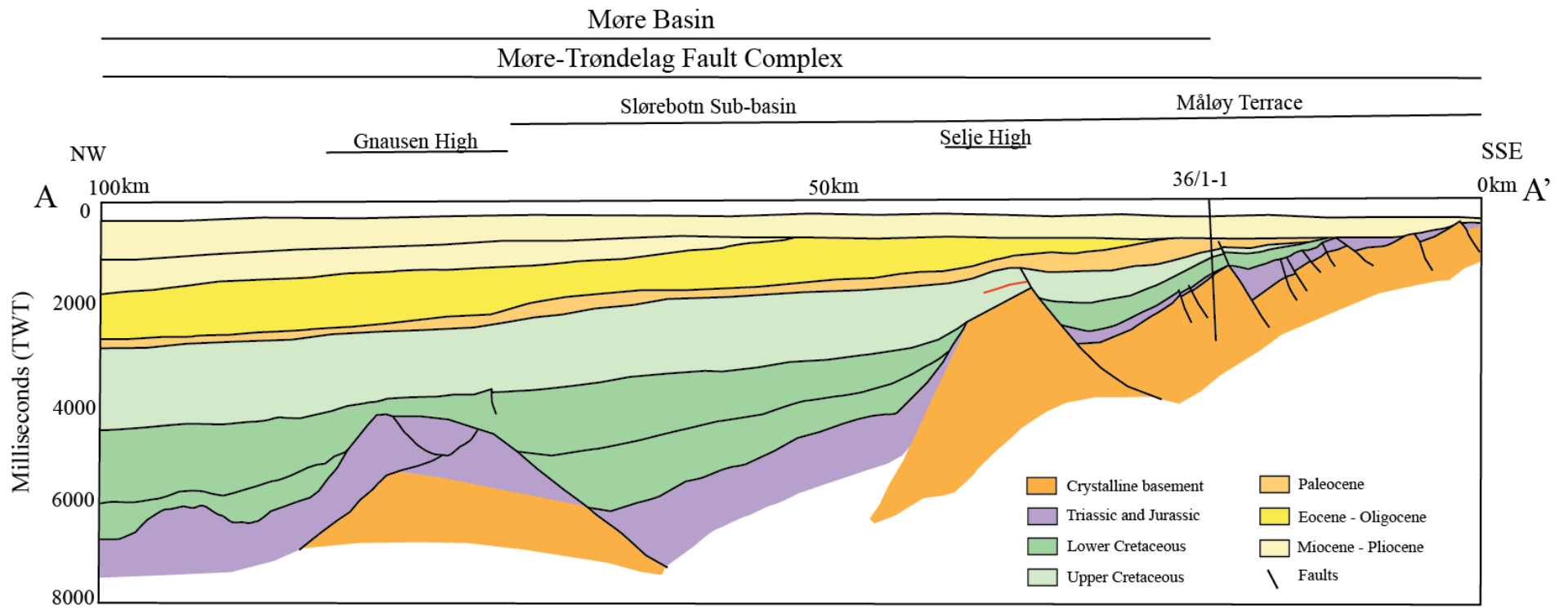


**Figure 5:** Regional line showing from the NW to the SSE from the Slørebotn sub-basin, Måløy Terrace and Selje High. This regional line is along the same line as interpreted in Figure 4. Modified by (Brekke, 2000).

## **2.2 Stratigraphy**

In the most southern parts of the Norwegian Sea, around 62-63°N, the lithostratigraphy is considered more like that of the northern North Sea than the Norwegian Sea, and the lithostratigraphic names in this area are therefore the same as in the North Sea (Figure 6) (Vergara et al., 2001). The deposition in the North Sea during Early Cretaceous has been interpreted as heavily dependent on the basin topography created by rifting during the Late Jurassic (Martinsen et al., 2005). The accommodation space, source area, and transport direction for the eastern margin were controlled by the structural highs, terraces, and the slopes (Martinsen et al., 2005).

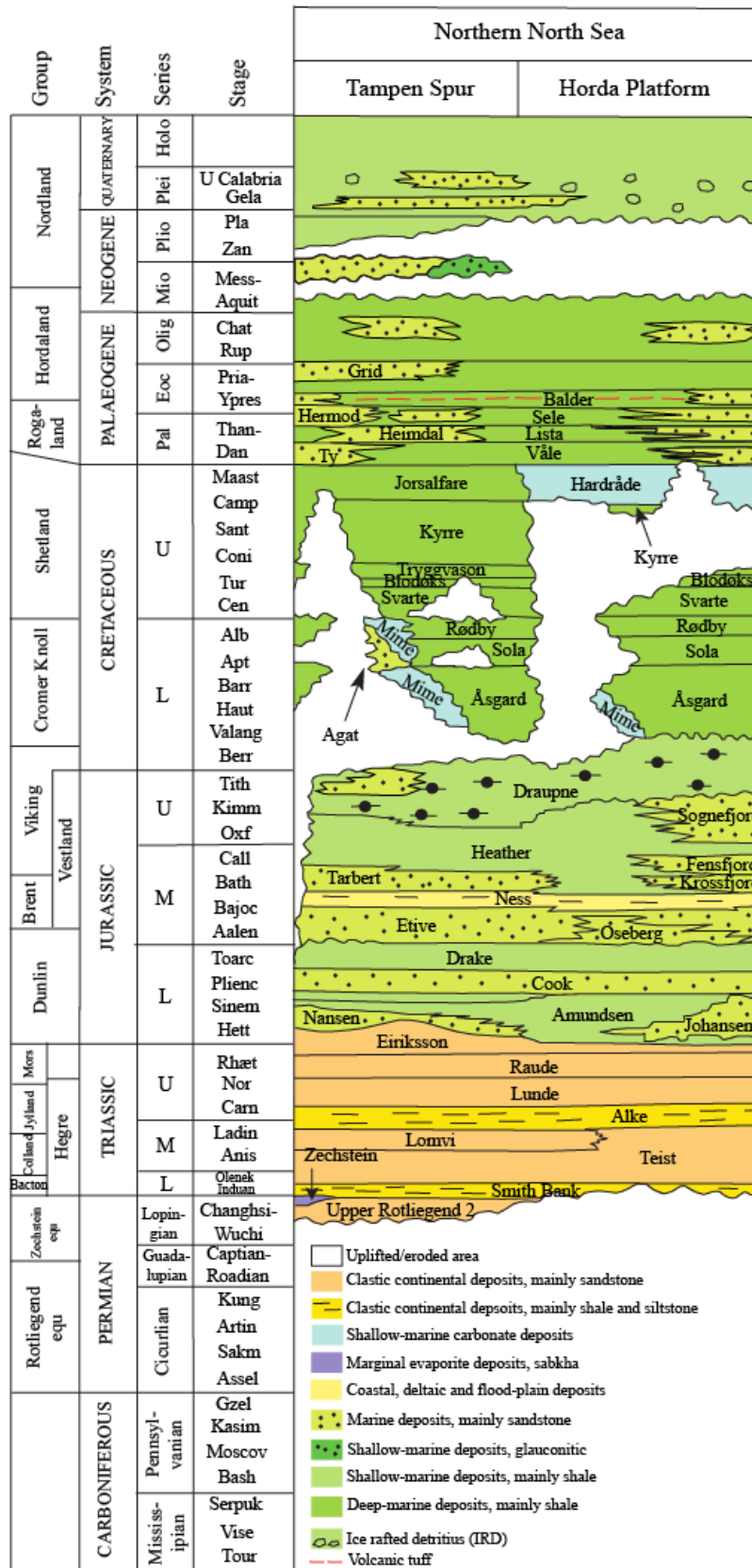


**Figure 6:** Lithostratigraphic chart of the Northern North Sea from the Tampen Spur and Horda Platform. The lithostratigraphy in the study area is believed to be similar. Modified from (NPD, 2014).

## 2.2.1 Pre-Devonian

A small number of the wells drilled in the Norwegian continental margin have penetrated basement rocks of Pre-Devonian age, thus this interval is fairly documented and has less certainty than overlying successions (Basset, 2003). The basement consist of several different rocks such as igneous rocks, metamorphic rocks, and metasedimentary rocks (Basset, 2003). The Pre-Devonian sediments are highly fractured and deformed due to metamorphism and are forming the basement of the northern North Sea and southern Norwegian Sea (Gee & Sturt, 1985; Pickering, Bassett, & Siveter, 1988; Basset, 2003).

The basement is encountered in two of the wells in the study area, wells 6204/10-1 and 6204/10-2R. It is therefore relevant to look at the well report for the two wells to compare the lithology found in the basement (Table 1); however, none of the wells have cores from the basement interval.

**Table 1:** Information about target, results, and lithology for the two wells 6204/10-1 and 6204/10-2R, which have drilled the basement. All information in the table is extracted from well reports for the two wells from NPD fact pages (NPD, 2019).

Well	Target	Results	Lithology of basement	Lithology of conglomerates above
<b>6204/10-1</b>	J-prospect (Turonian). Jurassic Lead. Stratigraphy in Tertiary, Turonian and Cenomanian levels.	Proved geological model of the J-prospect. Unexpected conglomerates in the lower parts of the well.	The lowermost part penetrated in the well consists of conglomeratic sediments with the same composition as the conglomerates described to the right. Uncertain age of sediments, either Triassic or Basement.	Conglomerate comprises of rock fragments (gneiss, quartzite, mica schist) locally quartz fragments, quartz/feldspar, different kind of mica, pyrite, and traces of rose quartz.
<b>6204/10-2R</b>	Jurassic L prospect. Turonian/Coniacian Q-prospect. Secondary target: Fractured basement.	Jurassic section missing. No hydrocarbons encountered in the basement. Thin Lower Cretaceous sandstone stringer with gas.	Cuttings show rock fragments of metamorphic rocks, gneiss, mica, schist, quartz, feldspar, muscovite and biotite. Traces of white opaque crystalline calcite constitute vein or fracture fill.	Thin conglomeratic sandstone on top of the basement which grades into sandy conglomerate. The conglomerate is sandy with rock fragments of the metamorphic basement.

### **2.2.2 Pre-Jurassic**

During Permian, the climate became arid and dry, and the basins were filled with continental sediments as alluvial fans and aeolian sand dunes of the Rotliegend formation (Larsen, Olausen, Sundvoll, & Heeremans, 2007; Faleide et al., 2010).

In the Triassic the climate was dry, and the period was dominated by sands, gravels and mud deposits coming from the elevated areas around creating alluvial plains (Ramberg, Solli, Nordgulen, Binns, & Grogan, 2008). Fine-grained material were deposited in the basins, while coarse-grained deposits were found in the marginal areas (Vollset & Doré, 1984). During the late Triassic, a dramatic change in climate led to seawater flooding the alluvial plains and ending the continental deposition (Vollset & Doré, 1984; Ramberg et al., 2008).

### **2.2.3 Jurassic**

The continental areas became covered in shallow seas due to a transgression in the Early Jurassic and marine shales were deposited over large areas (Vollset & Doré, 1984; Faleide et al., 2010). During Middle Jurassic, volcanic activity occurred in the central part of the North Sea causing dome structures. These structures worked as source areas for deltaic deposits, and the deposition of the Brent Group occurred in the northern North Sea (Vollset & Doré, 1984; Faleide et al., 2010).

In the Late Jurassic, the Viking Graben was exposed to normal faulting causing rotation of basement blocks, resulting in the blocks being tilted and the upper part of the footwall becoming exposed to erosion (Vollset & Doré, 1984; Faleide et al., 2010). This led to the removal of Lower to Middle Jurassic and in some areas even Upper Triassic strata (Faleide et al., 2010). A period of transgression in the Late Jurassic covered the northern North Sea with seawater leading to the deposition of the clay sediments of the Heather Formation; however, some coarse-grained sediments from turbidites and deltas were also deposited off from the margins (Sognefjord Formation and Heather Sandstone Formation) (Vollset & Doré, 1984; Faleide et al., 2010).

### **2.2.4 Cretaceous**

The Early Cretaceous is recognized by a transgression interchanging with minor regressive events resulting in mainly deposits of shales (Isaksen & Tonstad, 1989; Brekke & Olausen, 2008; Faleide et al., 2010). The change from Jurassic to Cretaceous is marked by a major

unconformity called the Base Cretaceous Unconformity (BCU) (Faleide et al., 2010). Several formations have been identified in the Early Cretaceous, such as the shaly Åsgard, which were deposited during quiet conditions and a transgression in Valanginian to late Barremian (Faleide et al., 2010). Movements along the North Sea rifts during Mid-late Aptian together with the occurrence of a regression caused changes in the lithology in the northern North Sea. As a result, the previously calcareous rich claystones in the basinal areas changed to more organic-rich claystones creating a new formation called the Sola Formation (Isaksen & Tonstad, 1989; Faleide et al., 2010). In addition, the sandstone rich sediments of the Agat Formation and the Ran sandstone Member were deposited during this period. These sandstone formations were a result of erosion along the flanks of structural highs and were deposited as gravity flows in some parts of the northern North Sea and the southern Norwegian Sea, like the Måløy Terrace and around the Selje High (Isaksen & Tonstad, 1989).

As the regression changed into transgression during Albian, the deposition of the Agat and Ran sandstones were still active as some of the higher parts of the structural highs were still exposed to erosion, while the overall area was covered by the sea (Isaksen & Tonstad, 1989). During this period, a new formation called the Rødby Formation consisting of fine-grained calcareous sediments evolved (Isaksen & Tonstad, 1989; Faleide et al., 2010).

In the Late Cretaceous, the northern North Sea was tectonically relatively quiet and the transgression reached its maximum, resulting in low clastic sedimentation and the area was now dominated by the marine shaly carbonate Shetland Group (Isaksen & Tonstad, 1989; Faleide et al., 2010).

Cores from the Åsgard Formation in well 6204/10-2R are extracted from NPD and displayed in Figure 7. The cores show the description of dark grey to grey shaly sediments as explained above.



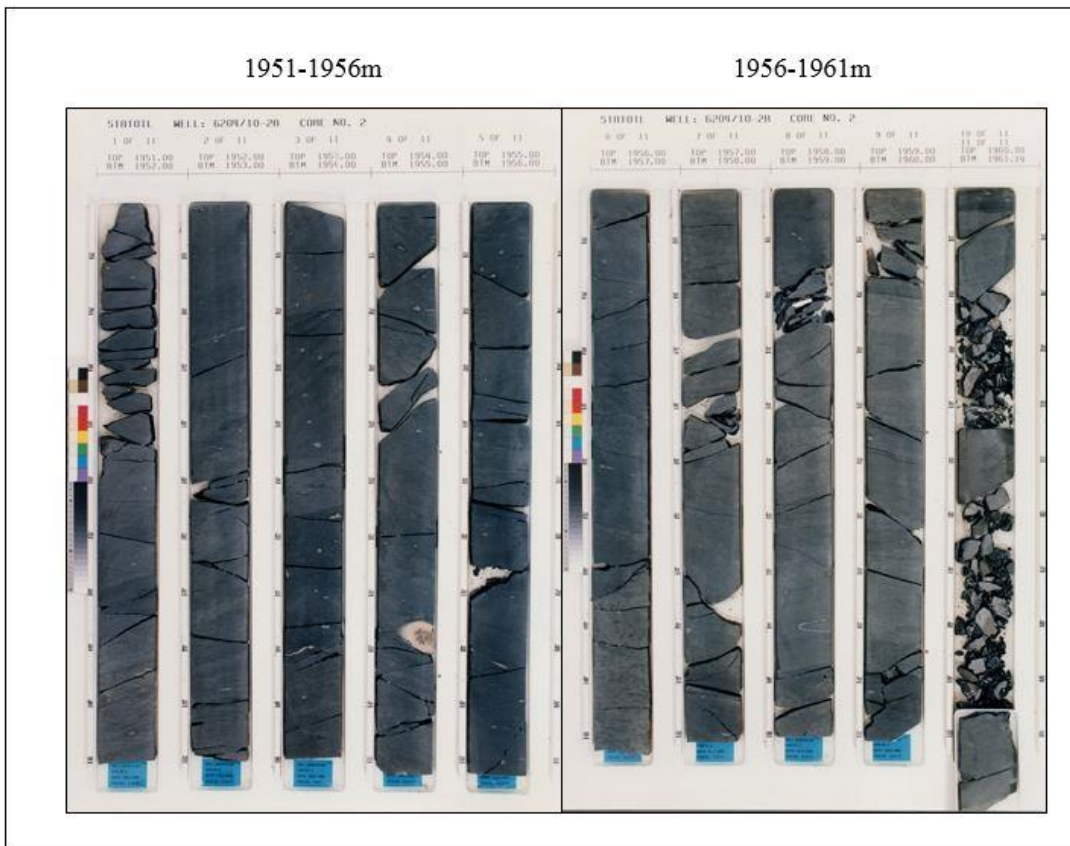


**Figure 7:** Cores from well 6204/10-2R showing the Åsgard Formation from 1951m to 1961m. The cores show dark fine-grained sediments. Collected from NPD fact pages (NPD, 2019).

#### 2.2.4.1 Agat Formation

The deposition of the Agat Formation occurred during the late Early Cretaceous on the Måløy Slope, illustrated in the chronostratigraphic chart in Figure 8 (Isaksen & Tonstad, 1989; Martinsen et al., 2005). The formation has a high content of coarse-grained sandstones that are the result of regressive events causing mass-flows along the slope (Bugge et al., 2001; Martinsen et al., 2005). The sandstones are therefore interbedded with shale creating sand beds with a thickness of 10-30 cm (Martinsen et al., 2005). Locally the sandstone beds can become tens of meters in thickness (Bugge et al., 2001; Martinsen et al., 2005).

The deposition of the Agat Formation is from the shelf in the east to the basin in the west (Gulbrandsen & Nyborkken, 1991; Bugge et al., 2001; Martinsen et al., 2005). Several different elements are proven, such as slumps, channels and sheet bodies, which might imply transformation in the slope angle. (Gulbrandsen & Nyborkken, 1991; Skibeli et al., 1995; Martinsen et al., 2005).

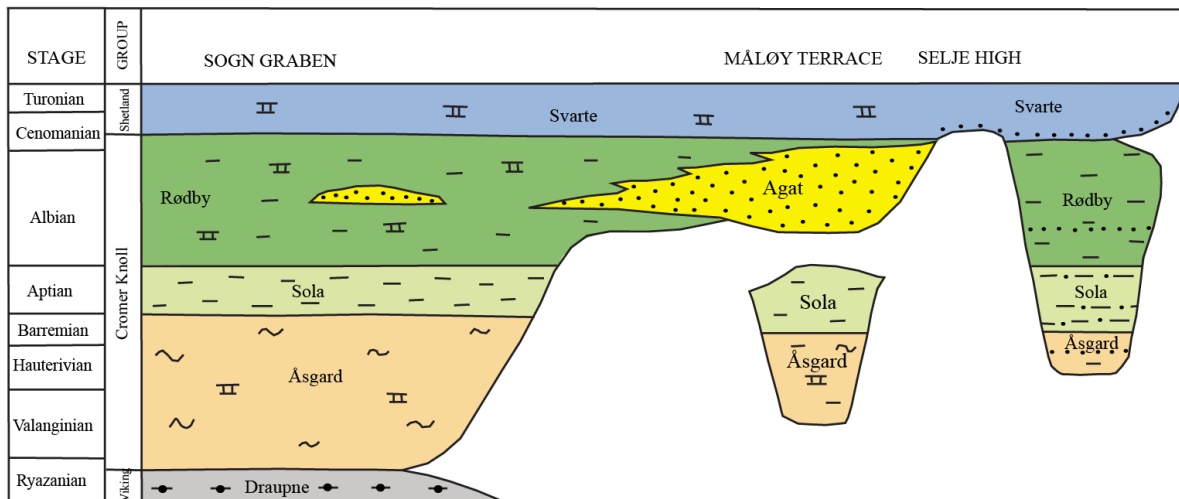


**Figure 8:** Chronostratigraphic chart for the Cretaceous from the Sogn Graben, Måløy Terrace, and Selje High. (Modified from (Vergara, Brunstad, Nordlie, Chranock, & Gradstein, 2006))

### 2.2.5 Post-Cretaceous

The sedimentation and deposition during the Cenozoic period were greatly affected by the uplift of surrounding clastic source areas (Faleide et al., 2010). The North Sea was not affected much by the spreading of the Norwegian Sea, and the area was relatively stable in Paleogene and Neogene except for some periods of uplift (Martinsen & Nøttvedt, 2007).

## 3. DATA AND METHODOLOGY

### 3.1 Data

A 3D seismic cube covering an area of 518 km<sup>2</sup> were available in the dataset. In addition to the 3D seismic, a large number of regional 2D seismic lines were available, however, these were used only for regional interpretation (Figure 9). The vertical resolution of cube ST9202 varies with depth, but the resolution for the Agat Formation in the area close to well 6204/10-1 is 42m, while in well 6204/11-2 the resolution in the Agat Formation is 48m.

The dataset contained six wells, where two are side-tracks of well 6204/10-2 (Table 2). The wells included conventional well logs such as gamma ray (GR), density (RHOB), sonic (AI), resistivity (Res), spontaneous potential (SP), and others. Three wells have check shots used for creating a time-depth table. Further well information and core descriptions were available at the fact pages of the Norwegian Petroleum Directorate (NPD). None of the wells in the study area has cores from the Agat Formation, the conglomerates or the Basement.

**Table 2:** List of wells in the seismic cube with additional information regarding check shots, side-tracks, target, and discoveries. Information is collected from the completion reports found on NPD fact pages (NPD, 2019).

Wells	Total depth (MD)	Check shot	Side-track	Target	Results
6204/10-1	2709 m	X		J-prospect (Turonian). Jurassic Lead. Improve stratigraphic understanding in Tertiary, Turonian and Cenomanian levels.	Dry
6204/10-2	1145 m			Jurassic L-prospect. Coniacian/Turonian Q-prospect. Secondary target: Fractured basement	Dry No discovery in the basement
6204/10-2 A	2290 m		X	Prove economic hydrocarbons and down-dip reservoir thickening of the gas-filled sand penetrated in well 6204/10-2R.	Dry
6204/10-2 R	2095 m	X	X	Jurassic L-prospect. Coniacian/Turonian Q-prospect. Secondary target: fractured basement.	Gas shows No discovery in the basement
6204/11-1	2966 m			Middle Jurassic Brent Group Equivalent in the E-prospect. Sandstones of Turonian age in the I-prospect.	Gas discovery GWC: 2792.5m TVD RKB
6204/11-2	2920 m	X		I prospect (Coniacian/Turonian). O-prospect (Albian/Aptian)	Oil shows

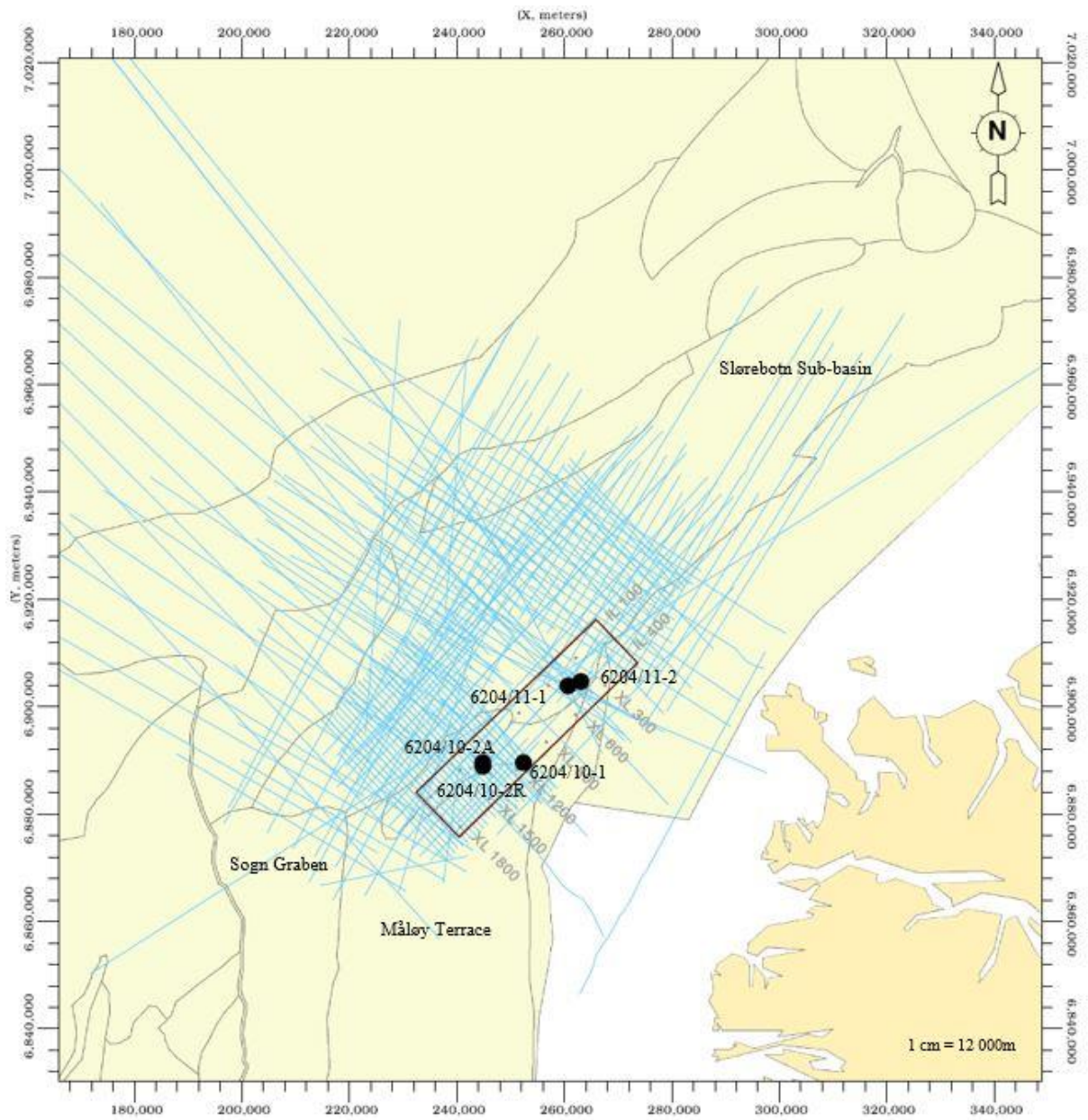


**Figure 9:** An overview of the dataset from the study area. Blue lines are 2D seismic lines, while the black box show the seismic 3D cube. Black circles are the wells. The Norwegian mainland are located to the east.

## 3.2 Methodology

### 3.2.1 Well correlation

Well correlation was executed based on the well tops information provided by NPD (2019). The well correlation was done with the intention of getting a better understanding of the wells in the area before starting the seismic interpretation. For that purpose, a structural well correlation with a focus on the Early Cretaceous and Jurassic interval to highlight structural features was done. The different formations were correlated across the area in all wells from SW to NE and the well correlation started at the top of Shetland Group (Early Cretaceous).

### 3.2.2 Seismic interpretation

Firstly, it is important to establish the polarity of the seismic data. To identify this the seabed was used where the acoustic impedance is going from low to high. If the reflector is red and red represents negative amplitude, then the polarity is considered reverse. In the opposite case, the polarity would be normal. Figure 10 displays the seabed in seismic cube ST9202, and the polarity is interpreted to be reversed for this cube.

A seismic well-tie was executed in the three wells that had check shots, wells 6204/10-1, 6204/10-2R, and 6204/11-2. The extracted wavelet was not a perfect fit, but by adjusting a Ricker wavelet to cover the dominant frequency it fitted well. For wells 6204/10-1 and 6204/11-2 a Ricker wavelet with a frequency of 20 Hz and phase rotation of 0 degrees was used. The synthetic seismogram is fitted specifically to the interval of interest, the Cromer Knoll Group, and Agat Formation. When displaying the seismic well tie in the seismic it fits well with the reflectors, and the horizons can easily be identified for mapping (Figure 11). The result from the synthetic well-tie in wells 6204/10-1 and 6204/11-1 are displayed in Figure 12 and Figure 13.

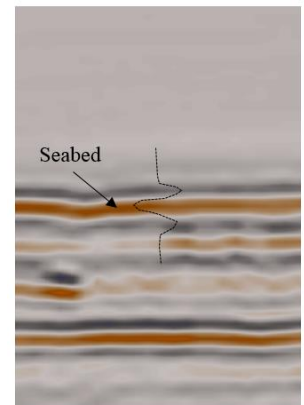


**Figure 10:** A close-up of the seabed highlighting the polarity of the seismic cube.

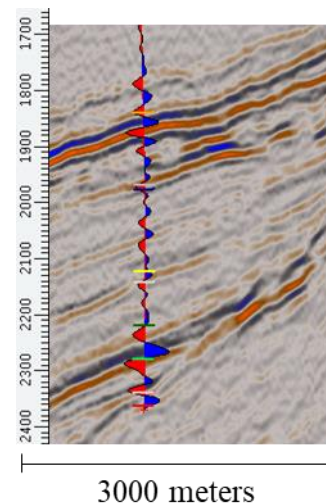


**Figure 11:** Seismic displayed with the synthetic seismogram to highlight the good correlation between the synthetic and the seismic.

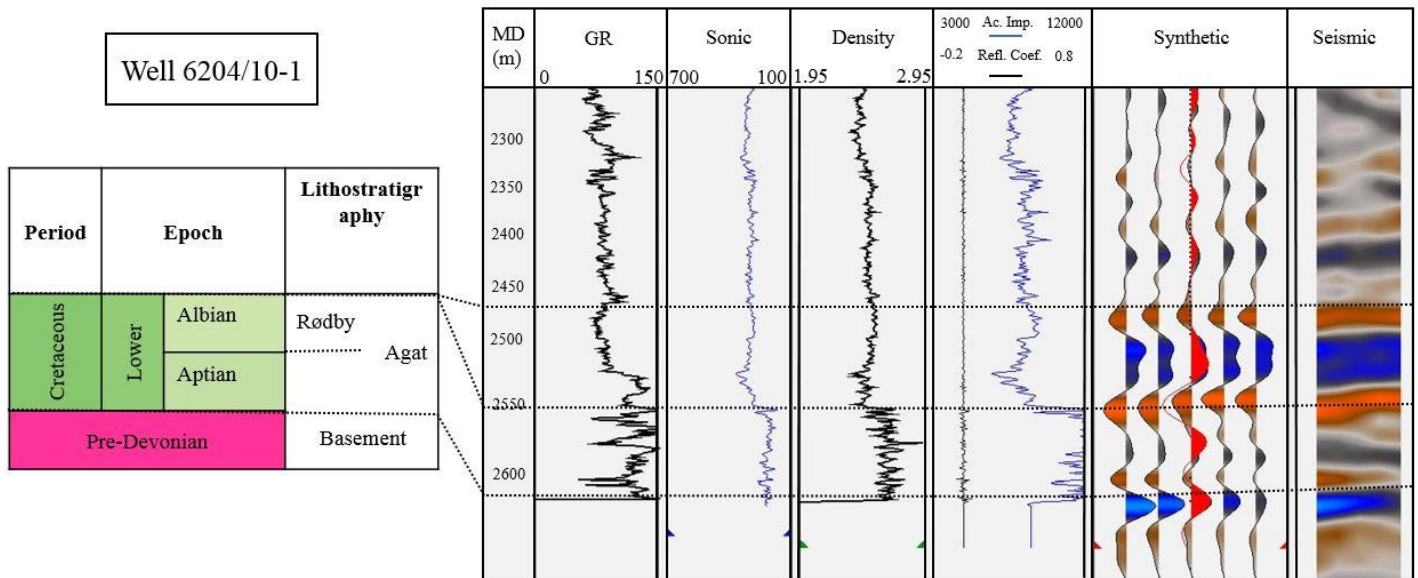


**Figure 12:** Seismic well-tie for well 6204/10-1. The following well logs displayed are: GR, sonic, density, acoustic impedance, and reflection coefficient. The top of present formations are marked.

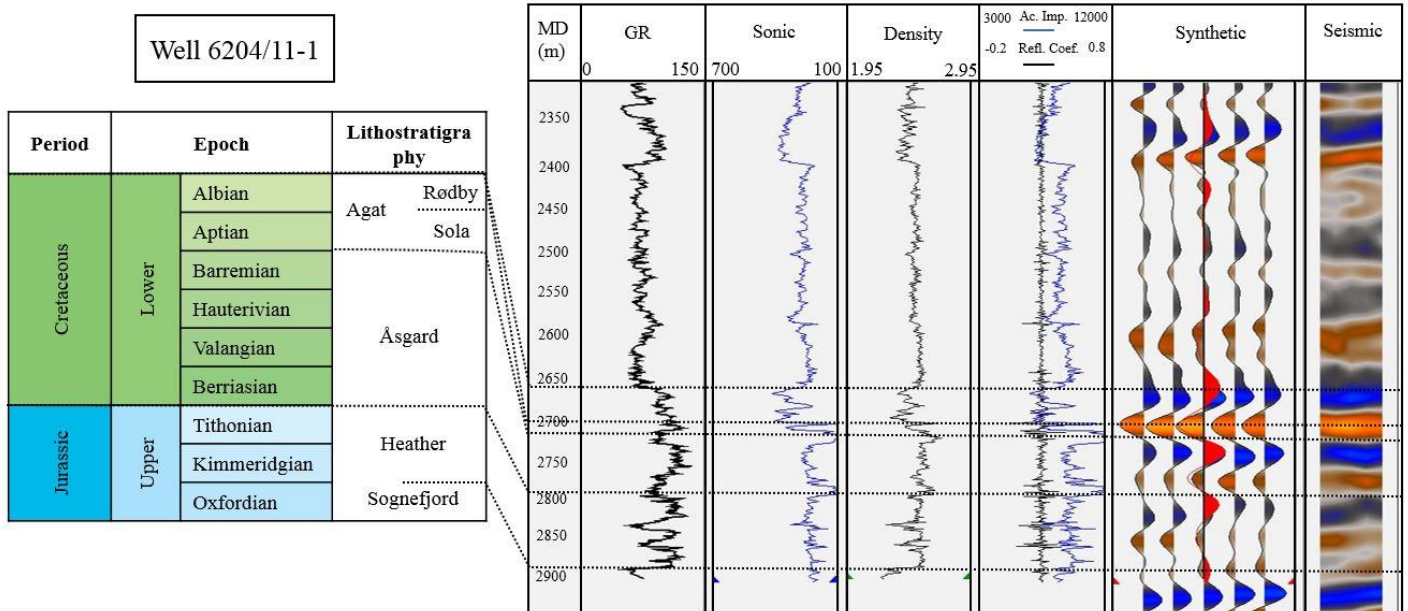


**Figure 13:** Seismic well-tie for well 6204/11-2. The following well logs displayed are: GR, sonic, density, acoustic impedance, and reflection coefficient. The top of present formations are marked.

Four key horizons were identified based on answering the objectives; Top Basement, Base Cretaceous Unconformity, Base Agat Formation, and Top Agat Formation. The BCU in the study area is defined as the base of the Cretaceous Cromer Knoll Gp. All the key horizons have only been identified in some of the wells, which made the interpretation slightly difficult in certain areas. An overview of the different horizons and in which wells they are identified are given in Table 3. Well 6204/10-2 did not contain any of the chosen horizons.

**Table 3:** List of the seismic horizons interpreted in the study area and which wells have the well picks for the given horizons.

<b>Seismic horizon</b>	<b>6204/10-1</b>	<b>6204/10-2</b>	<b>6204/10-2R</b>	<b>6204/10-2A</b>	<b>6204/11-1</b>	<b>6204/11-2</b>
<b>Top Basement</b>	X		X			
<b>Top Agat Fm</b>	X					X
<b>Base Agat Fm</b>	X					X
<b>BCU</b>	X		X	?	X	X

All the main faults in the study area were interpreted and displayed on the structural map created from the interpreted horizons. It is worth mentioning that only the major faults from the Basement to Lower Cretaceous have been mapped in this thesis.

Furthermore, all the main faults in the study area were interpreted with respect to syn-rift and post-rift, based on the elements shown in Figure 2. The faults were separated into fault families containing similar age, strike, and location.

Lastly, the integration of the data contained in this study was used to create conceptual sketches of the paleogeography from the Late Jurassic to Base Cretaceous interval.

### 3.2.3 Spectral decomposition

For further investigation of the interval of interest, spectral decomposition was done in GeoTeric. The Agat Formation is a thin sandstone unit (106m in well 6204/10-1 and 30m in well 6204/11-2), which is difficult to distinguish in some areas of the seismic due to the vertical seismic resolution (40-48m).

#### *Theory*

Spectral decomposition is a method used to highlight seismic features and attributes and can help distinguish the top and base of a layer beneath the seismic resolution (Partyka, Gridley, & Lopez, 1999). By using spectral decomposition, it increases the accuracy and effectiveness of seismic interpretation by highlighting geological features such as channels, faults and bed thickness that otherwise could be buried in seismic broadband data (Li, Qi, Marfurt, & Stark, 2015; Chopra & Marfurt, 2016).

Iso-proportional slicing is a method to slice up the 3D seismic volume (Posamentier, Davies, Cartwright, & Wood, 2007). Well-mapped horizons can be used as a base for the slicing in between an interval of interest. The interval between the two horizons are divided into a number of chosen slices, thus revealing better the stratigraphic features of the interval (Posamentier et al., 2007; Cader, 2017). Lastly, the color blending can be applied to the slices.

Color blending is a powerful tool, where different colors are assigned to different volumes (Moore & Smith, 2017). Thus, multiple spectral components are blended into one image. White color indicates that all the three volumes are high, however, if one of the volumes dominate, the assigned color for that volume will be evident (Li et al., 2015). Black indicates that all three volumes are present at more or less the same amount (Li et al., 2015; Moore & Smith, 2017).

The different spectral decomposition options are listed in Table 4, highlighting the methods and use.



**Table 4:** Information about the three different spectral decomposition methods that are available and are used in this thesis. Information extracted and modified from a GeoTeric video tutorial online (GeoTeric, 2017b, 2017a).

	<b>Decomposition options</b>	<b>Methods</b>	<b>Use</b>
<b>Standard Frequency Decomposition</b>	Constant Bandwidth	Similar to Fourier Transform	Estimation of bed thickness and thin bed interference.
	Constant Q (Exponential and Uniform)	Similar to a Continuous Wavelet Transform	Regional studies and reconnaissance.
<b>High Definition Frequency Decomposition</b>	HD Frequency Decomposition	Modified matching pursuit	Reservoir-scale analysis and understanding depositional layers.

### ***Methodology***

The software used to do spectral decomposition is GeoTeric. The main attributes used from the software were frequency decomposition, HD frequency decomposition and iso-proportional slicing all with color blending (GeoTeric, 2017b).

All four different decomposition options were tested on the seismic cube in GeoTeric. After evaluating the results of the decomposition, only two composition methods were used to describe the results; Constant bandwidth for both Basement and Agat Formation and HD frequency decomposition for only the Basement. In the HD frequency decomposition, the following frequencies were used: 15Hz – 30Hz – 45Hz for the different volumes for the Basement. For the constant bandwidth, another set of frequencies were used for the Basement and Agat Formation: 17Hz – 24Hz – 31Hz and 17Hz – 30Hz – 42Hz respectively. These volumes were assigned to different colors to create the color blend, where the lowest frequencies are red, medium are green and highest are blue. The resultant color blends were used on the surface of both the Basement and the Agat Formation to highlight stratigraphic features on the surface.

In addition, iso-proportional slicing between the top and base of the Agat Formation with 3 slices in between were executed. The constant bandwidth color blend for the Agat Formation was assigned to these slices and used to evaluate the changes in the formation.

## 4. OBSERVATIONS AND RESULTS

### 4.1 Structural well correlation

#### *Observations*

The structural well correlation (Figure 14) is concentrated mainly in the interval of interest from the Basement until the Upper Cretaceous. All the well tops used in this correlation are collected from the Norwegian Petroleum Directorates facts pages (NPD, 2019).

The section goes from the Selje High in the south to the Slørebotn Sub-basin in the north (map in Figure 14). The basement is only encountered in two of the wells, 6204/10-1 and 6204/10-2R. The difference in elevation is striking, with a much thicker interval of the basement for the well drilled in the Selje High.

The Jurassic section is only present in two of the five wells in the correlation (6204/11-1 and 6204/11-2), and only the Upper Jurassic is penetrated (Heather and Sognefjord formations). Whereas in the Jurassic the thickest interval is located in well 6204/11-1, in the Cretaceous the thickest interval is located in well 6204/11-2. The Jurassic interval in well 6204/11-1 has a thickness of 314m, while in well 6204/11-2 the thickness is at least 92m, however, this well is not drilled deeper. The Lower and Middle Jurassic is missing, and the Upper Jurassic in well 6204/11-1 overlays a thin Triassic interval while well 6204/11-2 is terminated in the Jurassic Sognefjord Formation. The BCU is defined at the base of the Cromer Knoll Group, which is located at 2602m in well 6204/11-1 and 2769m in well 6204/11-2.

The Lower Cretaceous Cromer Knoll Group consists of a thin interval varying from 138m in the elevated basement to 0-205m in the lower areas; however, the thickness variation between wells is significantly less compared to the Upper Cretaceous. Still, there are some small variations in thickness and elevation.

Furthermore, the wells drilled on the Selje High, have the Lower Cretaceous interval drilled at 1935m and 2233m, while two of the remaining wells (6204-10/1 and 6204/11-2) have drilled the same group at a much deeper level at 2465m and 2659m. Moreover, the well 6204/11-1 did not encounter the Lower Cretaceous interval. Thus, the Lower Cretaceous interval have varying formations present in the wells. The Rødby Formation and the Agat Formation is only present in wells 6204/10-1 and 6204/11-2. It is worth mentioning that these two wells are located in the structural lows in the study area. The two formations, Rødby and Agat, show a much thicker interval in well 6204/10-1 located in close proximity to the Selje High, with

99m and 106m, respectively, compared to 31m and 30m in well 6204/11-2. Thus, the Agat Formation is not observed in any of the wells drilled in the structural highs (wells 6204/10-2A, 6204/10-2R, and 6204/11-1).

The Åsgard Formation underlies the Agat Formation in well 6204/11-2 as a thin unit of 39m, however, this formation is not present below the Agat Formation in well 6204/10-1 which non-conformably lies on top of the basement. In addition, the Åsgard Formation is penetrated in wells 6204/10-2A and 6204/10-2R at the Selje High with a thickness of 138m in the latter. Moreover, this is the only formation encountered of Lower Cretaceous age in the Selje High.

The Shetland Group marks the top of the correlation, with either Jorsalfare Formation or the Kyrre Formation depending on the well. The Upper Cretaceous section consists of a very thick interval varying from approximately 1250m to 1400m in the three wells 6204/10-1, 6204/11-1 and 6204/11-2, while the other two wells have considerably thinner sections varying from approximately 650m to 950m of Upper Cretaceous succession.

Lastly, the cores in Figure 7 of the Åsgard Formation are relevant to mention here as it might give indications of the depositional environment during the Early Cretaceous. The cores are from well 6204/10-2R drilled in the Selje High. The main observation is the dark gray color which becomes slightly lighter towards the end at 1961m. Moreover, the cores look overall fine-grained and well sorted, with a small interval of coarser material at the bottom of 1656-1657.

### ***Interpretation***

The most evident observation is the displacement between the wells drilled on the Selje High and the surrounding areas. Before doing any seismic interpretation, this looks like a major normal fault displacing the wells 6204/10-2A and 6204/10-2R up compared to the other wells, which could also explain why the sediments of the Jurassic interval are eroded away or not deposited at the structural high. However, well 6204/10-1 has also been exposed to erosion or non-deposition of the Upper Jurassic interval. These wells are located at the Selje High and the Måløy Slope (6204/10-1), while wells 6204/11-1 and 6204/11-2 are located in the deeper Slørebotn Sub-basin.

In addition to the possible major fault in the south, the elevation difference between the Jurassic intervals in wells 6204/11-1 and 6204/11-2 might indicate another normal fault in the correlation, however, this would be a minor fault. Moreover, the change in thickness from

Jurassic to Cretaceous across faults further confirm the possible fault activity. The presence of the Heather Formation in Late Jurassic suggests deep marine conditions associated with the transgression during this period (Faleide et al., 2010), while the Sognefjord Formation and the Heather Sandstone (SS) Formation are indicating infill of elastic sediments from the platform area, likely during minor regressive events as explained in the geological setting (Bugge et al., 2001).

Furthermore, the thickness variations and absence of the Upper Jurassic and the Agat Formation in the structural highs and the shift in the thickness of the Upper Jurassic and Lower Cretaceous between wells 6204/11-1 and 6204/11-2 further indicate fault activity during the deposition of the Late Jurassic and the Early Cretaceous.

The presence of the Åsgard Formation in some of the structural highs suggests that they were partially flooded in the Early Cretaceous before the deposition of the Agat Formation in the structural lows. However, it is interesting that the Åsgard Formation is only present in the Selje High and well 6204/11-2, which is good indications of a period of active rifting and erosion after the deposition of the Åsgard Formation. In addition, the cores displayed in Figure 7 showing fine-grained dark sediments are good indications that the Åsgard Formation was deposited during a transgression, which corresponds well with the Early Cretaceous transgression suggested by Faleide et al. (2010).

However, this hypothesis needs to be further investigated with seismic data.

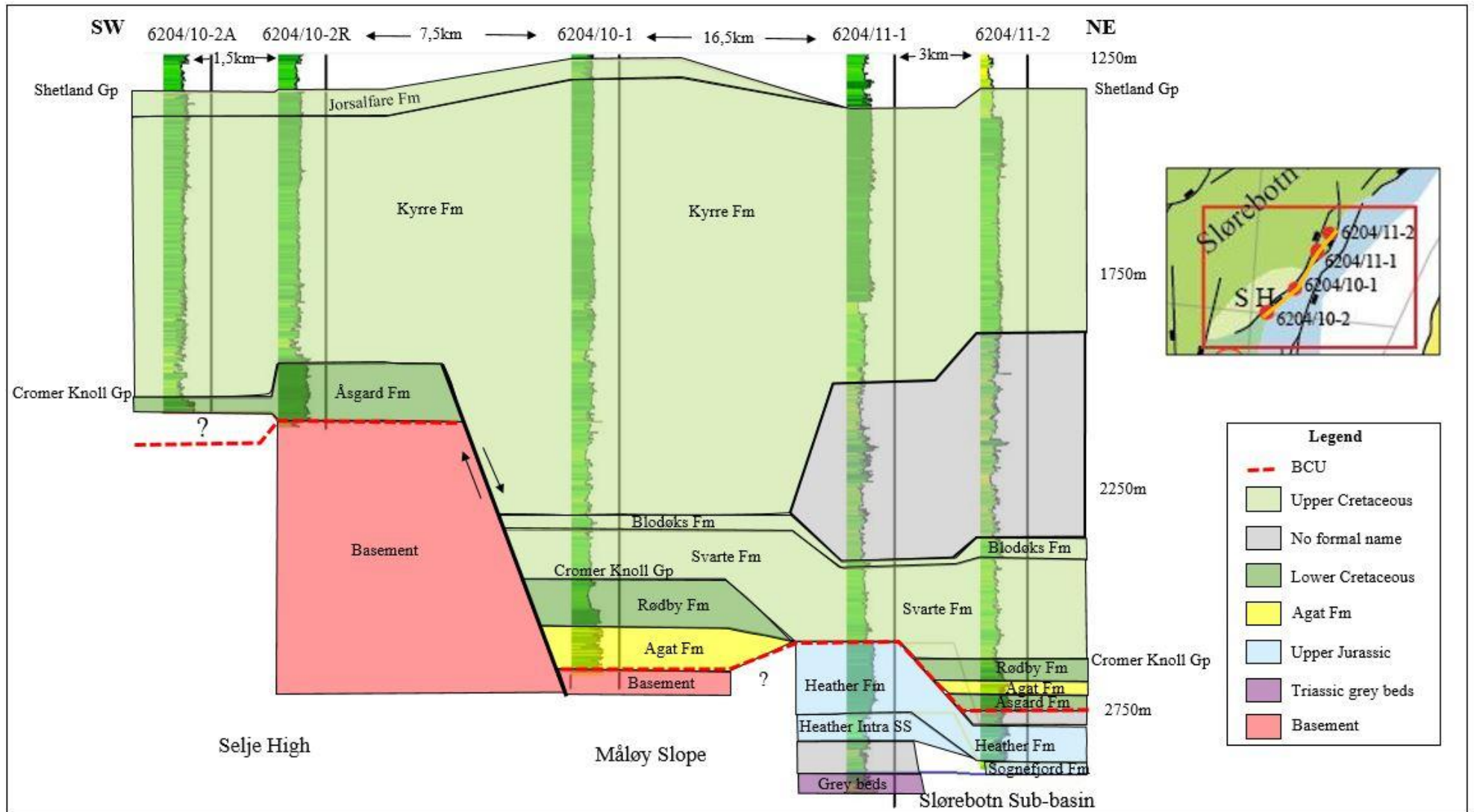


**Figure 14:** Structural well correlation between all wells in the study area going from southwest to northeast (yellow line in map), through the Selje High, Måløy Slope, and Slørebotn Sub-basin. The correlation is from Basement until the top of Upper Cretaceous.

## **4.2 Seismic interpretation of the main intervals**

In this subchapter, the observations based on the three main units; Basement, Pre-BCU, and Agat Formation will be presented separated into faulting, mapping, seismic character, and spectral decomposition. In addition, some basic interpretations are presented for further discussion in Chapter 5.

### **4.2.1 Basement**

In this part, the observations and interpretations based on the basement are presented. These are crucial for understanding the structural elements in the study area but might also contain important information about the depositional history and help with the understanding of the overlying sediments.

#### **4.2.1.1 Faulting**

Three fault families were identified in the study area during the structural interpretation and these are differentiated based on orientation, timing, and location. Figure 15 shows all the eleven major faults mapped in the study area. Faults are marked with the given fault family in a structural map of the basement. A further detailed description of the different families is provided below.

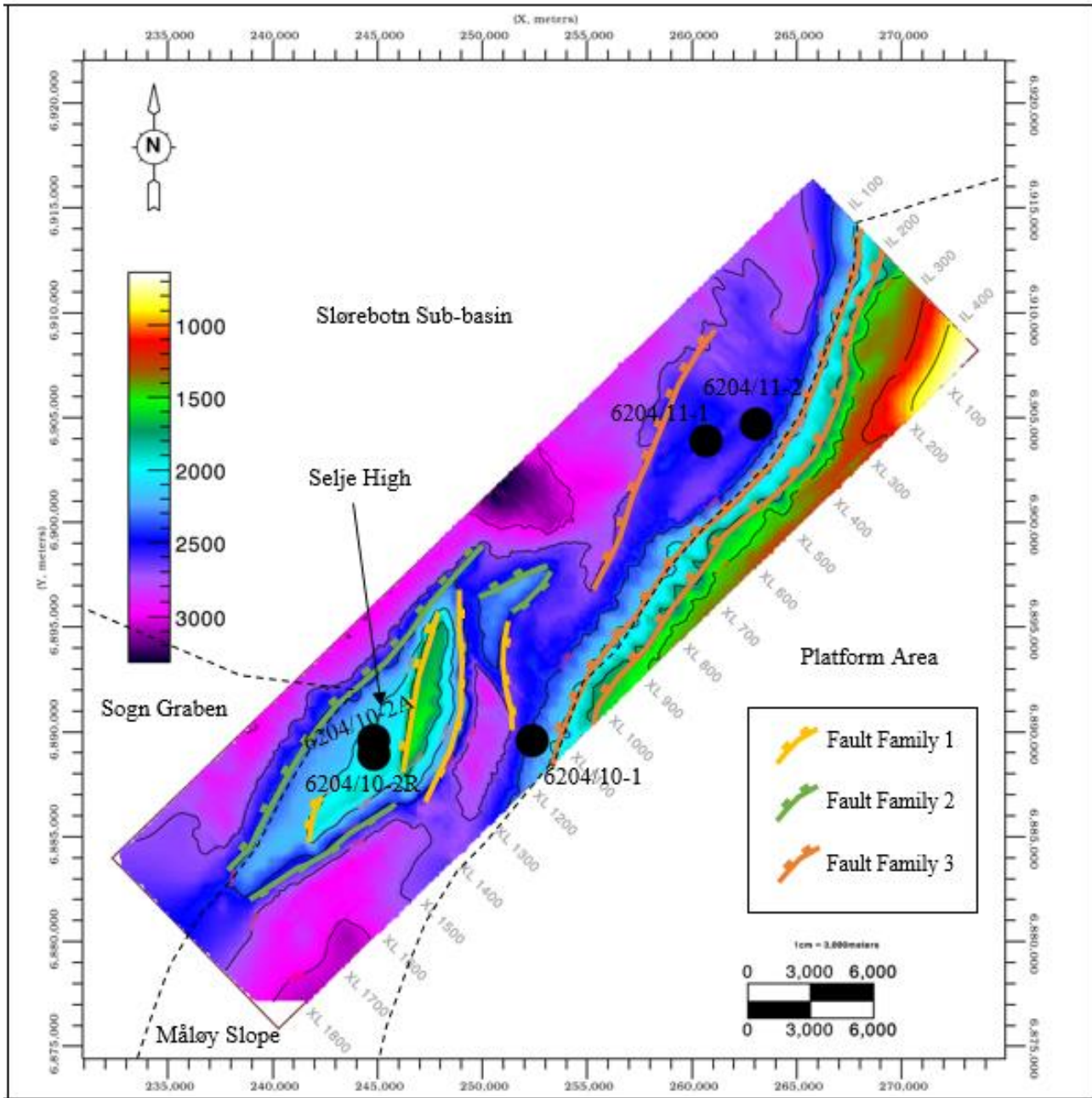


**Figure 15:** Structural map of the basement with all the faults divided into three fault families. Fault family 1 (FF1) in yellow, Fault family 2 (FF2) in green and Fault family 3 (FF3) in blue.

### **Fault family 1 (FF1): N-S striking normal faults**

Four of the eleven major faults are striking in an N-S direction (Figure 15). These faults are found in the immediate area of the Selje High and are normal faults bounding this structural high (Figure 15). FF1 represents faults with variable displacement and dip, however, all faults intersect the basement and continue into the Lower Cretaceous where they terminate. Upward dragging of the reflectors in the Cretaceous interval towards the fault plane is evident for the faults bounding the Selje High (Figure 16 and Figure 17).

The most prominent fault of FF1 is the major N-S striking normal fault that is bounding the Selje High basement block in the east (Figure 16 and Figure 17). This fault shows the biggest displacement in the study area and has a listric appearance. In addition, a small fold is observed in the hanging wall of this major fault. Three of the four faults in FF1 are shown in Figure 16 and Figure 17.

### ***Interpretation***

As FF1 is only present in the southern part of the study area in close proximity to the Selje High, an immediate thought is that these faults have triggered the uplift of the Selje High basement block, likely during the Jurassic as no Jurassic sediments are present at the Selje High. The N-S strike is common for the North Sea and the southern Norwegian Sea (Brekke, 2000; Færseth & Lien, 2002) and corresponds well with FF1. As these faults are major faults affecting from the basement and all the way to Cretaceous with upward dragging reflectors of several different ages, it is likely that the faults have been subjected to reactivation during several younger rift periods. Furthermore, the mound observed in close relation to the major fault might be a fold due to a reverse fault reactivation at a later time which is also suggested for the Norwegian Sea by Brekke (2000), Gabrielsen, Odinsen, and Grunnaleite (1999), and Færseth and Lien (2002).



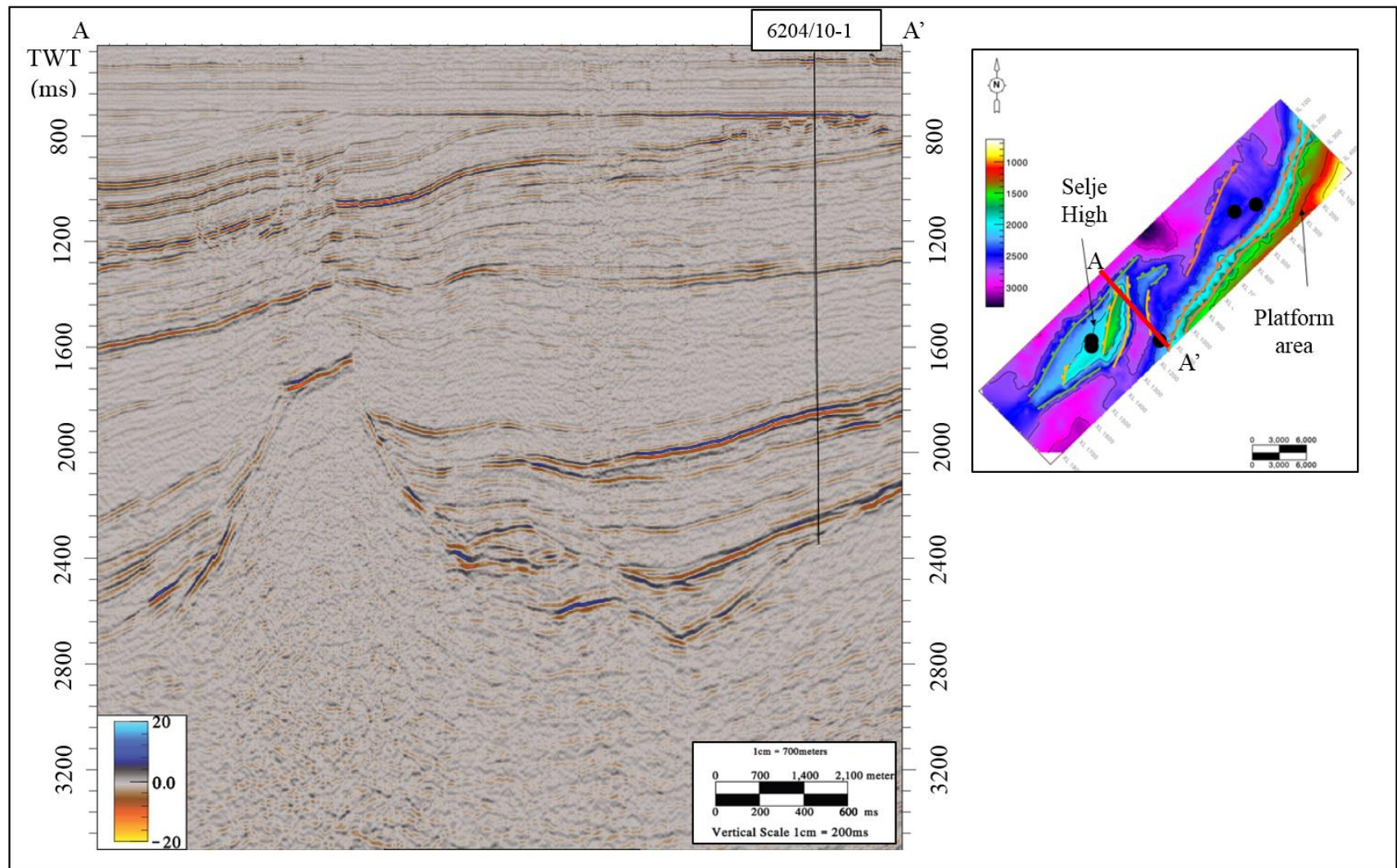


**Figure 16:** Seismic line displaying faults from fault family 1. Uninterpreted seismic line.

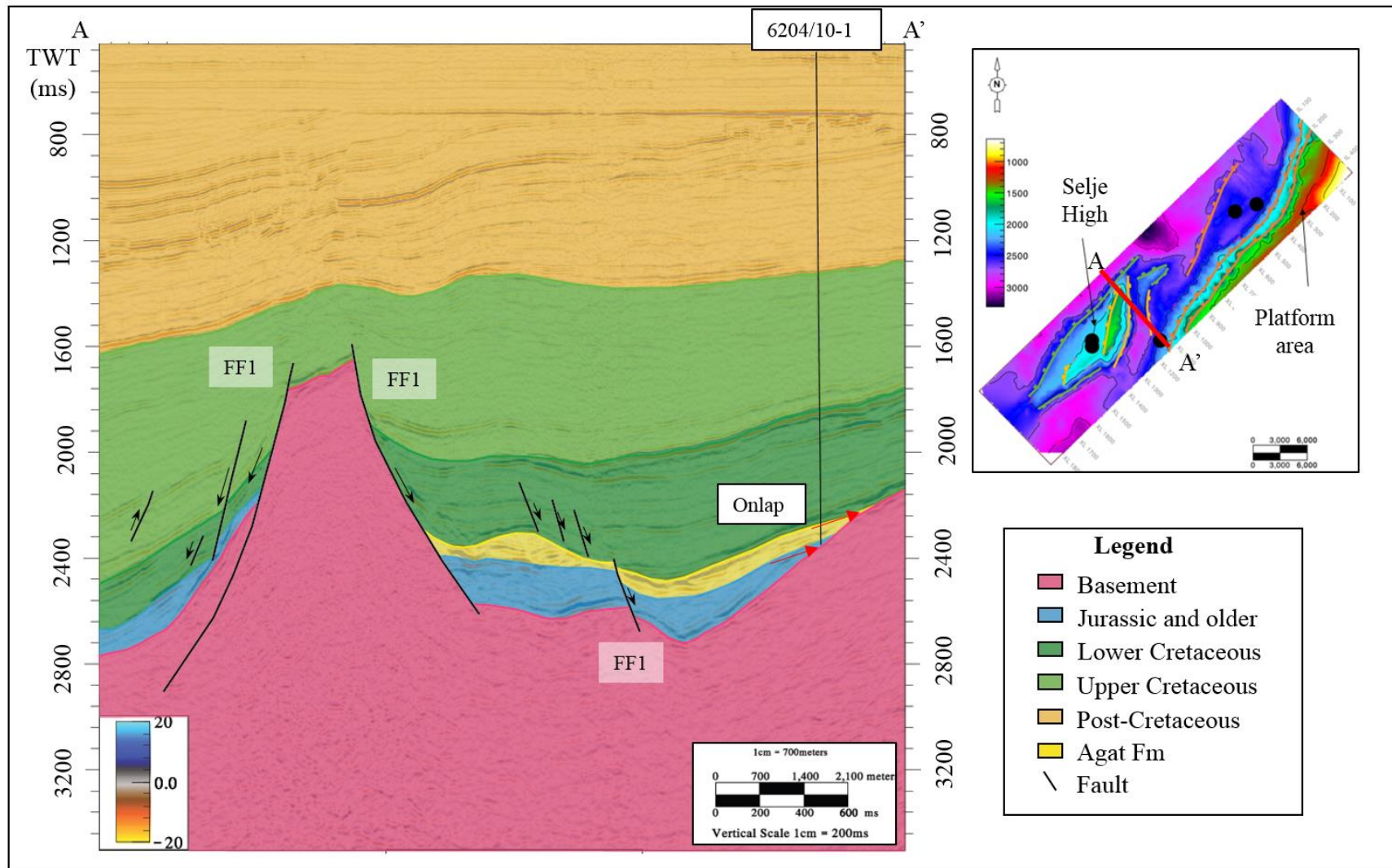


**Figure 17:** Seismic line displaying faults from fault family 1. Interpreted seismic line showing the Selje High and the main characteristics of fault family 1. Red arrows indicates lap relationships. Two major faults bounding the

### **Fault family 2 (FF2): NE-SW striking normal faults**

FF2 is the second fault family that contains faults affecting the basement. These are normal faults with a NE-SW strike located in the southern part of the study area in near proximity to the Selje High (Figure 15). The faults display a variation in the lateral extent and dip direction. Two of the faults are dipping in the N-W direction, while two faults are dipping in the S-E direction (Figure 18 and Figure 19). The major fault bounding the Selje High in the east has similar characteristics to the major fault in FF1, where both are large listric normal faults. However, the faults show different orientation in the strike and are therefore separated into different fault families.

The faults bounding the Selje High in FF2 show similar dragging of reflectors as observed for FF1 along the fault plane from Pre-Cretaceous to Upper Cretaceous. The most prominent dragging is seen in the Lower Cretaceous close to the BCU and in the Upper Cretaceous close to the top of the structural high. In addition, an incipient fold in the hanging wall of the east bounding fault is noted, as observed in FF1 (Figure 18 and Figure 19).

### ***Interpretation***

The dragging of the Lower Cretaceous reflectors along the fault plane can be evidence of active rifting during the deposition of the Cretaceous, or reactivation of the faults during later rifting phases in the Upper Cretaceous or Paleogene. However, this can be better explained by further investigation of the tectonic activity during the Upper Cretaceous and Paleogene, however, this interval has not been studied in this project. These major faults in FF2 bounding the Selje High are likely the cause of the uplift, as explained for FF1.

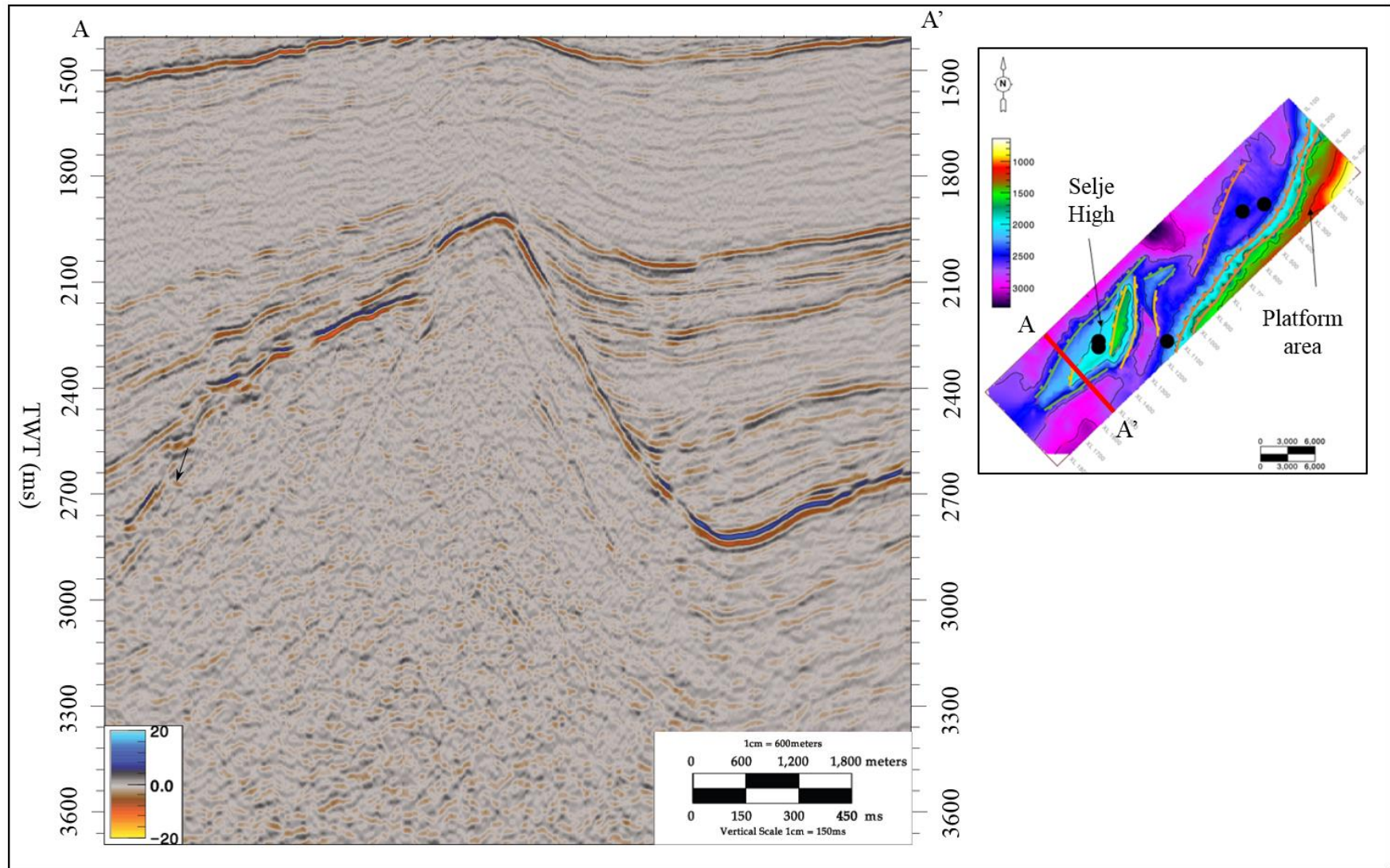


**Figure 18:** Seismic line displaying faults from fault family 2. Uninterpreted seismic line.

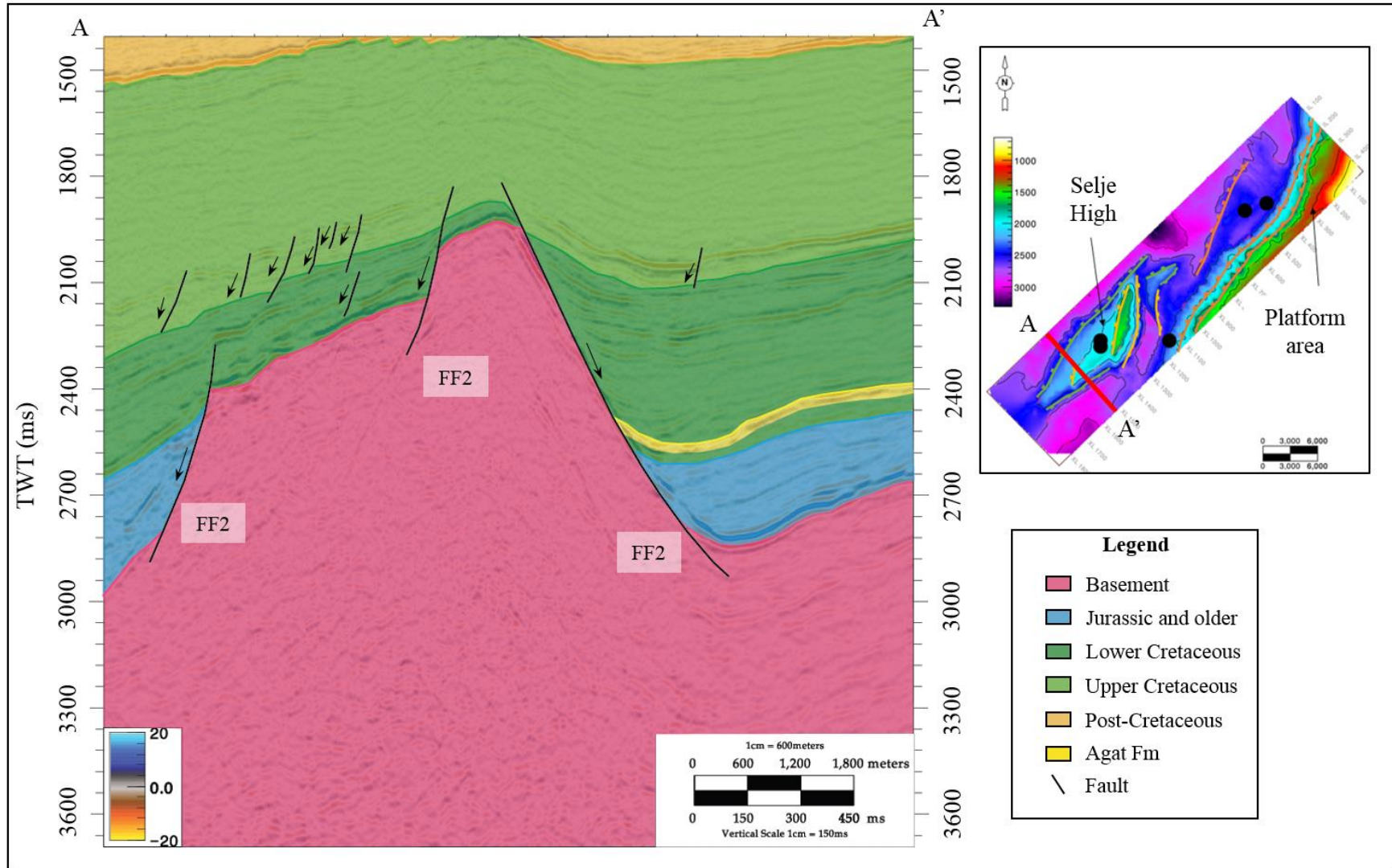


**Figure 19:** Seismic line displaying faults from fault family 2. Interpreted seismic line showing the Selje High and the main characteristics of fault family 2.

### **Fault family 3 (FF3): Normal faults striking NNE-SSW**

FF3 consists of two major faults and one smaller fault in the northern part of the study area (Figure 15). These three faults are bounding the two wells 6204/11-1 and 6204/11-2. The faults are striking in an NNE – SSW direction with dip direction towards the Slørebotn Sub-basin in the west. The major faults bounding the platform area have large throws and slightly listric appearance (Figure 20 and Figure 21). The smaller fault in the west show less throw, however, it has a listric appearance as the other faults in FF3. Two minor faults have been interpreted in Figure 20 and Figure 21 in between the two of the larger faults. These smaller faults also belong to FF3 and are affecting the basement and Jurassic section with termination in the BCU. The most western fault of the two major faults also terminates in the BCU, while the eastern major fault is ending at the top of Lower Cretaceous (Figure 20 and Figure 21). This fault family bear resemblance to FF2, however, as these are located further north and not bounding the Selje High, a separate fault family were suggested.

#### ***Interpretation***

The major faults in the east are marking the transition between the platform area and the Cretaceous basin of the Slørebotn Sub-basin (Figure 15). The large relief observed between the hanging wall and the footwall for the major faults is good indication of extensive rifting same as for FF1 and FF2.

#### ***Interpretation of faults affecting the basement***

These uplifted basement areas bear the potential of being source areas due to the high elevation and therefore the possibility of subaerial exposure, resulting in erosion of the basement and deposition down the fault plane. Moreover, these basement highs constitute as good barriers for sediments being sourced from other areas and will mark the boundary of the lateral extent of these formations. As all the fault families are affecting the basement until the Cretaceous, it is likely to believe that these faults have been subjected to several phases of reactivation. However, further investigation on strikes of older faults is needed to compare with the faults interpreted in this thesis.

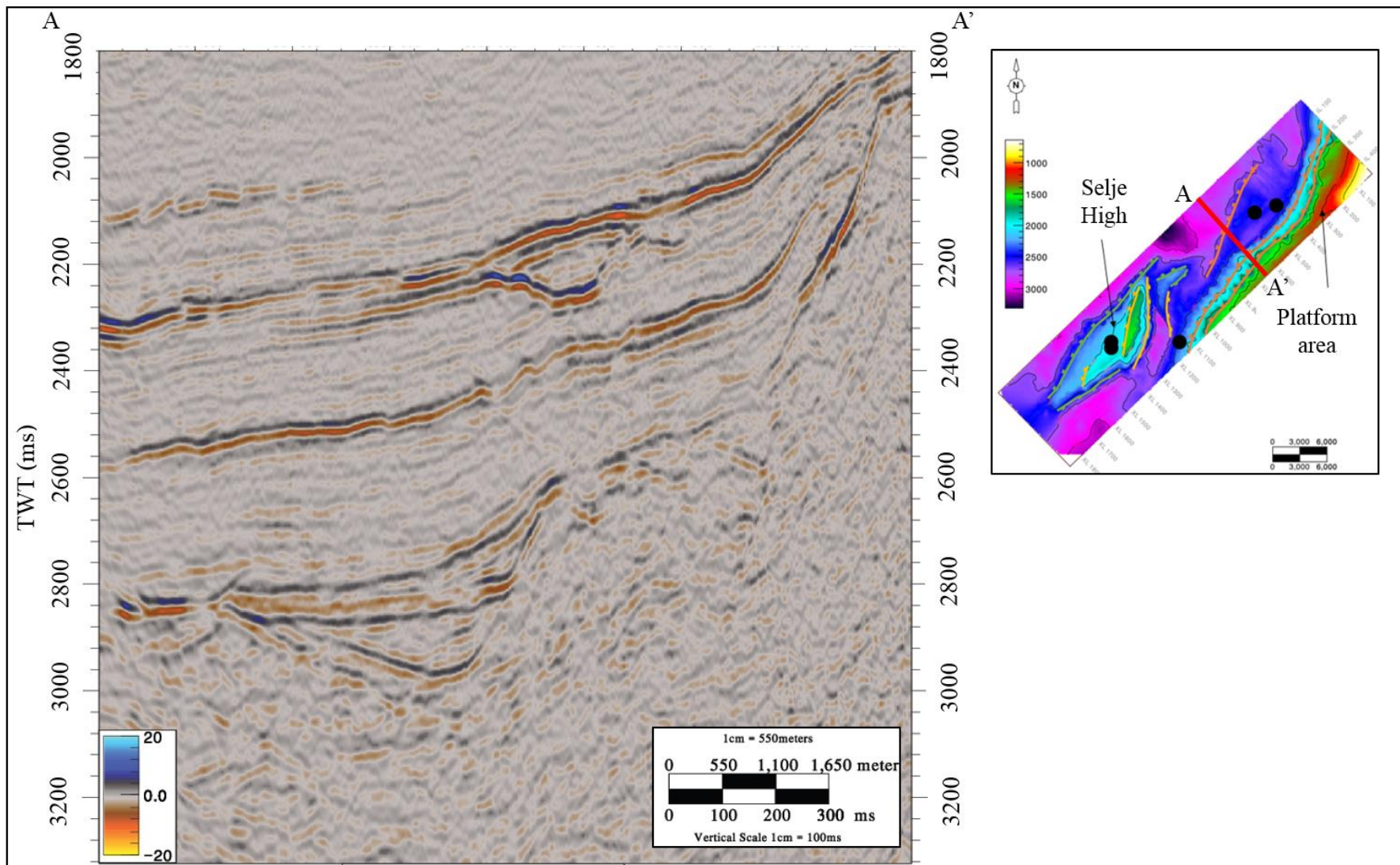


**Figure 20:** Seismic line displaying faults from fault family 3. Uninterpreted seismic line.

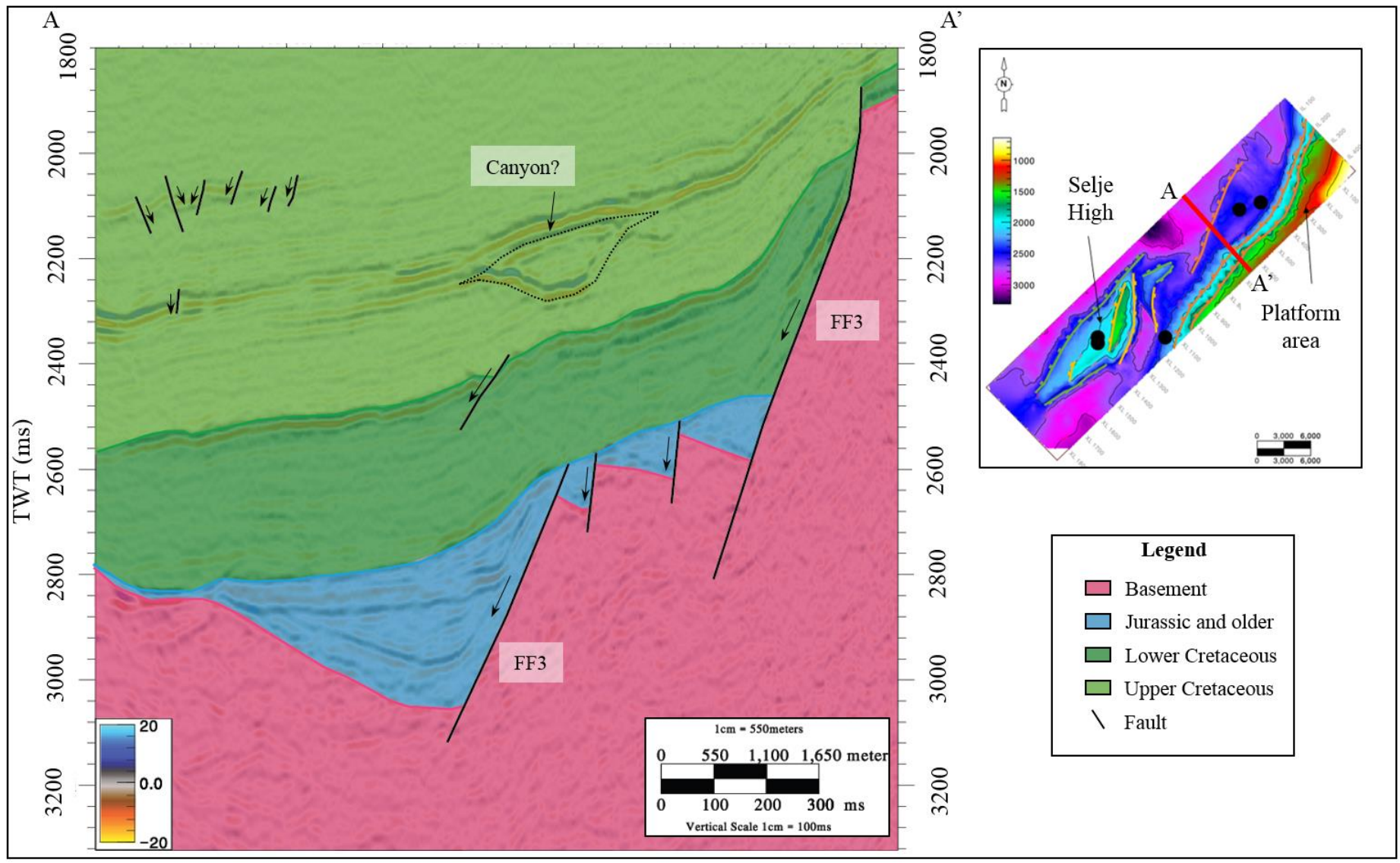


**Figure 21:** Seismic line displaying faults from fault family 3. Interpreted seismic line showing the faults in the north and the main characteristics of fault family 3.



### **4.2.1.2 Mapping of Basement**

#### *Observations*

The interpreted surface of the basement is displayed in Figure 22a, highlighting the changes in elevation throughout the study area. To the northeast, the depth of the basement is the least, with areas between 0-2000ms below the seabed. In this area, the depth increases abruptly moving towards the southwest where the two major faults of FF3 separates the higher areas from the lower areas. Moving further west, the depth continues to increase to 3000ms, however not as abruptly as in the eastern part.

In the southwest, a basement high is observed, which is called the Selje High. One can observe from the contour lines that the steepness of the basement block varies on the eastern and western flanks. On the western side towards the Sogn Graben and Slørebotn Sub-basin, the slope is gentle, while the eastern side closer to the platform area is considerably steeper. Several faults from FF1 and FF2 are bounding the Selje High. A small elevation bounded by two minor faults of FF2 in the basement is seen to the northeast of the Selje High.

In the northwestern area, the basement was difficult to interpret, however, the surface shows a relatively flat area, with deepening towards the west into the Slørebotn Sub-basin. It is worth mentioning that two of the wells in the south (6204/10-2A and 6204/10-2R) are drilled in a basement high.

An important observation on the basement surface (Figure 22) is the wavy contour lines along the basement highs, eastern steep platform area, and the western edge of the Selje High. The waves observed on the eastern side of the Selje High are different with a wider appearance, while the two other areas have shorter wavelengths.

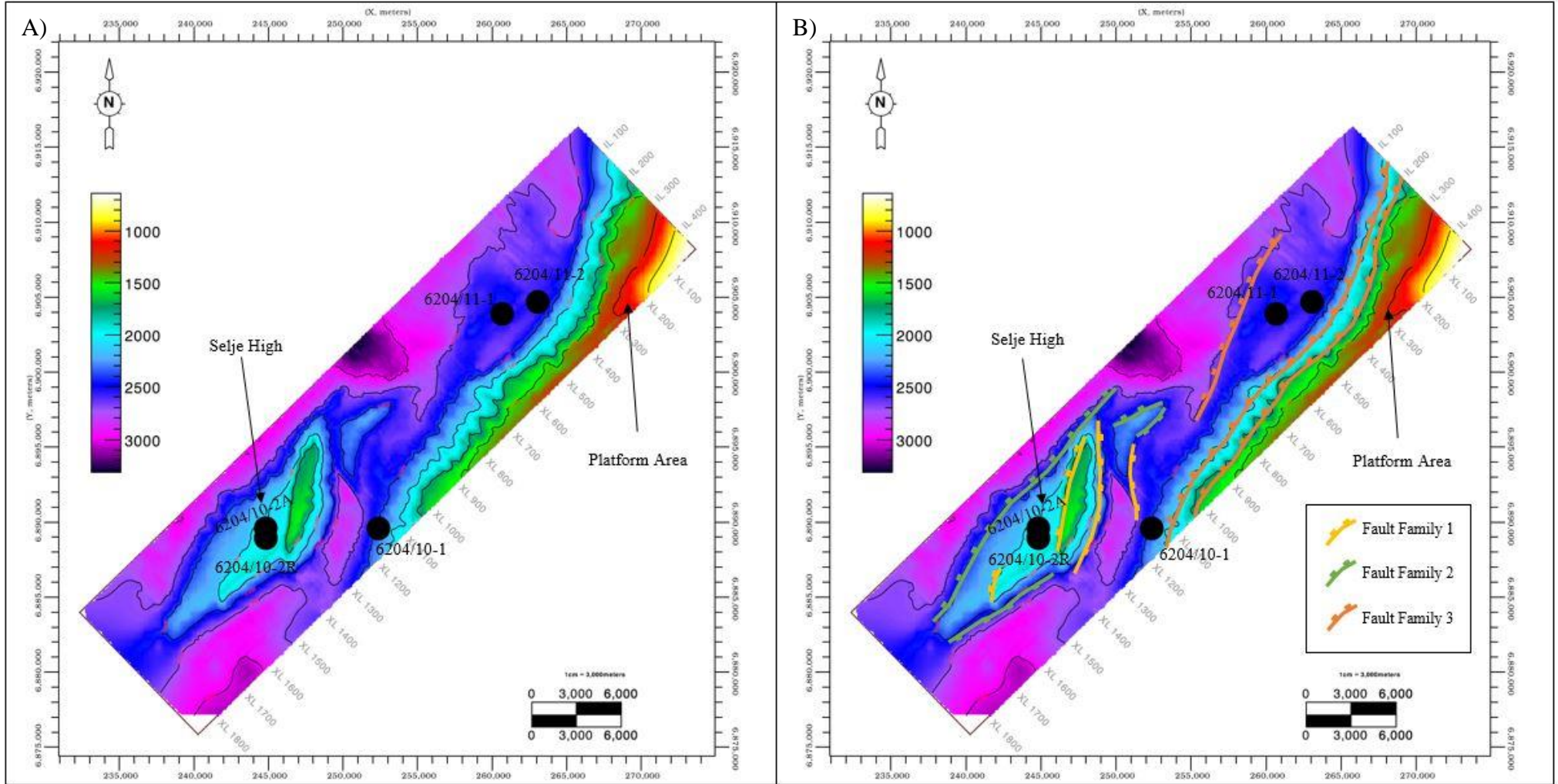


**Figure 22:** Basement map. a) Surface map of the basement in time (ms). b) Structural map of the basement in time (ms) with faults active during the period. Contour interval: 300ms. Elevated basement areas are marked as the Selje High and the Platform area.

### *Interpretation*

The higher elevated area in the northeast is located very close to the Norwegian mainland and resembles the edge of the shallow platform area. Moreover, the major drop in the elevation along with close contour lines indicates the two major faults interpreted that are displacing the basement down relative to the platform area.

The Selje High in the southwestern area is a basement high which was created due to uplift by fault movements as explained in the faulting. The faults interpreted on both sides show that this basement high is a horst. The western side of the Selje High being much gentler than the eastern indicates that the fault block might be tilted to the west with dip-direction into the Sogn Graben and Slørebotn Sub-basin. The tilting of the basement block is related to the extensional faulting of FF1 and FF2. Moreover, one can see from Figure 16, Figure 17, Figure 18, and Figure 19 that the faults on the eastern boundary of the Selje High have higher relief which might indicate higher fault activity and therefore explain the tilting of the Selje High.

Lastly, the waves along the basement highs and the fault planes might indicate erosion of the elevated basement, hence these waves are likely incisions into the basement which can be gullies, submarine canyons or slump scarps. However, these are only assumptions, therefore further investigation of the seismic and spectral decomposition might give better answers to these wavy contour lines.

### 4.2.1.3 Seismic character

#### *Observations*

In Figure 23 a seismic line intersecting along the major fault bounding the platform area highlights the wavy seismic character of the basement observed in the structural map. The incisions in the study area are observed along the higher basement areas. In Figure 23 and Figure 24, one can observe the vertical extent of the incisions. The incisions furthest north are higher up in the strata comparing to further south and affecting strata of younger age (Late Cretaceous to Paleocene). In addition, the reflectors of the younger strata are following the geometry of the incisions as the basement and the BCU. Further south, the incisions are lower in the strata, and only the BCU and the Basement is incising, while the remaining overlaying reflectors are infilling the incision with onlapping of the BCU (Figure 24).

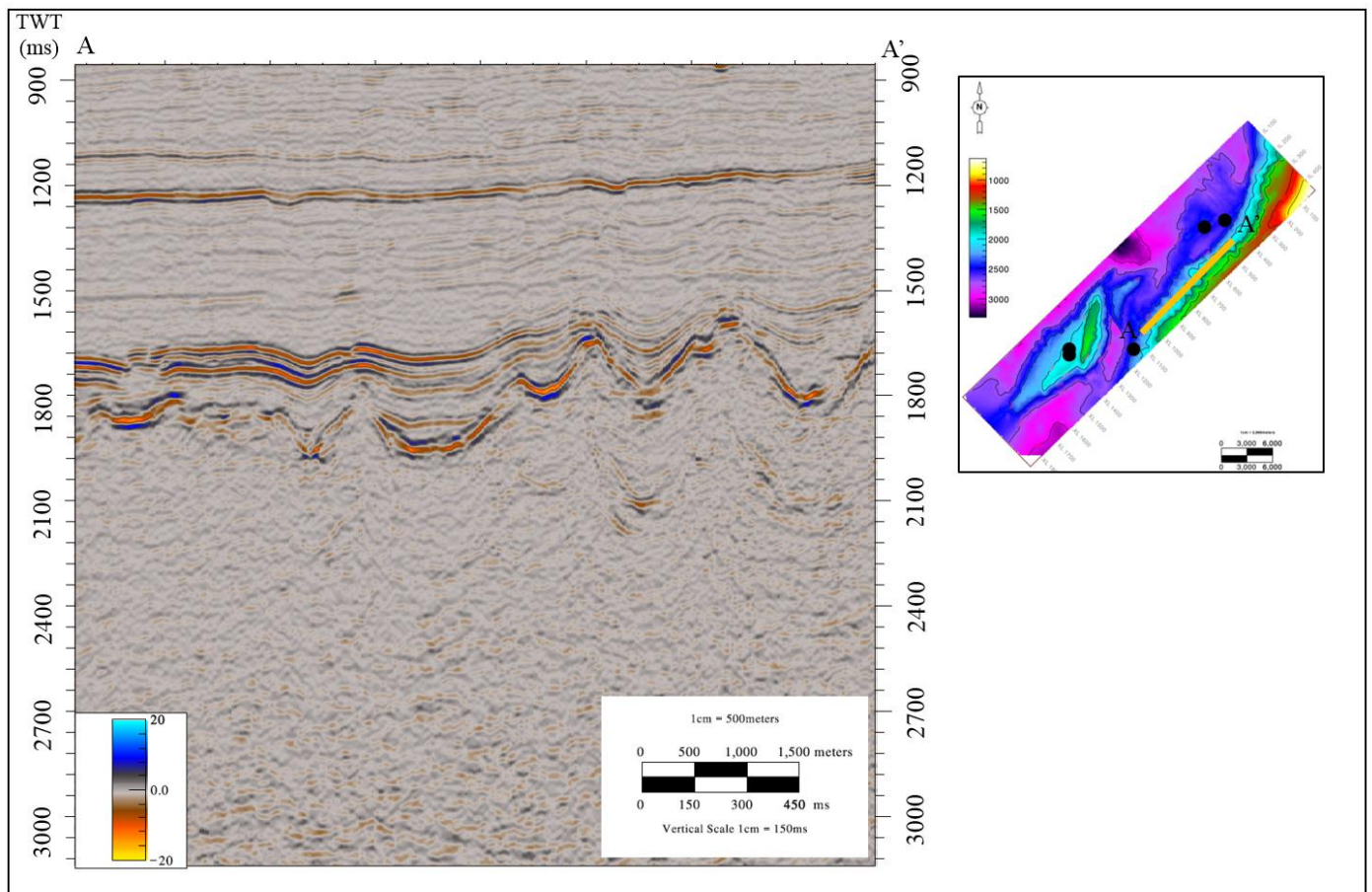


**Figure 23:** Seismic inline crossing along the platform area to highlight the basement incisions observed in the structural map. The seismic line is along the yellow line in the structural basement map. Uninterpreted section.

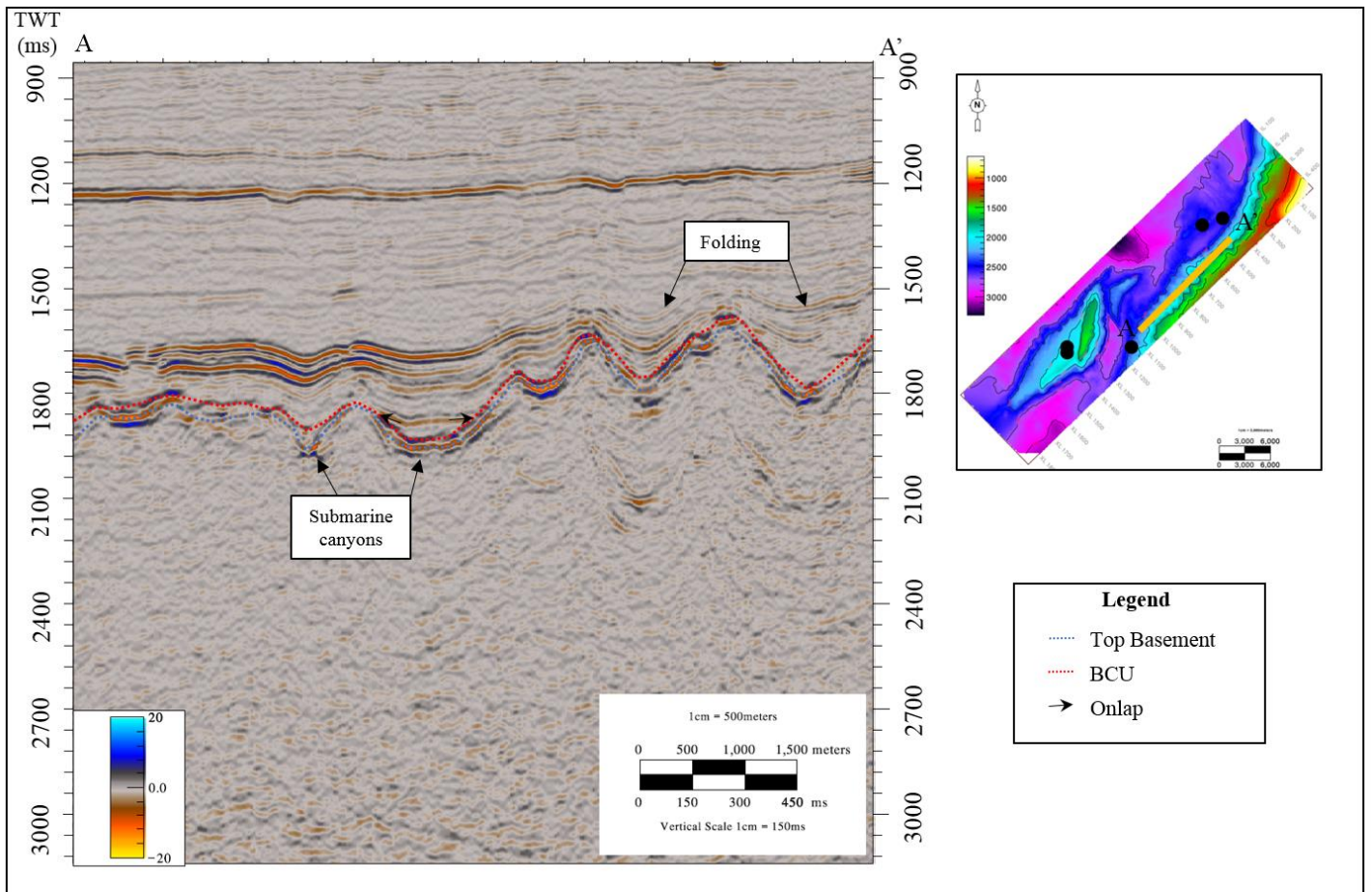


**Figure 24:** Seismic inline crossing along the platform area to highlight the basement incisions observed in the structural map. The seismic line is along the yellow line in the structural basement map. The top basement (blue) and BCU (red) are marked in the seismic line, along with onlap within the submarine canyons. Folding is also observed.

The clearest incision in marked in Figure 24, is approximately 1,5km in width and 500m in depth. However, the incisions even further south show a narrower appearance. The basement is clearly affected based on the wavy appearance in Figure 23 and Figure 24, along with the BCU which is situated directly over the basement and show similar wavy characteristics. These incisions are mainly observed along the elevated basement areas where the BCU lies directly above the Basement.

### *Interpretation*

The incisions observed in the seismic lines can be separated into two different types. The ones affecting the younger strata are likely caused by folding of the elevated areas and are not a stratigraphic result, but rather caused by compressional forces. The incisions further south, however, are stratigraphic features. These incisions have infilling of younger strata that onlaps on both sides of the incision. Thus, the incisions are interpreted as submarine canyons or gullies, which are often associated with active rifting. This due to the uplift and subaerial exposure resulting in erosional features along the elevated areas. As observed, the vertical extensions of the incisions thus imply which formations the erosion influenced, in this case, the basement and the BCU (Figure 23 and Figure 24). The association with the active rifting imply that the formation of the submarine canyons occurred during the Late Jurassic rifting, eroding away sediments deposited prior to Late Jurassic on the structural highs, resulting in deposition of Late Jurassic deep marine sediments in the structural lows. Sømme and Jackson (2013) suggested the same interpretation of these incisions in the same area, however, it was also suggested that there were several episodes of cutting and filling of the canyons, which occurred during later tectonic phases when exposed to erosion.

Lastly, it would be interesting to find these incisions in other parts of the study area, where the Jurassic succession still is present. However, in the seismic data used in this thesis, all the incisions detected are only in the structural highs.

#### **4.2.1.4 Spectral decomposition**

The initial purpose of doing the spectral decomposition was to investigate the Agat Formation with the aim of finding stratigraphic features giving implications on the depositional system and source area. However, the basement itself also proved to be important.

##### ***Observations***

In Figure 25 and Figure 26, spectral decomposition using constant bandwidth and high definition with an RGB color blend is presented. The top of the basement highs is evident by very clear light color, indicating an overlap of all the frequencies within the frequency band.

Along the northeastern boundary, the edge of the platform area, the elevation drops drastically, and some interesting features are observed along the slope. Along the fault plane of FF3, a series of light stripes are evident going all the way down the slope to where it flattens out (Figure 25, Figure 26, Figure 27 and Figure 28). These same stripes are observed along the western edge of the Selje High, along the gently dipping flank of the basement block. However, on the eastern steeper flank of the Selje High, the stripes are not evident.

In addition, a wavy character along the edge of the basement highs are evident for both the platform area (along FF3) and the western flank of Selje High (marked in Figure 25 and Figure 26). However, on the eastern flank of Selje High, these wave characteristics are less prominent and are wider and less carved into the high. A close up of the eastern edge of the Selje High is presented in Figure 29. It is also worth mentioning that these stripes and wave features at the top of the basement corresponds well with the incisions observed in the structural map and the seismic line (Figure 15 and Figure 24).

Lastly, Figure 30 shows several lines on top of the Selje High oriented in the same direction as FF1. One of these lines shows displacement along the plane, with a change of orientation towards the east. The other observed lines show little to no displacement. There are a few very small lines crossing perpendicular to the other lines.

### ***Interpretation***

The spectral decomposition highlighted the lineaments along the fault plane from the basement highs. These very evident white stripes going along the fault planes give implications of the basement being severely altered by erosion creating these incisions interpreted as gullies, submarine canyons and/or slump scarps. These canyons create a fairway for the sediments being deposited at a later time, resulting in deposition of clastic sediments in the deep marine basin. The incisions observed are related to basement highs, where the Jurassic succession is missing, which are good indicators of erosion or non-deposition of this interval. It is therefore likely to believe that these incisions in the basement were caused during the extensional period in Jurassic. Which has also been suggested by Sømme, Jackson, and Vaksdal (2013).

Furthermore, the two different wavy geometries observed on the gentle western edge and the steep eastern edge of the Selje High are indications of different mechanisms influencing the fault planes. The wider waves with no stripes along the fault plane are interpreted as affected by slumps creating slump scarps or mass failure. The basement highs with stripes and smaller and deeper wiggles are interpreted as submarine canyons depositing gravity flows such as submarine fans.

Lastly, the alignments of these lines across the top of the Selje High are likely minor faults with the same orientation as FF1 with little displacement. However, it is possible that these lines are fractures caused by the faulting and uplift of the Selje High due to the small lines crossing perpendicular along with the non-observed displacement for some of the lines.

The results from the spectral decomposition seem to correspond well with the results from the previous sections. Moreover, the basement lays the foundation for understanding the deposition of the Pre-Cretaceous sediments and the Agat Formation.



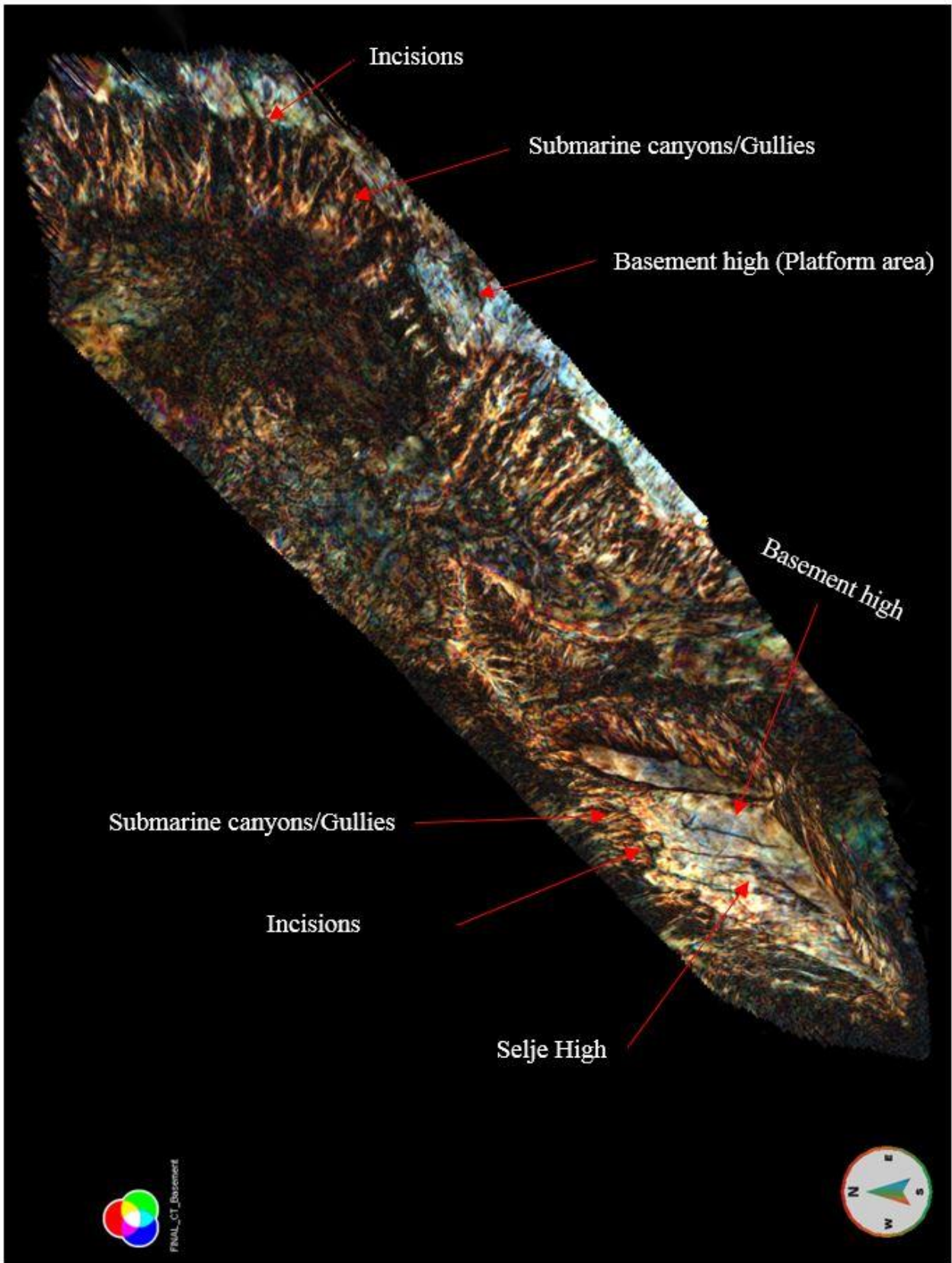


**Figure 25:** Basement horizon seen from above with constant bandwidth frequency decomposition in GeoTeric. The result of a frequency decomposition with an RGB color blend (17Hz - 24Hz - 31Hz) displayed on the basement surface. Submarine canyons/gullies, incisions and the elevated basement areas are marked.

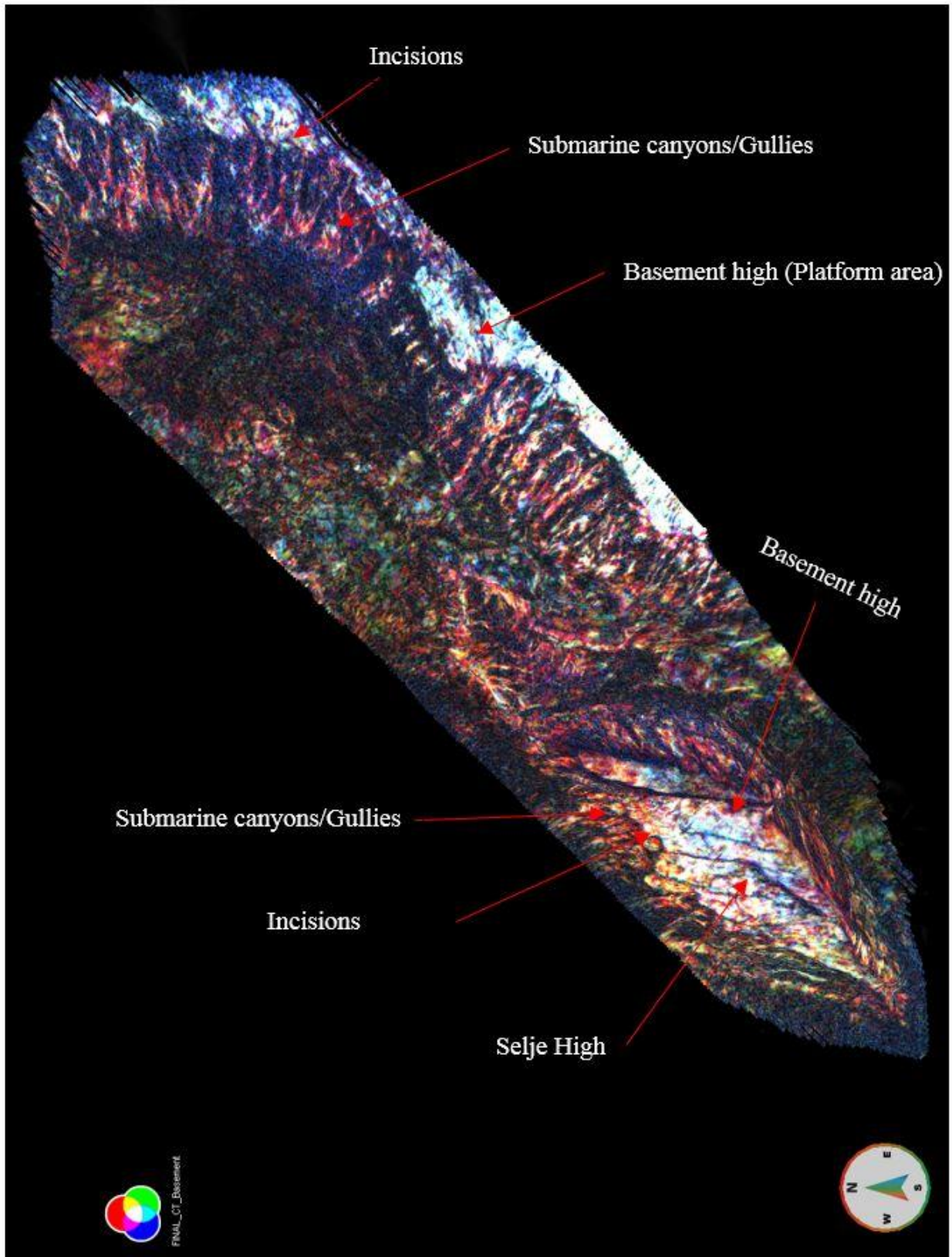


**Figure 26:** Basement horizon seen from above with constant high definition frequency decomposition in GeoTeric. The result of a frequency decomposition using with an RGB color blend (15Hz - 30Hz - 45Hz) displayed on the basement surface. Submarine canyons/gullies, incisions and the elevated basement areas are marked.

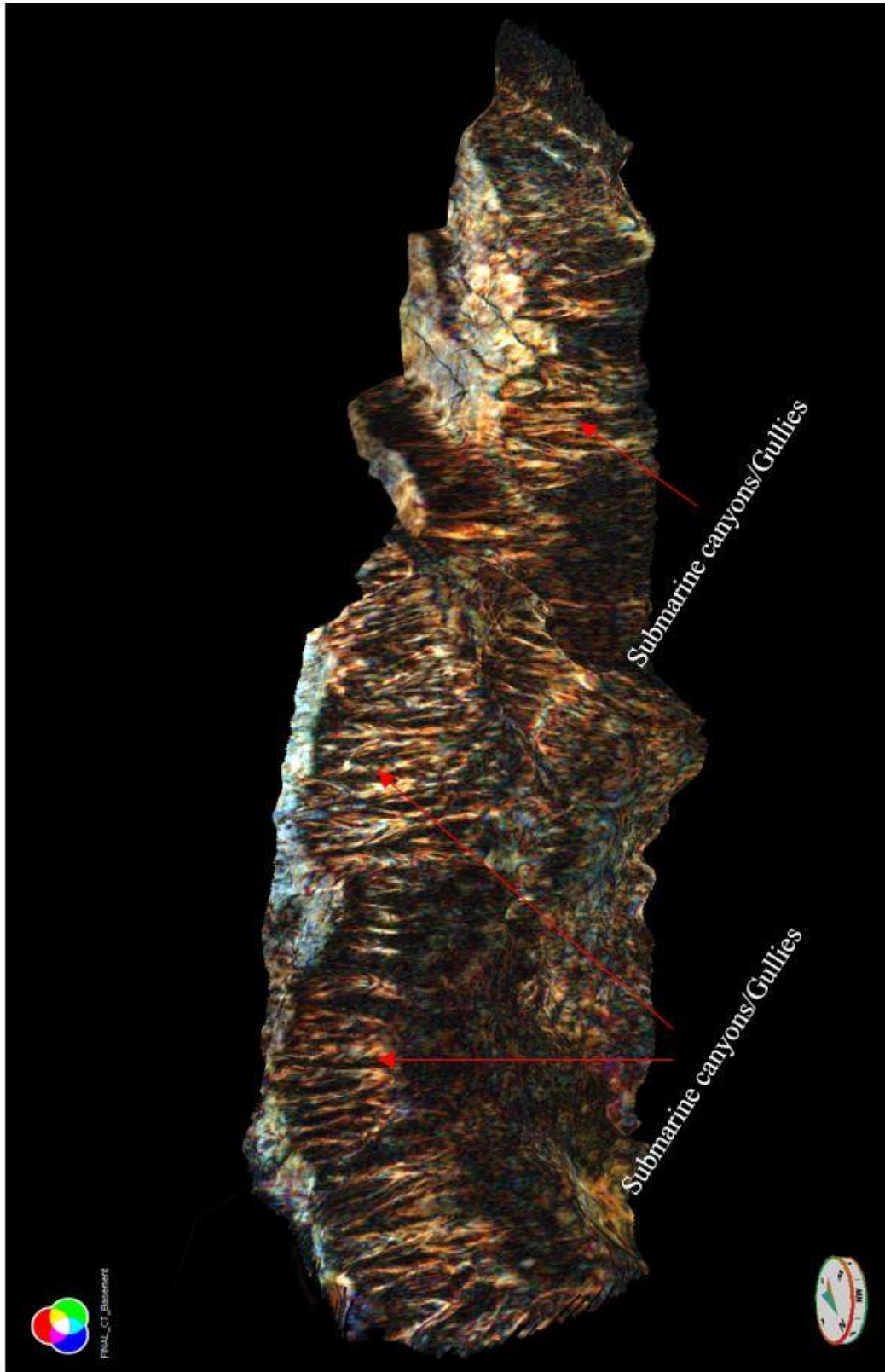


**Figure 27:** Basement horizon with constant bandwidth frequency decomposition in GeoTeric. The result of a frequency decomposition with an RGB color blend (17Hz - 24Hz - 31Hz) displayed on the basement surface and seen from the NW to highlight the submarine canyons along the fault plane of the platform area.

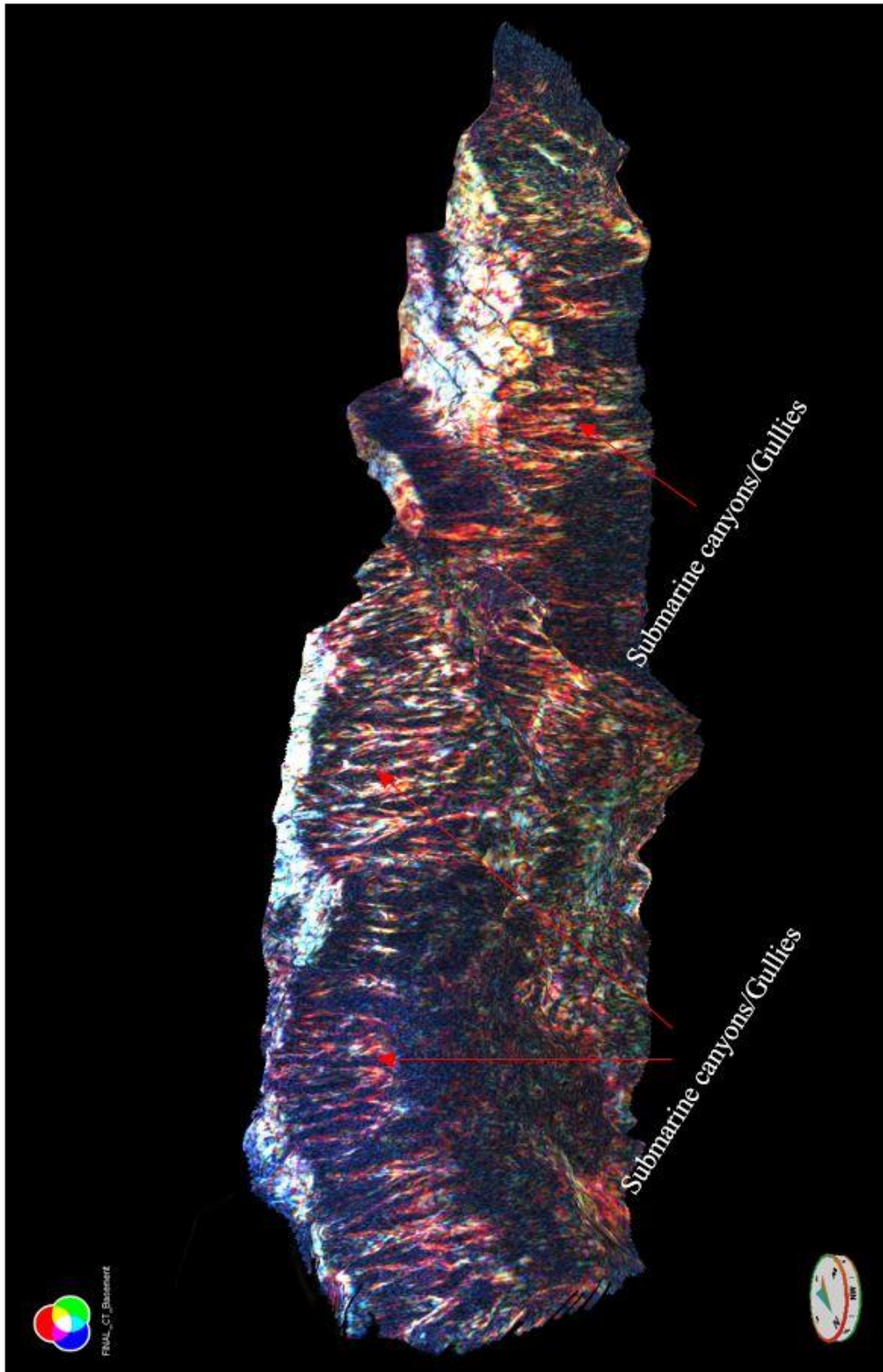


**Figure 28:** Basement horizon with HD frequency decomposition in GeoTeric. The result of a frequency decomposition with an RGB color blend (15Hz - 30Hz - 45Hz) displayed on the basement surface and seen from the NW to highlight the submarine canyons along the fault plane of the platform area.

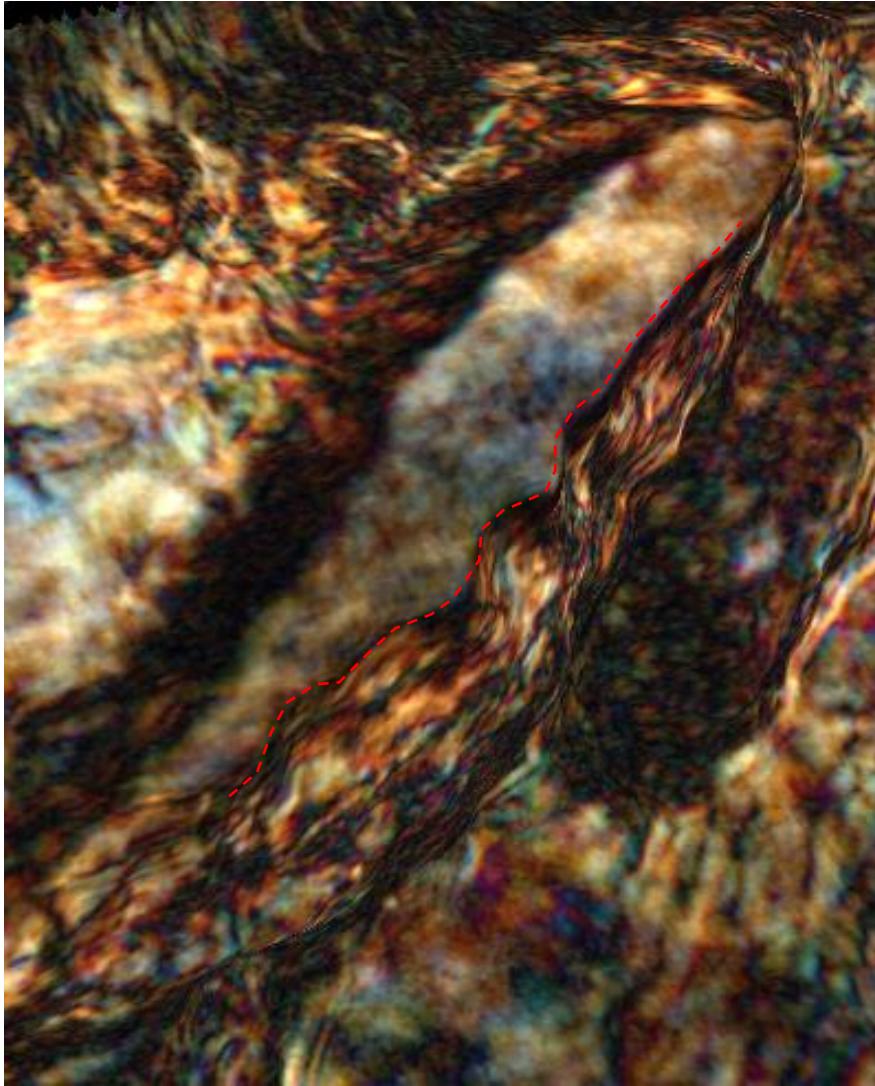


**Figure 29:** Close-up of the highest part of the Selje High, marking the possible slump scarps in the basement with a stippled red line.

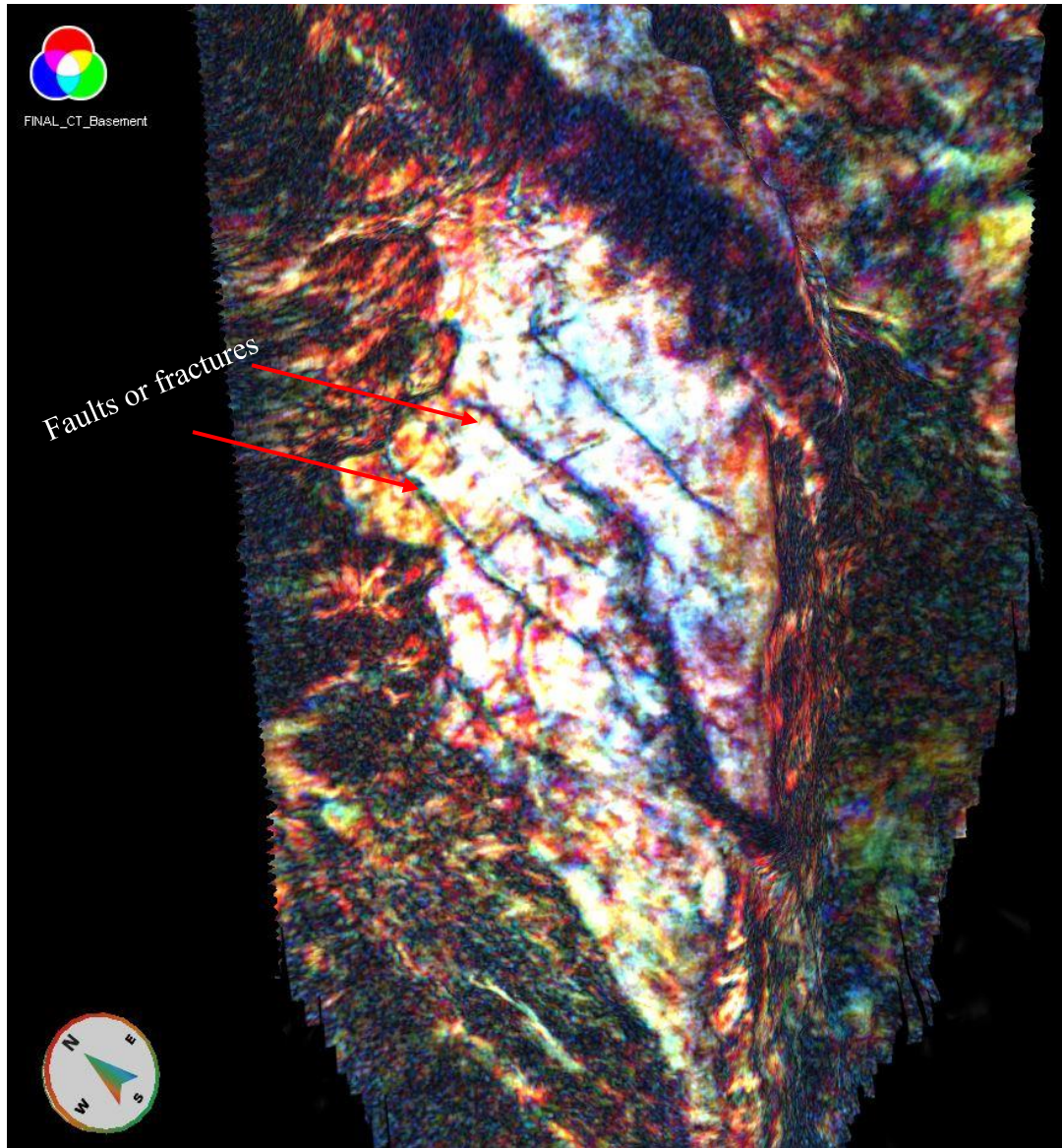


**Figure 30:** Close-up of the top of Selje High seen from above, highlighting the possible faults or fractures oriented N-S.

## 4.2.2 Pre-BCU

### 4.2.2.1 Faulting in Pre-BCU

#### *Observations*

The Pre-BCU succession is, as in the basement, affected by all the major faults in the study area. The Jurassic or older interval is thin comparing to the Cretaceous in the areas close to the Selje High and in relevance to the faults in FF1 and FF2 (Figure 16, Figure 17, Figure 18, and Figure 19). Thickness variations across faults are evident in FF1 as thickness increases in the hanging wall towards the fault plane for the east-dipping faults, which is clear growth strata. However, the west-dipping fault is thinning towards the fault plane in the hanging wall and is thickening towards the Sogn Graben and Slørebotn Sub-basin (Figure 16 and Figure 17). The Jurassic succession is missing in the footwall for both the east and west-dipping faults in FF1.

Moreover, the western major fault in FF2 shows similar thickness variations, with thickening in the hanging wall towards the Sogn Graben in the west (Figure 18 and Figure 19). The second fault in FF2 dipping to the west has no Jurassic or older sediments neither in the footwall or the hanging wall (Figure 18 and Figure 19). Furthermore, the major fault bounding the Selje High dipping east have a continuous succession of Jurassic or older in the hanging wall, with only minor evidence of dragging of the reflectors close to the fault plane (Figure 18 and Figure 19). However, the interval is likely thinning towards the east as seen further north in the study area. Thus, the interval is thickening towards the major fault of the Selje High. The Jurassic or older succession is missing in the footwall of this major east-dipping fault.

Additionally, the FF3 shows large variations in thickness towards the fault plane. Figure 20 and Figure 21, shows several faults dipping west, with the Jurassic or older succession having growth strata towards the fault in the hanging wall. Especially the major platform fault shows a large displacement resulting in extensive growth strata. The figures displaying seismic used to mark fault families highlights several areas with Pre-BCU growth strata in the study area (Figure 16, Figure 17, Figure 18, Figure 19, Figure 20, and Figure 21).

FF1 in Figure 16 and Figure 17 also shows a clear onlap of the Jurassic or older succession on the basement in the hanging wall of the major east-dipping fault. This is likely to occur for the

east-dipping fault in FF2 as well, however, the edge of the hanging wall is not presented within the study area.

Lastly, no rocks of Jurassic age or older are observed in the elevated basement areas.

### ***Interpretation***

All the major faults show variations in thickness across faults with hanging wall growth strata, which is good indications that the Jurassic or older succession was deposited during active rifting. Likely are these rifts reactivated in later periods, as the reflectors of the Jurassic or older succession are slightly dragged up along the fault plane in the hanging wall. However, the main period of rifting is in the Jurassic.

In addition, the onlaps observed in FF1 in the hanging wall along with growth strata are indications of active rifting as well as rotation of the fault blocks. Hence, the accommodation space towards the fault plane increased mainly due to the tectonic subsidence and eustatic sea level rise along the footwall block in Late Jurassic. Moreover, the Jurassic succession absent in the basement highs, is a further indication of rotation and active rifting during this period.



#### 4.2.2.2 Mapping of BCU

##### *Observations*

The BCU marks the boundary between the Cretaceous and the underlying formation. In the study area, the BCU marks the change from Cretaceous to Jurassic in wells 6204/11-1 and 6204/11-2, while in wells 6204/10-1 and 6204/10-2R the unconformity marks the boundary between Cretaceous and the Basement.

Figure 31 shows the time structural map of the BCU for the entire seismic 3D-cube with and without faults affecting the BCU. By observing the time structural map, one can see clear similarities with the time structural map of the Basement. The Selje High is still a prominent structural feature in the southwestern part of the study area, and the contour lines on the western side have larger spacing in between than on the eastern side, which is also observed on the Basement surface (Figure 22).

Looking closer at the map, some differences compared to the basement are evident. The two wells 6204/11-1 and 6204/11-2 are located approximately at the same depth (time) in the Basement map; however, in the BCU map, there is a clearer difference in elevation between the two wells. Well 6204/11-1 is situated at a small high or area with a higher elevation compared to surrounding areas. Lastly, a look at the contour lines around the major faults in the east and the Selje High to compare the wavy geometries from the Basement. The two major faults of FF3 in the northeast also show these waves as seen in the Basement, however, the contour lines around the Selje High looks more smooth compared to the Basement surface, especially on the eastern side (Figure 31).

In addition, a time thickness map between the BCU and the Basement is displayed in Figure 32. The map shows small variations in thickness at the basement highs due to some uncertainty when interpreting the basement. In the basement highs, the BCU lies directly above the basement and no thickness should be observed. However, the areas in the structural lows in close relation to the elevated basement highs show greater thickness varying from 200-400ms, especially on the eastern side of Selje High (Figure 32). Moreover, a thicker sequence is also observed around the two wells in the northern part (wells 6204/11-1 and 6204/11-2). A general increase in thickness is seen towards the Sogn Graben and Slørebotn Sub-basin in the west, however, the difficult mapping in this area can be seen as variations in thickness in the northwest.

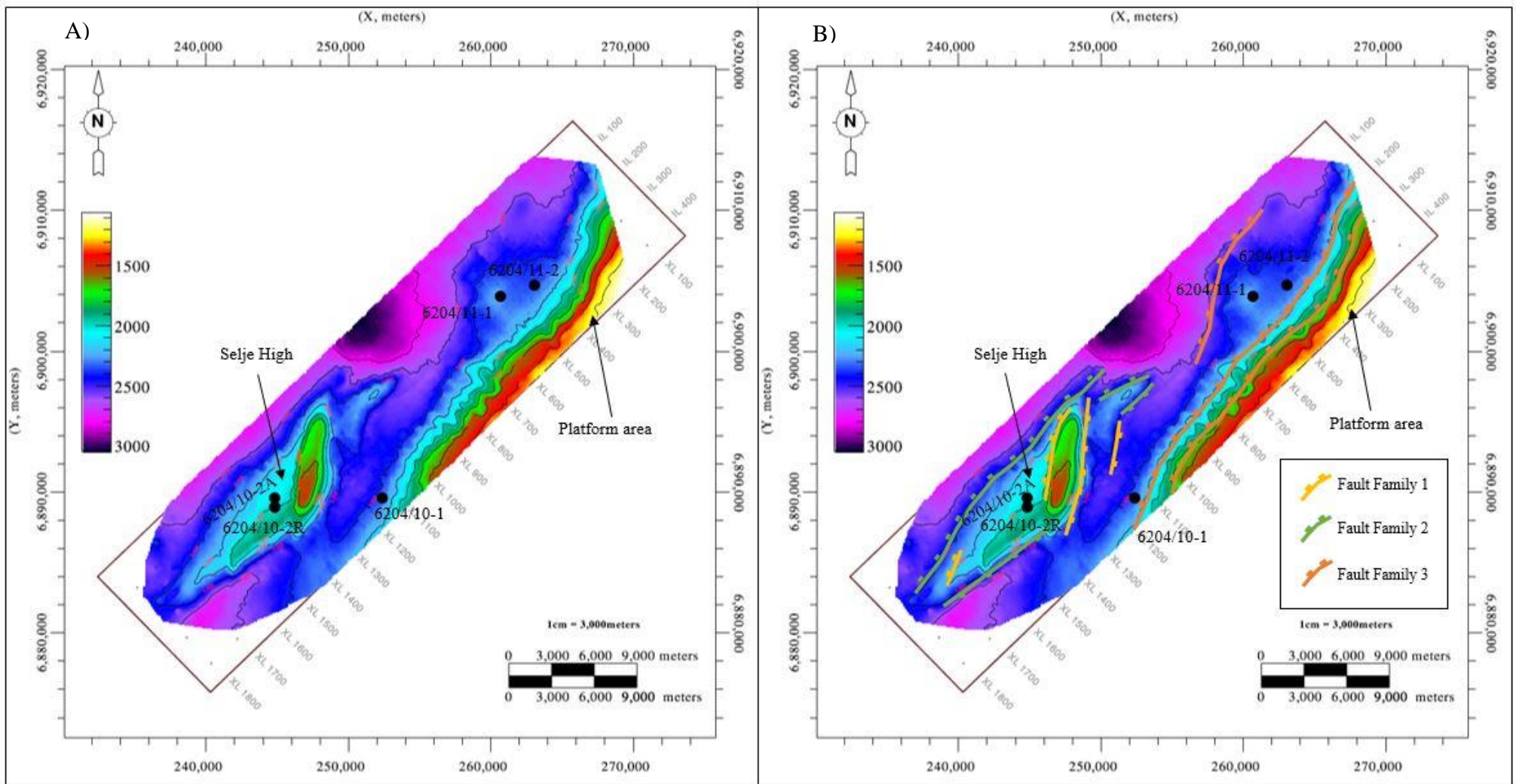


**Figure 31:** Maps of the Base Cretaceous Unconformity (BCU). A) Surface map of the BCU in time (ms) B) Structural map of the BCU in time (ms) with faults active during the period. Contour interval: 200ms. Elevated basement areas are marked as the Selje High and the Platform area.

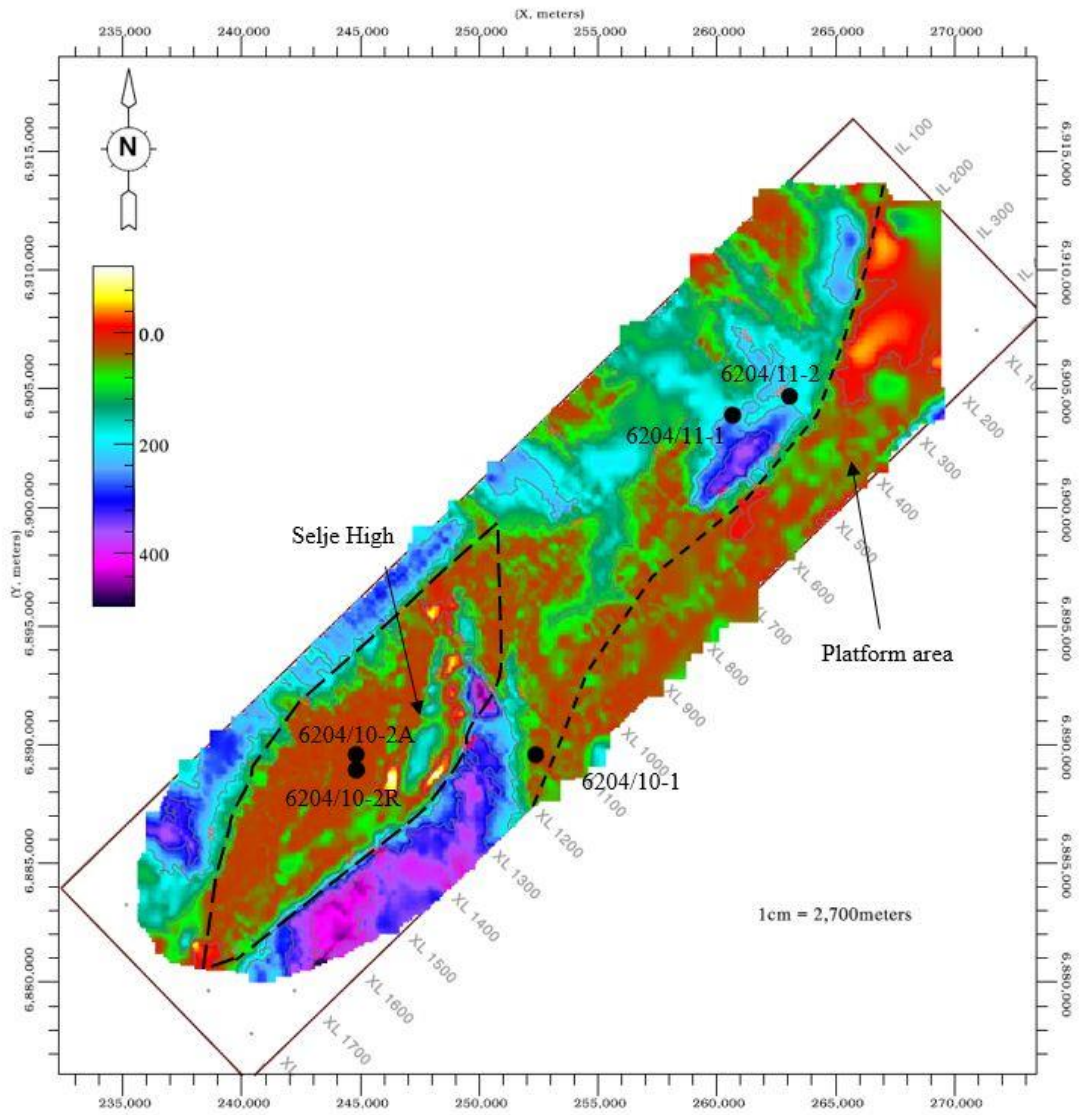


**Figure 32:** Time thickness map between the BCU and the Basement with thickness in time (ms). The elevated basement areas have lowest thickness (red) and the structural lows have varying thickness of 100-400 ms.

### ***Interpretation***

The BCU structural map showing similar features around the Selje High with a steeper flank in the east and a gentler flank in the west indicates as in the basement, that the Selje High was tilted during the Late Jurassic.

The differences in elevation between wells 6204/11-1 and 6204/11-2 might indicate a minor fault or minor anticlinal shape. However, this needs further investigation in the 3D seismic. Moreover, the wavy geometries observed in the basement are now absent around the Selje High, indicating that the submarine canyons or gullies created in the Basement are not present in the BCU for the Selje High, however, the incisions are still evident along the platform area and are likely affecting the BCU there.

Lastly, the time thickness map shows areas with increased thickness related to the hanging wall of faults, which give implications of growth strata towards the fault plane in the hanging wall. This should be confirmed by looking at the seismic, however, growth strata are a good indication of the interval being tectonically active during the Late Jurassic. In addition to the lack of Jurassic thickness on the basement highs.

### 4.2.2.3 Seismic character

#### *Observations*

The main stratigraphic features observed in the Pre-BCU succession are wedges. These wedges in the stratigraphic interval are found in the hanging wall of the main faults. Figure 20 and Figure 21 illustrating FF3 shows a good example of several Pre-BCU wedges. The wedges represent growth strata towards the fault plane, as the thickness of the stratigraphic layer increases towards the fault.

Several Pre-BCU wedges are marked in the figures below; Wedge 1 (Figure 33), Wedge 2 (Figure 34), Wedge 3 (Figure 35), Wedge 4 (Figure 36) and Wedge 5 (Figure 37). Since the wedges are covering the entire study area, the seismic characters are varying some.

Wedge 1 shows varying amplitude strength with some strong and some weak dipping prograding reflectors which are downlapping on the basement (Figure 33).

Wedge 2 has very low amplitude reflectors that are chaotic to wavy with downlap on the underlying Basement (Figure 34).

Wedge 3 can be separated into two minor wedges, where the one to the left has weaker chaotic reflectors, while the wedge to the right shows a combination of strong amplitude reflectors and weak (Figure 35). In addition, the right wedge contains more continuous sub-parallel dipping reflectors in the lower section and more chaotic in the upper section.

Wedge 4 is similar to Wedge 3, however, this wedge contains more weak amplitude reflectors that are chaotic in the middle of the wedge and is onlapping the basement in the hanging wall (Figure 36).

The last wedge, Wedge 5 observed in the south of the study area contains two wedges on each side of the Selje High (Figure 37). These contain weak amplitude reflectors that are sub-parallel to wavy with varying dip. The wedge in the west is truncating at the fault, while the one in the east is likely onlapping the basement in the east. In addition to seismic lines, a map showing the outline of the wedges is displayed in Figure 38. The thickness map (Figure 32) can be used to make some inferences about where you can expect to find growth strata and wedges, however, it must always be confirmed by seismic. Naturally, all the wedges are located in the hanging walls of the major faults in the study area, which corresponds well with the thickest areas in the thickness map.

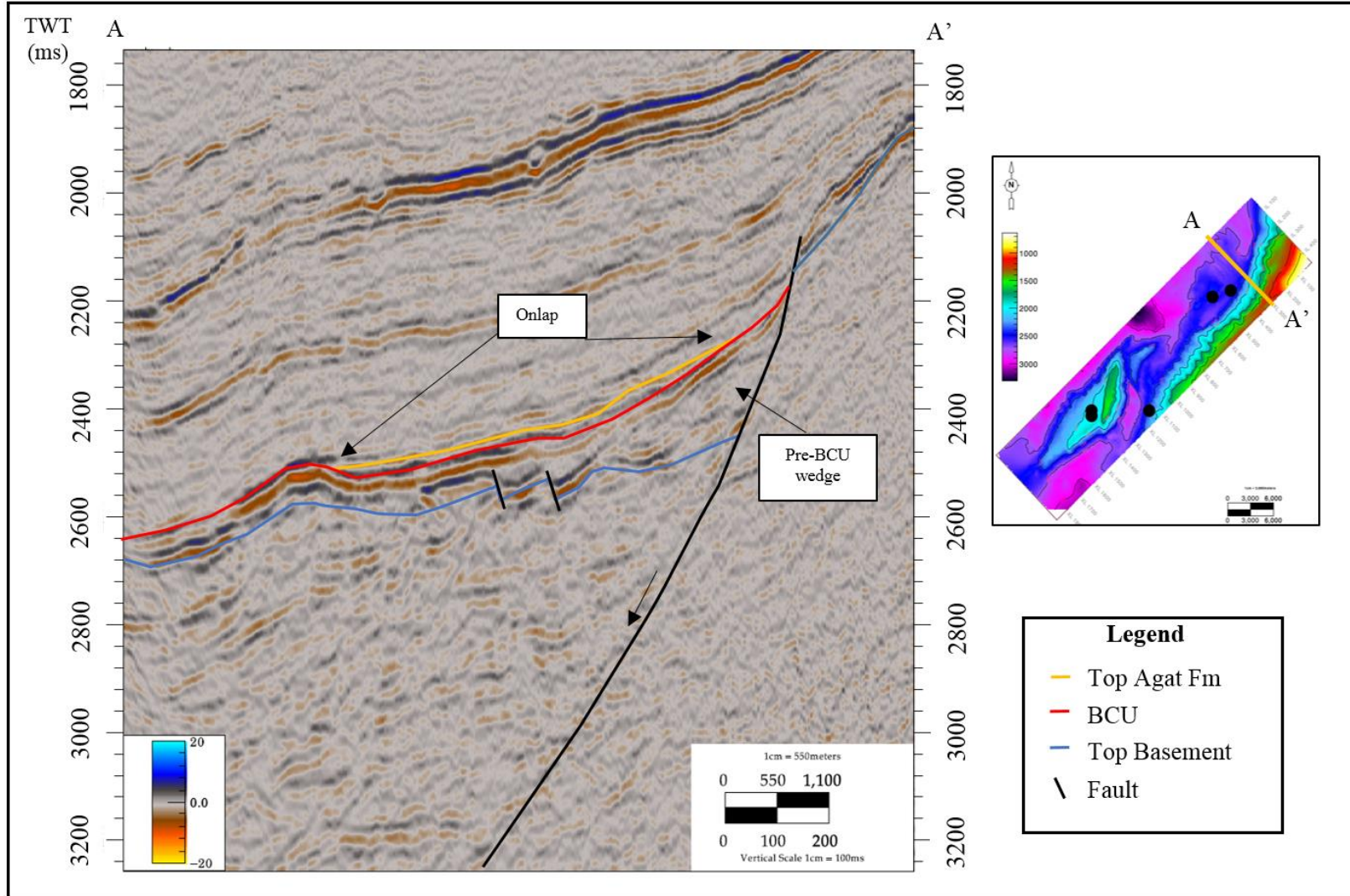


**Figure 33:** Seismic XL 300 highlighting the Pre-BCU wedges and the Agat Formation. Onlaps are marked for the Agat Formation. Seismic line going from A to A' as marked in the structural map.

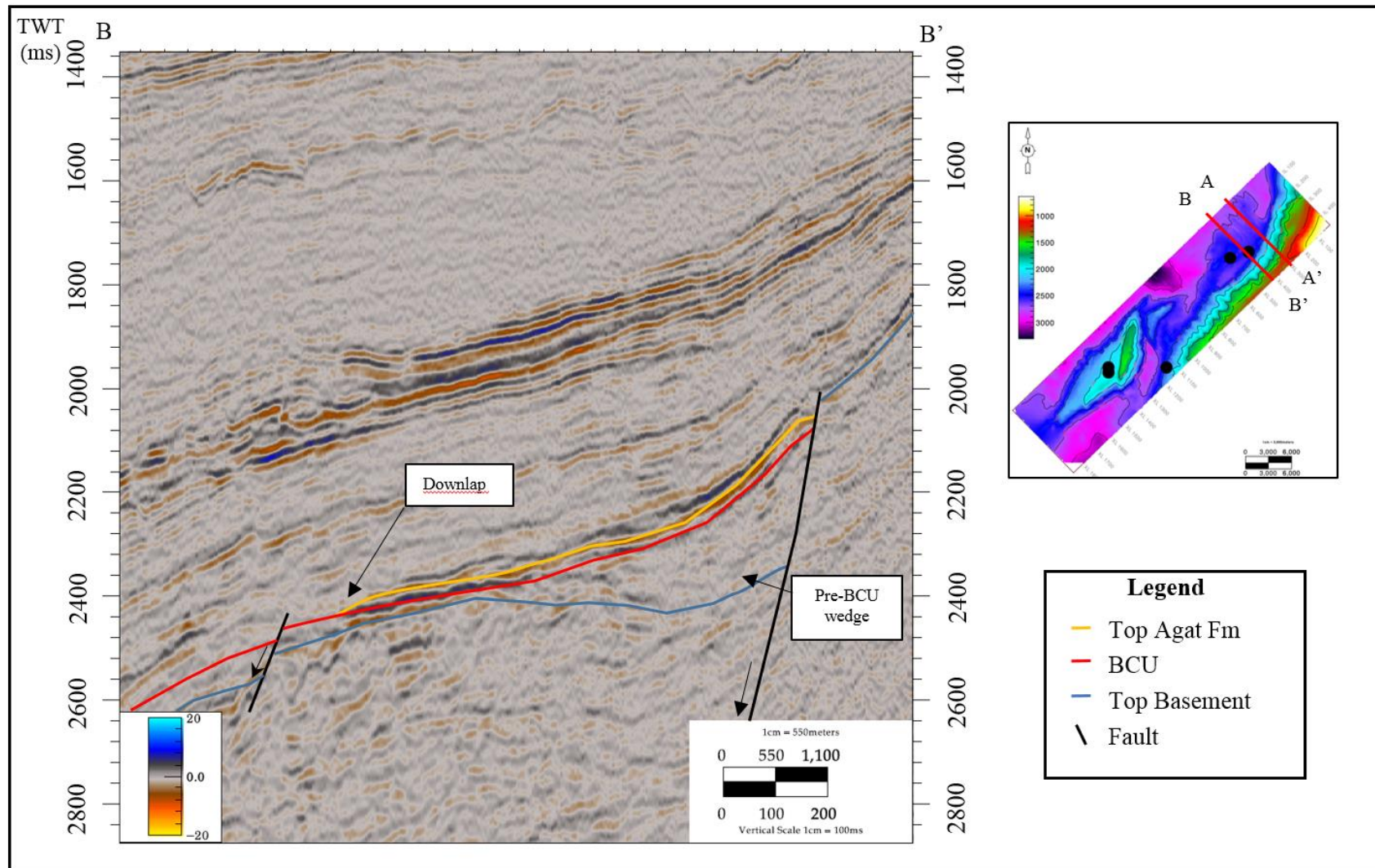


**Figure 34:** Seismic XL 404 highlighting the Pre-BCU wedges and the Agat Formation. Downlap is observed of the Agat Formation on the BCU. Seismic line going from B to B' as marked in the structural map.

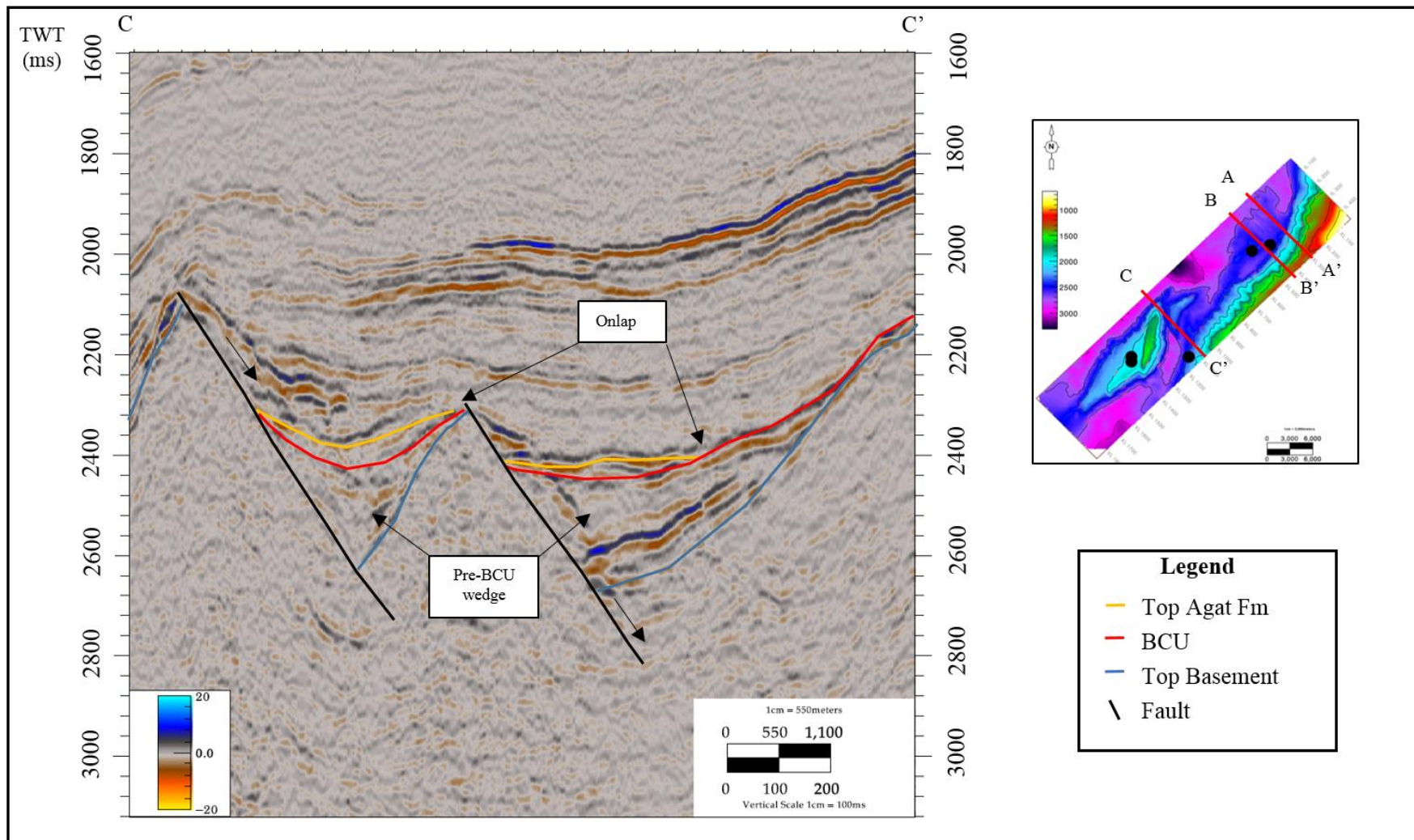


**Figure 35:** Seismic XL 1073 highlighting the Pre-BCU wedges and the Agat Formation. Two wedges are defined in this seismic line. Onlap in the hanging wall is observed for the Agat Formation in both wedges. Seismic line going from C to C' as marked in the structural map.



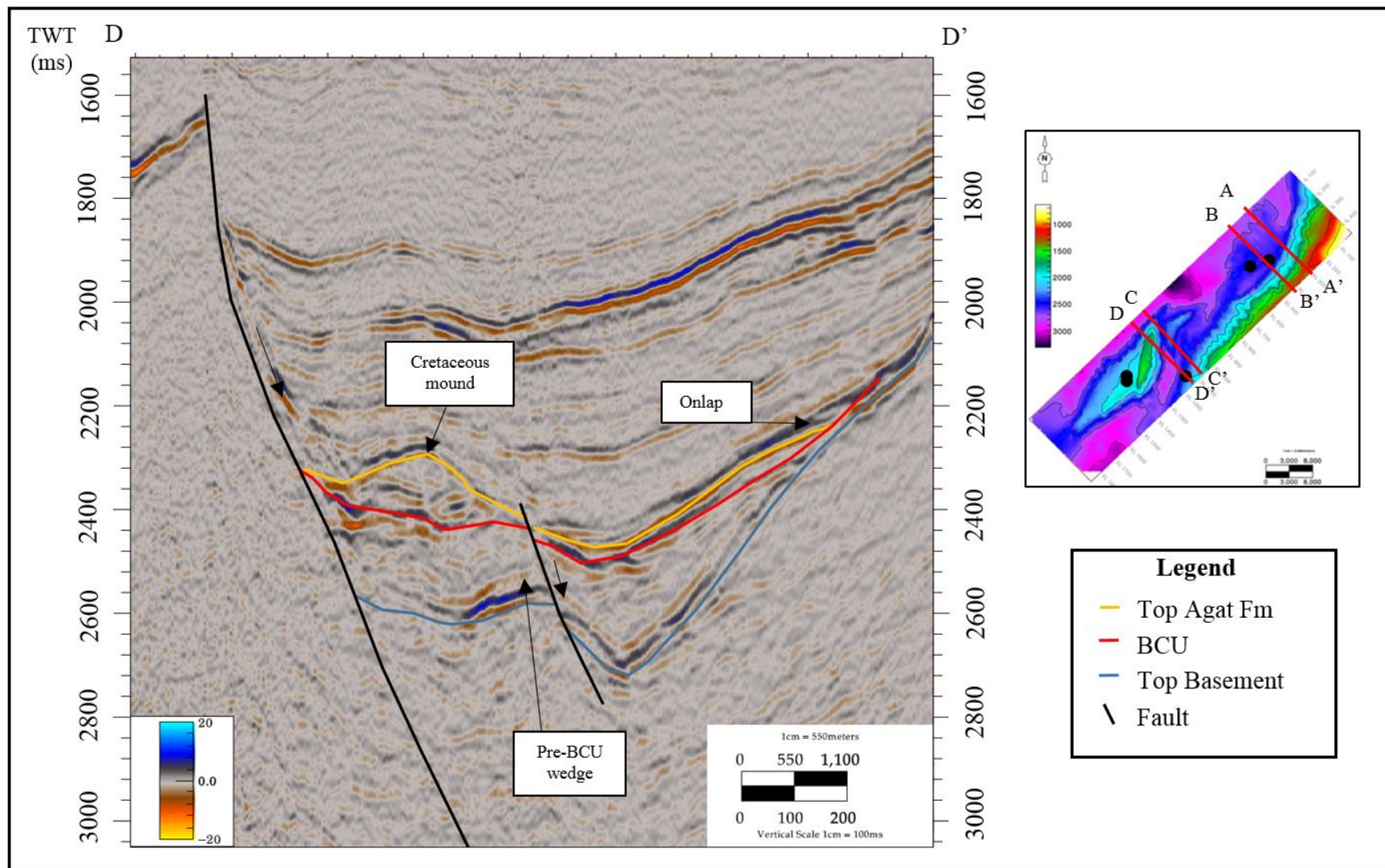


**Figure 36:** Seismic XL 1125 highlighting the Pre-BCU wedges and the Agat Formation. The same two wedges as observed in Figure 36 have now merged to one large wedge with a minor fault in between. Onlap in the hanging wall is observed for the Agat Formation on both sides of the minor fault. Seismic line going from D to D' as marked in the structural map

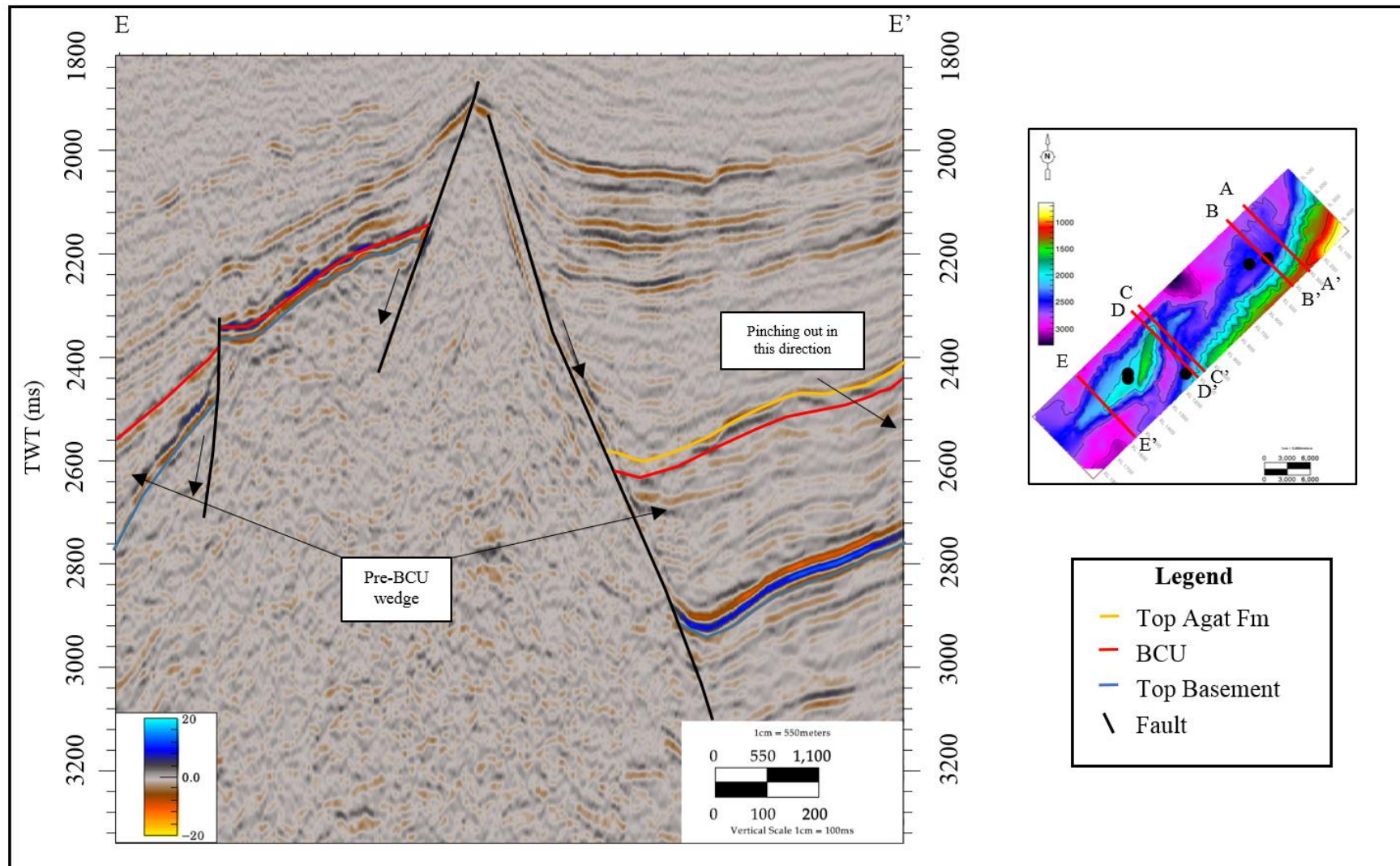


**Figure 37:** Seismic XL 1550 highlighting the Pre-BCU wedges and the Agat Formation. The entire wedge is not observed in seismic, however, the Pre-BCU succession is likely pinching out in the east. A Pre-BCU wedge is also observed on the west of Selje High thickening towards the Sogn-Graben. Seismic line going from E to E' as marked in the structural map

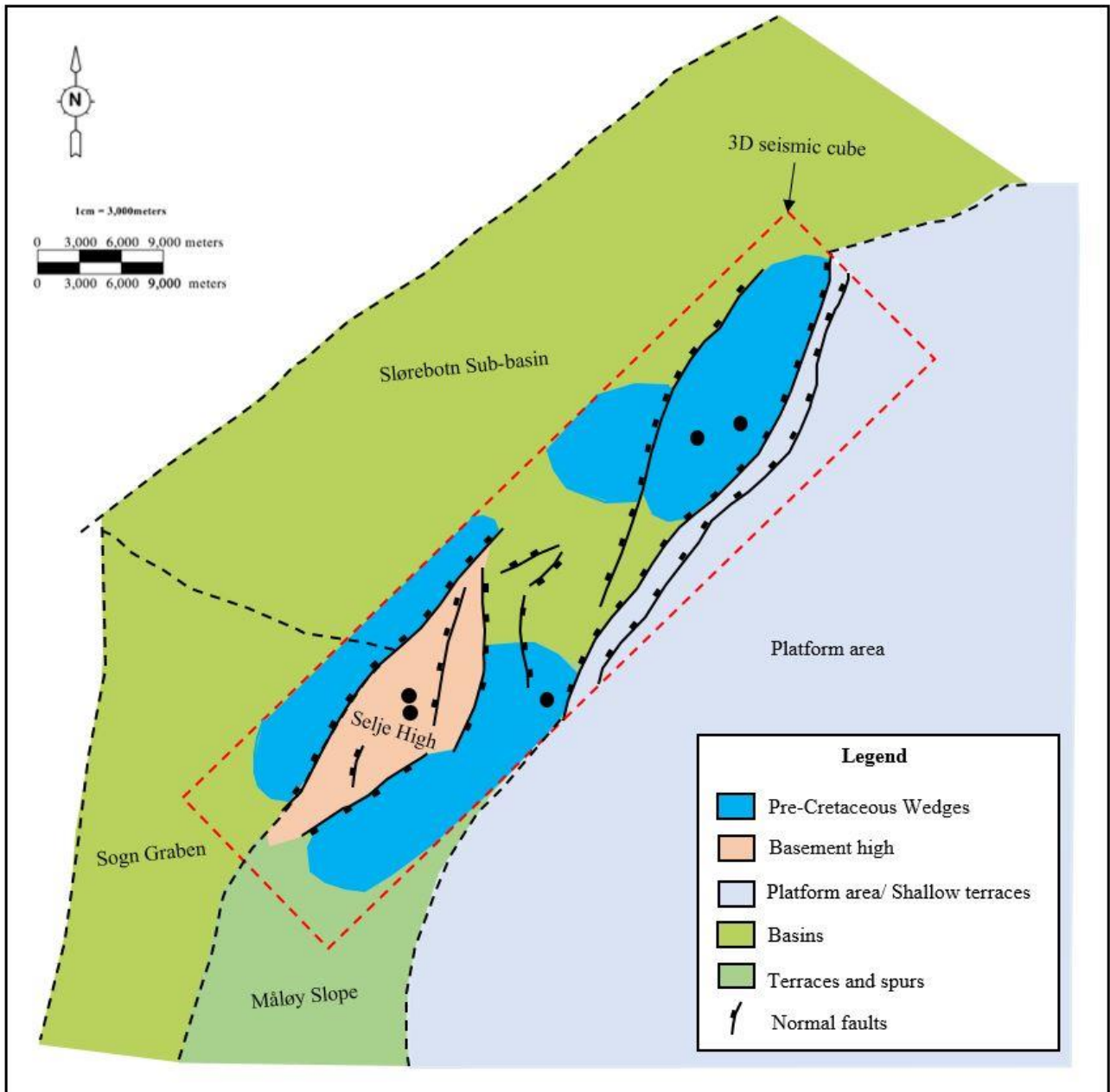


**Figure 38:** A map with the structural elements highlighting the location of the Pre-Cretaceous wedges in the area. As explained above. These are located in relation to the faults.

### *Interpretation*

The wedges are found in the hanging walls of the faults across the entire study area and are good indications of fault activity during the Jurassic. Moreover, as the wedges are found in the entire study area it is likely that the active rifting was a major event and not a local incident. In addition, the fact that the wedges are dipping towards the fault plane in the hanging wall with some of them having onlaps on the edge of the hanging wall might infer that the faulting period was affected by the rotation of fault blocks as mentioned in the previous section and discussed in Jongepier and Rui (1996).

Additionally, the wedges do not only give important information about the timing of the faults in relevance to syn-rift deposits, but it also gives implications of the source area of the sedimentation. Thus, the wedges can help predict whether the sediments are sourced from the Selje High or from the platform area. The thickest part of the wedge located against the Selje High in the southeast, therefore, implies that the sediments are mainly deposited from the footwall in Selje High, with an influx from the tilted hanging wall in the platform area, while the wedges in the north are deposited from the footwall in the platform areas.

Lastly, the internal configuration of the wedges might give some indications on the deposition. Several of the wedges contain chaotic reflectors which might indicate mass transport deposits and the sub-parallel stronger reflections might be shale layers in between the mass transport.

### **4.2.3 Agat Formation**

The Agat Formation has only been observed in two of the wells in the study area, well 6204/10-1 and 6204/11-2. These are situated in different parts of the study area; however, they are both drilled along the base of the slope of the major faults defined in the basement and Pre-BCU sequences.

#### **4.2.3.1 Faulting**

##### *Observations*

Figure 20 and Figure 21 shows a seismic line along the major fault in the east from FF3. This fault show a Lower Cretaceous section which is overall continuous in thickness in the hanging wall, but significantly thinner in the footwall. The reflectors of the Lower Cretaceous interval are dragged up along the fault plane of the major fault in FF3.

Furthermore, the Lower Cretaceous interval close to FF1 has the same characteristics as FF3, with the succession appearing uniform in thickness in the hanging wall of the major east-dipping fault. However, the thickness for the same succession in the hanging wall of the west-dipping fault is much thinner, and it shows a small increase in thickness towards the Slørebotn Sub-basin in the northwest. Additionally, the Lower Cretaceous succession is not present at the top of the Selje High. Moreover, dragging of reflectors along the fault plane of the major faults is observed (Figure 16, Figure 17, Figure 18, and Figure 19).

The minor east-dipping fault in FF1 shows a uniform thickness in the Lower Cretaceous succession from well 6204/10-1 and down to the minor fault (Figure 16 and Figure 17) but shows thickness variation across the fault. The Agat Formation has a thicker succession between the major and the minor east-dipping faults, resulting in a mound shape of the deposits (Figure 16 and Figure 17), which was described previously. It is important to highlight that the interpretation of reflectors close to the faults is uncertain, and therefore interpretations can vary.

Lastly, the onlap of the Agat Formation on the basement is observed in the hanging wall for FF1 to the east for Selje High (Figure 16 and Figure 17) and is likely occurring also for FF2 to the east of Selje High. Furthermore, the Åsgard Fm was present partially at the Selje High, however, it is not present below the Agat Fm in well 6204/10-1 and it is not at the highest point of Selje High, which is important to highlight (Figure 14, Figure 16, and Figure 17).

### ***Interpretation***

The Agat Formation shows thickness variation due to the mound observed in Figure 16 and Figure 17, which can either be interpreted as a reverse reactivation of faults or erosional deposits as a slump from the elevated basement high. Thickness variations across faults are typically an expression for tectonic activity, and large differences in thickness are observed for the Lower Cretaceous succession.

The onlap surface in the hanging wall of the major Selje High bounding fault of FF1 can be interpreted as both evidence for active faulting and rotation, however, it may also indicate that this formation is immediate post-rift deposits infilling the rift bathymetry. The upward dragging of the reflectors close to the fault plane can be used as evidence for explaining the reactivation of the faults during a later rifting phase, which could also explain the lack of Åsgard Formation in well 6204/10-1.

#### **4.2.3.2 Mapping of Agat Formation**

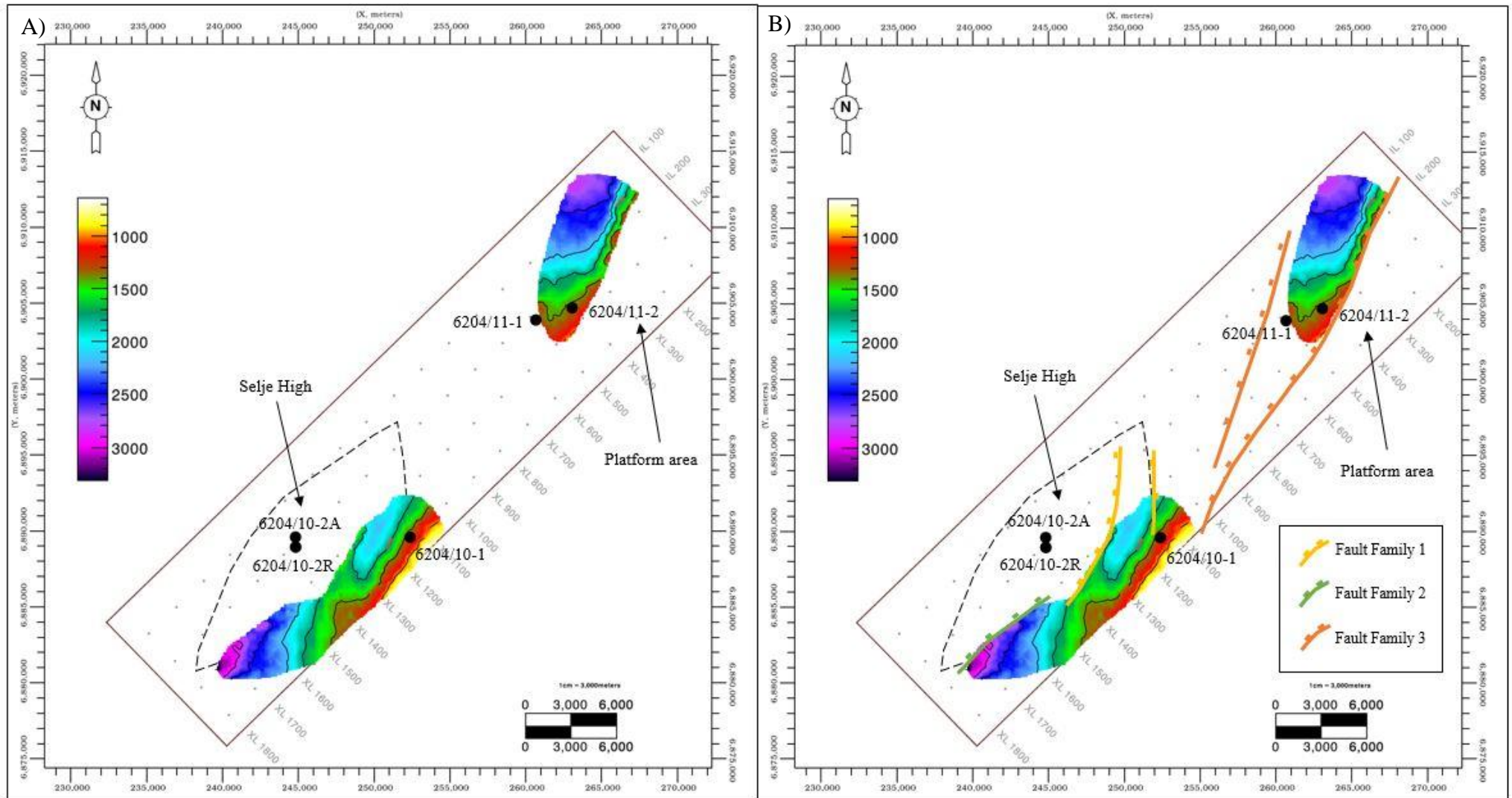
Since the Agat Formation is only present in two of the six wells (6204/10-1 and 6204/11-2), the seismic tie to the wells is restricted to the areas surrounding these two wells. Hence, the seismic interpretation and mapping of the formation are limited in the areas far away from the wells in addition to the areas located behind structural highs.

##### ***Observations***

Figure 39a presents the structural map of the Agat formation and defines its lateral extent based on seismic interpretation. In the southeast, the Selje High constitutes the maximum lateral extent of the Agat Formation to the northwest. The formation is not present at the top of Selje High, however, whether the Agat Formation is present on the western side of the high would be open for discussion, but in this study, the Agat Formation is not interpreted to the west. This could be due to the Agat Formation having a thickness below the seismic resolution in this area.

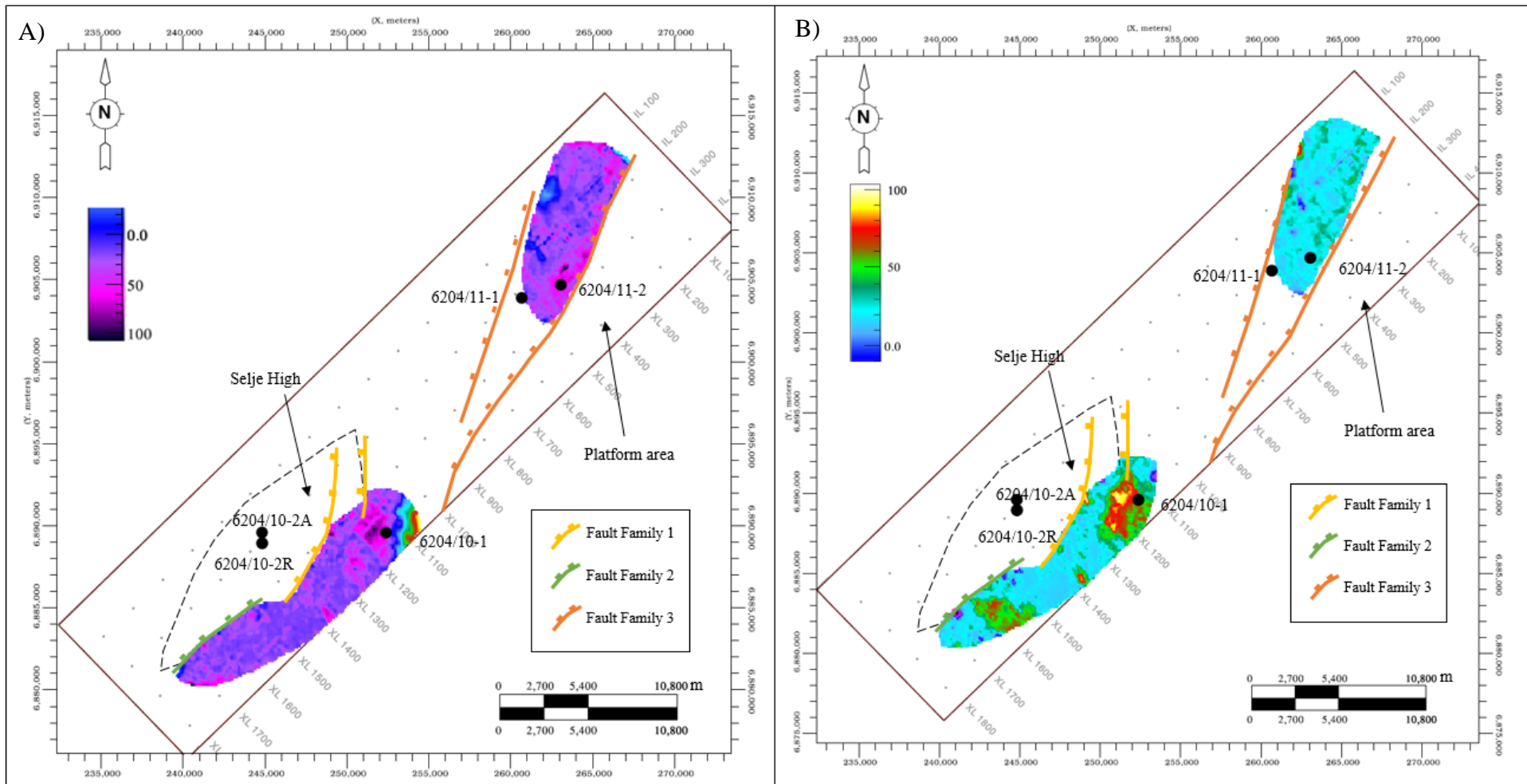
Additionally, the Agat Formation in the north is restricted in both west and east by major faults, thus the Agat Formation is not present in the remaining areas. It is worth mentioning that the formation is deepening towards the northwest, opposite direction as in the formation in the south. The Base Agat Formation show the same depth and distribution trends as the Top Agat Formation (Figure 39b).

Figure 40a and Figure 40b represent the time thickness maps between the Top Agat Formation and the BCU, and the Top Agat Formation and the Base Agat Formation, respectively. The map between Top Agat and BCU has mainly thicknesses between 0-100ms, with largest thicknesses around well 6204/10-1 and 6204/11-2 with 100ms, in addition to a greater thickness along the major fault of FF3. For the time thickness map between the top and the base of the Agat Formation, the thickness varies from 0ms to 100ms, with the thickest areas around well 6204/10-1 and furthest south in the study area.



**Figure 39:** Structural maps of the Agat Formation. a) Top Agat b) Base Agat Maps of the Base Cretaceous Unconformity (BCU). a) Surface map of the BCU in time (ms) b) Structural map of the BCU in time (ms) with faults active during the period. Contour interval: 200ms. Elevated basement areas are marked as the Selje High and the Platform area.





**Figure 40:** Time thickness map for the Agat Formation A) Time thickness map between the BCU and Top Agat Formation and B) Time thickness map between the Base Agat Formation and the Top Agat Formation. The faults are displayed in the figure to highlight that these are marking the lateral extent of the Agat Formation.

### ***Interpretation***

As mentioned in the section about faulting, the Agat Formation contains evidence of the deposition being influenced by the previous fault activity in the Late Jurassic. The onlapping of the basement in the hanging wall and the thickness variations across faults can be interpreted as both tectonically active and inactive. What can be indicated from the results is that the Agat Formation is influenced by the Jurassic faults in the sense that it marks the boundary of the lateral extent of the formation.

As the Agat formation is located close to the major fault in Selje High, it is likely that at least some of the Agat Formation in the south are deposited from the structural high, however, it is possible that it was also sourced from the east outside the study area. The thickness map does not show any clear evidence of thickening towards any of the source areas. Thus, this cannot be concluded before looking at seismic lines at faults and stratigraphic features.

Furthermore, the formation in the north only has one plausible source area, which would be the platform in the east. In addition, the formation is restricted in the west by the west-dipping normal fault, which is another indication of the deposition coming from the east. The continuous thickness in the north show a thin uniform distribution of the formation, however, in this area, the formation is below seismic resolution which makes the interpretation uncertain. Nevertheless, the main depocenter seems to be around well 6204/10-1.

### 4.2.3.3 Seismic character

#### *Observations*

The Agat Formation is observed in the seismic around wells 6204/10-1 and 6204/11-2. The deposits lay directly on top of the BCU in the northern area (Figure 41). In well 6204/11-2, the seismic well-tie shows that the interval of the Agat Formation (30m) is below the seismic resolution (40-48m), with the top and base being within the same event (Figure 41), and the base of the formation is therefore interpreted at the BCU. An example of this can be seen in Figure 41, where the Agat Formation is located from the fault laying on top of the Jurassic or older syn-rift succession.

In the southern area, the Agat Formation (106m) is above the seismic resolution (40-48m), thus the interval can be seen as two separate events (Figure 42). The Agat Formation in the south lies on top of the Jurassic or older syn-rift wedge bounded by the major east-dipping fault in FF1 (Figure 42). The formation onlaps the basement in the east, close to well 6204/10-1. The thickness from the well and down to the minor FF1 fault is continuous, nevertheless, the thickness in the footwall of the minor fault is thicker with a mound feature observed in the hanging wall close to the major fault in FF1.

Looking at the internal configuration of the Agat Formation can be difficult as the interval is quite thin in some areas. In the northern area (Figure 41), the Top Agat Formation is a strong red, negative reflector pinching out into a downlap on the BCU. Moreover, in the southern area, the interval of the Agat Formation is thicker and therefore contained more than one reflector (Figure 42). The reflector of the Top Agat Formation is strong and continuous close to well 6204/10-1, however, the reflector becomes weaker above the minor east-dipping fault, then gets stronger closer to the fault plane of the major east-dipping fault in FF1. The remaining reflectors close to well 6204/10-1 are sub-parallel with varying amplitude strength. In the mound feature observed, the reflectors are wavy to sub-parallel with varying in amplitude strength and continuity.

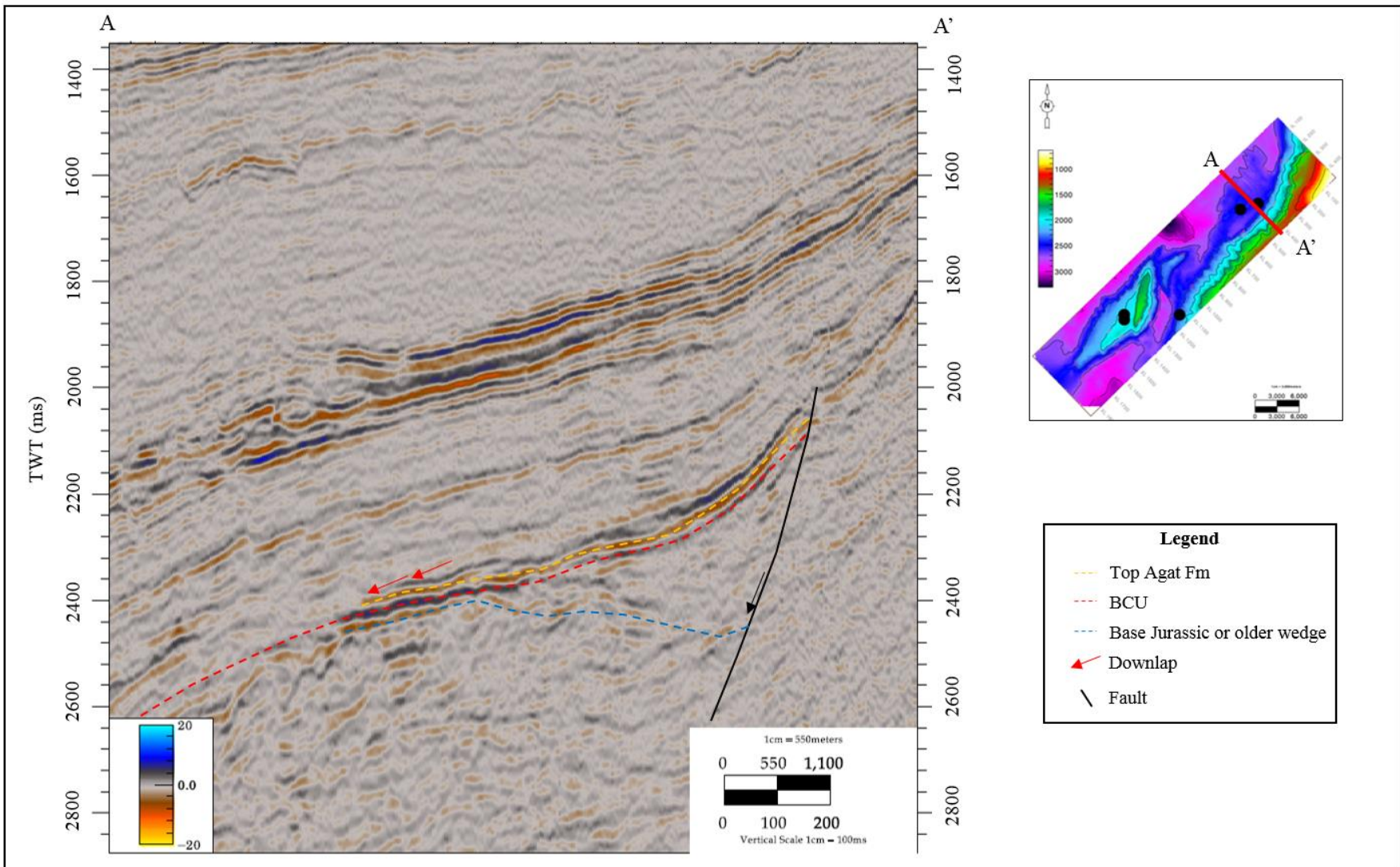


**Figure 41:** Seismic X-line 404 highlighting the Agat Formation with a yellow stippled line. The Agat Formation is downlapping the BCU in the west marked with red arrows.

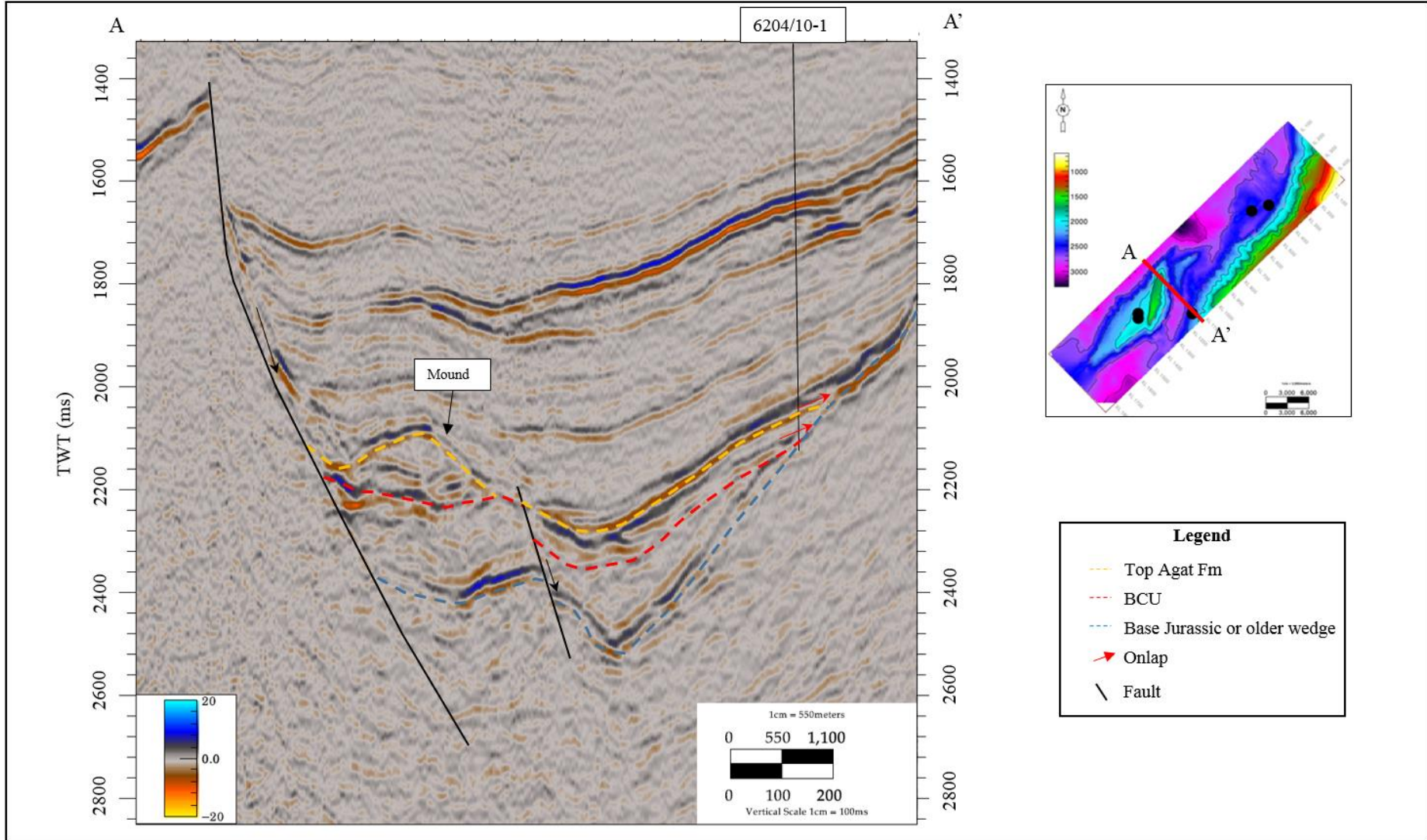


**Figure 42:** Seismic X-line 1125 highlighting the Agat Formation with a yellow stippled line. The Agat Formation is onlapping the BCU in the west marked with red arrows. A mound or a fold is observed in the hanging wall of Selje High.

### *Interpretation*

The Agat formation deposited in the northern area (south in the Slørebotn Sub-basin) show that the deposits are coming from the elevated platform areas, as the formation is deposited on the slope and downlaps the BCU in the west.

The Agat Formation deposited in the south show thickness variations across a minor fault due to the deposits of a mound close to the major fault bounding the Selje High which has been highlighted before. This mound seems to be deposited from the basement high in the west, likely as a slump which coincides well with the internal configuration of chaotic reflectors. If the faults were reactivated during the Early Cretaceous, the mound would likely be a fold caused by the compressional forces, as discussed in previous chapters.

The onlap of the Agat Formation on the Basement was for the Jurassic succession interpreted as active rifting and rotation of fault blocks. For the Agat Formation it can either be the same explanation, or it can be that the Agat Formation was infilling the wedge geometry caused by the Late Jurassic rifting. The same explanation as Sømme et al. (2013) fits well with the observations made for the Agat Formation in the north, where the deposits are deposited from the eastern platform area along canyons or gullies. However, a more detailed investigation of facies would be necessary to more accurately define the exact canyons which deposited the sediments.

Lastly, it is important to highlight the area in between the Agat Formation in the north and the south, which show no presence of the Agat Formation. This might be the result of starved canyons not depositing sediments down the slope.

### ***Seismic observations in well 6204/11-1 and 6204/11-2***

Figure 43 shows a random seismic line crossing wells 6204/11-1 and 6204/11-2 used to investigate the thickness and elevation variations between the wells observed in the structural well correlation. Here one can observe the elevation difference in the Pre-BCU section in the seismic and it is also evident that the Agat Formation of Lower Cretaceous is onlapping the BCU around well 6204/11-1 (Figure 44). In the seismic, the reflectors are continuous close to the faults and become more chaotic closer to well 6204/11-1. Moreover, an anticlinal shape in well 6204/11-1 are observed with a flat reflector within. No minor fault is observed in this seismic line.

### ***Interpretation***

In the seismic line, the Agat Formation and Lower Cretaceous sediments onlapping the BCU is likely infilling the basin topography created from the Jurassic rifting. The seismic should be helpful in explaining the increased elevation well 6204/11-1, however, it is not very clear from the seismic what caused the anticlinal shape. One explanation could be reactivation of faults in the Early Cretaceous causing inversion of depocenters, however, no faulting is observed in this seismic line. The antclinal shape works as a trap and the flat reflector is interpreted as the GWC, which is also described at NPD (NPD, 2019).

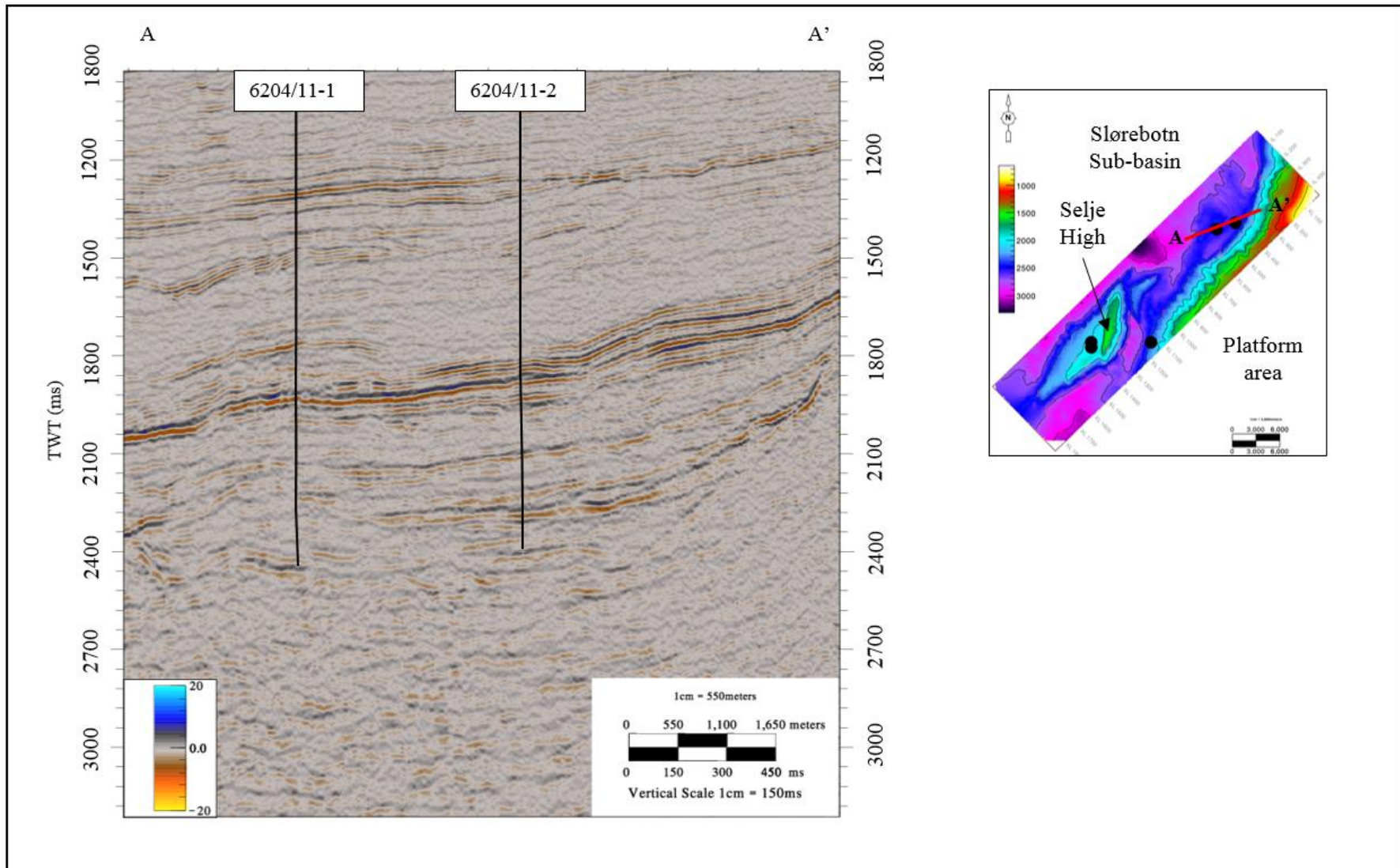


**Figure 43:** Uninterpreted random seismic line between well 6204/11-1 and 6204/11-2.



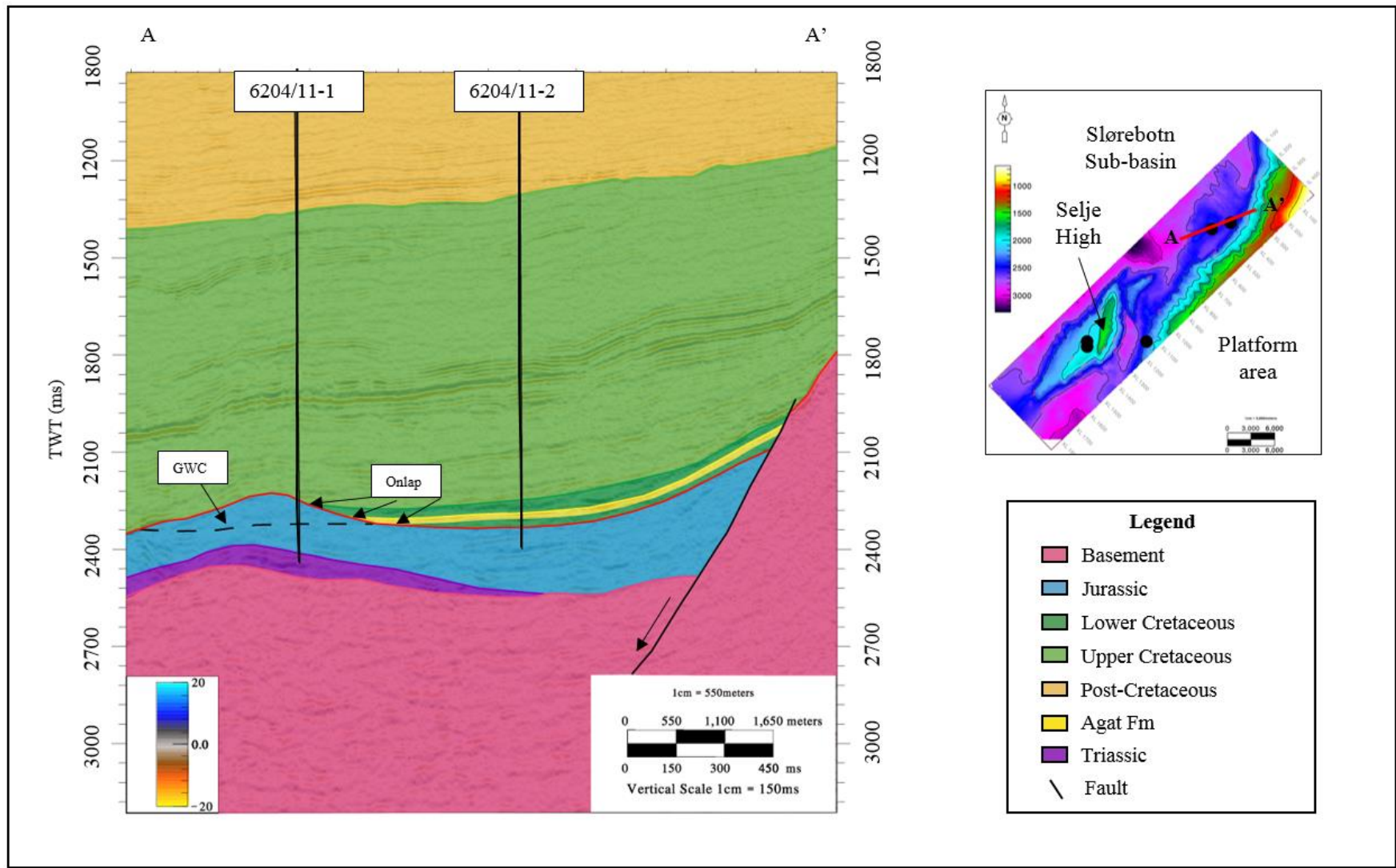


**Figure 44:** Interpreted random seismic line between well 6204/11-1 and 6204/11-2. Agat Formation is onlapping the BCU and a GWC are defined in the anticlinal shape of well 6204/11-1.

#### 4.2.3.4 Spectral decomposition

##### *Observations*

A constant bandwidth spectral decomposition RGB color blend was applied to the Top Agat Formation (Figure 45). At first glance, no very distinct shapes are evident from the color blend, however, after a more detailed look, some relevant features are observed. The spectral decomposed surface has areas with red to yellow colors which are areas with low to medium frequencies. In addition, a set of linear geometries are highlighted, especially in the northern part of the surface (marked with arrows in Figure 45). These lines are alternating between green, blue and red colors, where the red marks the lower frequencies, green marks the middle frequencies and blue the higher frequencies.

In the southern area of the Agat Formation, the decomposition does not highlight the red colors in the same sense as the northern area; however, the areas around well 6204/10-1 show significantly brighter colors than further south. Moreover, some dark circular features are evident along the edge of Selje High.

The iso-proportional slicing in Figure 46 and Figure 47, between the Top Agat and Base Agat, highlights the changes in frequencies and textures within the formation. The lower frequency lines discovered in the Top Agat surface is evident in the Upper part of the formation, however, in the lower part, the lines become weaker. The overall brightness in the colors dims towards the base of the formation and results in less variation in frequencies.

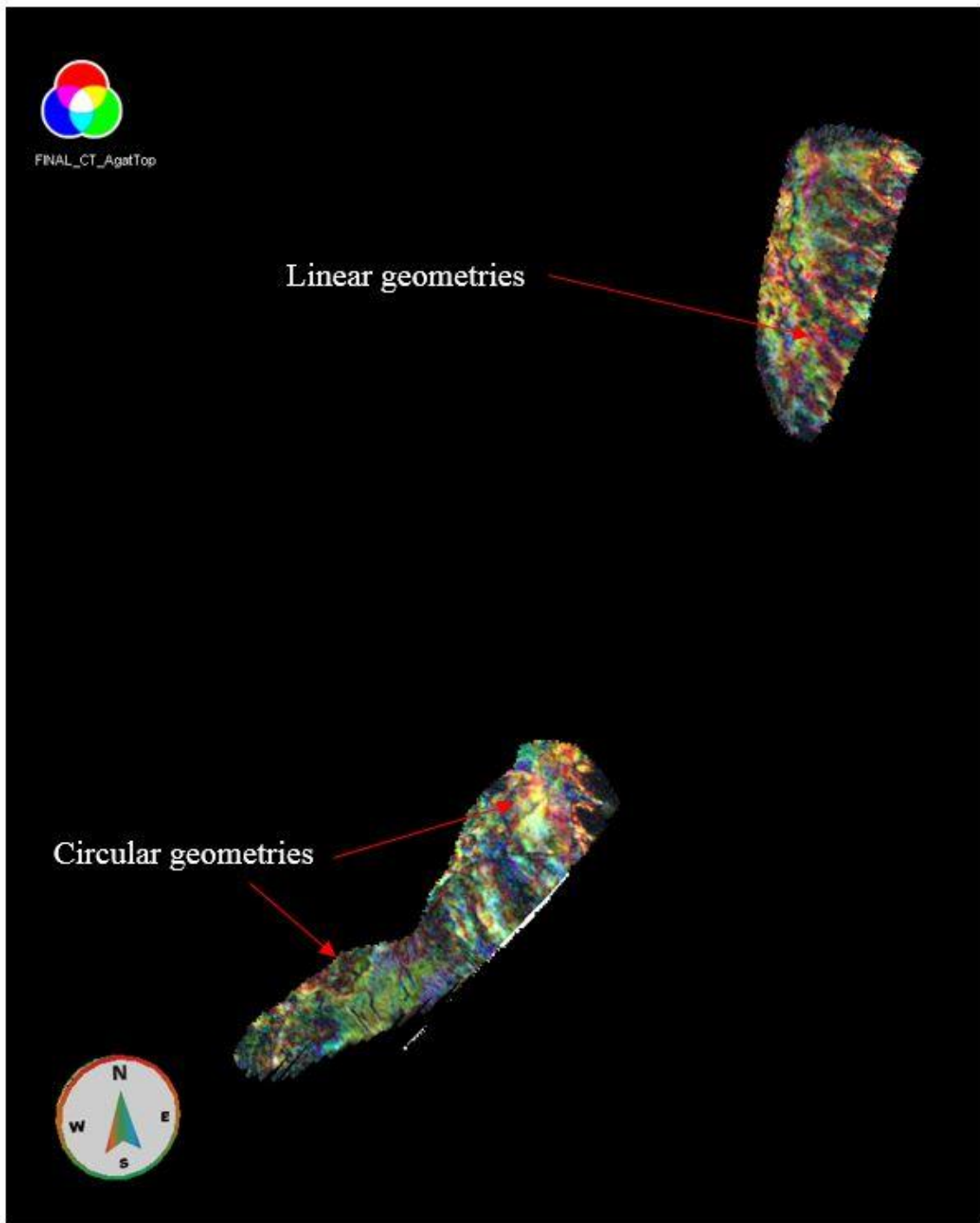


**Figure 45:** Top Agat Formation with a constant bandwidth spectral decomposition with an RGB color blend (17Hz – 30Hz – 42Hz). Circular and linear geometries are observed in the south and in the north, respectively.

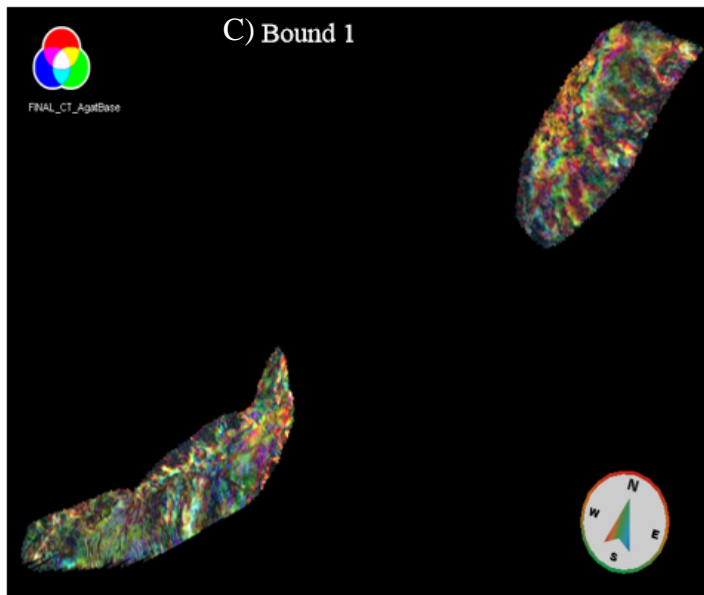
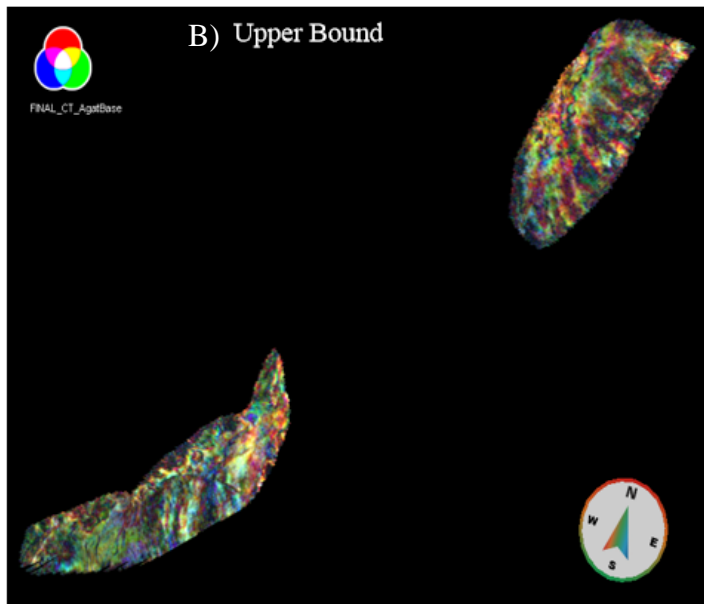
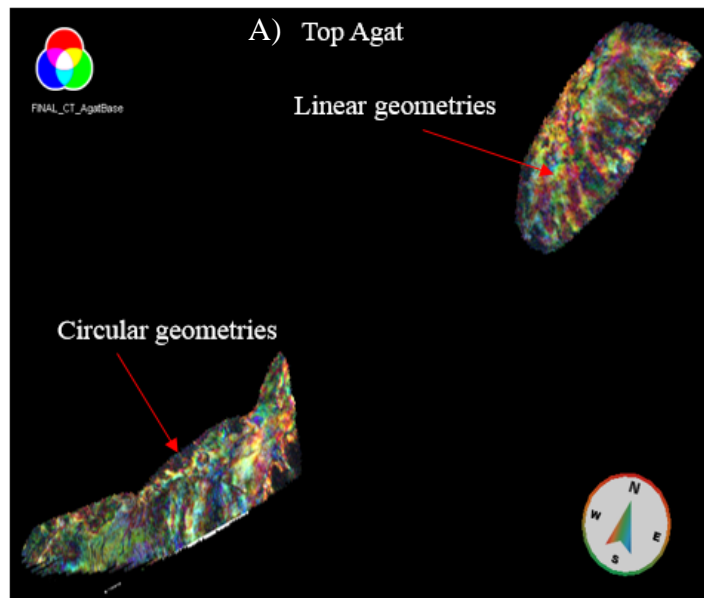


**Figure 46:** Iso-proportional slicing between top and base of Agat Formation. Constant Bandwidth Spectral decomposition with a RGB color blend (17Hz – 30Hz – 42Hz). a) Top Agat b) Upper Bound c) Bound 1. The same geometries as observed in Figure 46 are observed here. Marked in a).

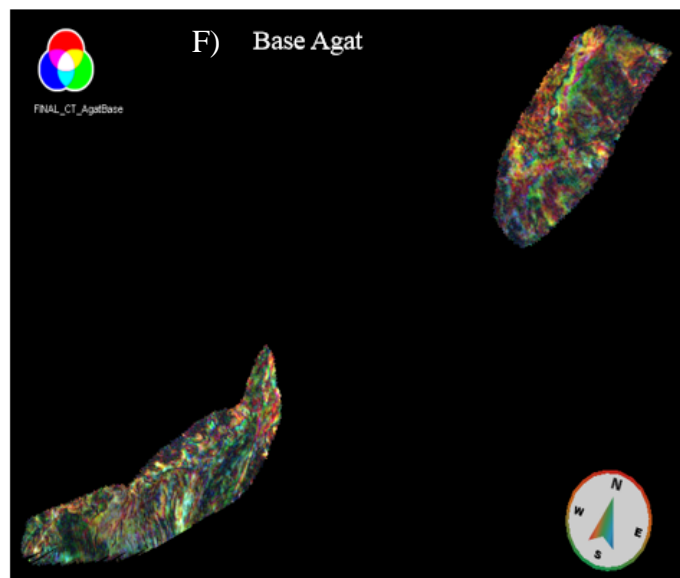
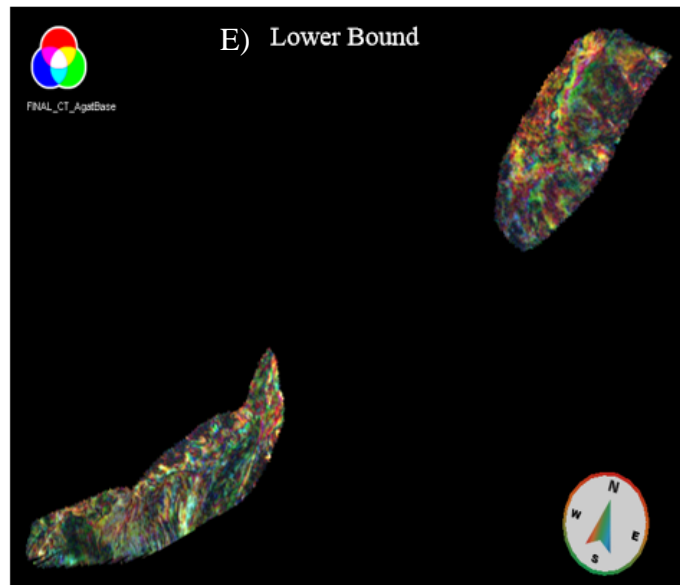
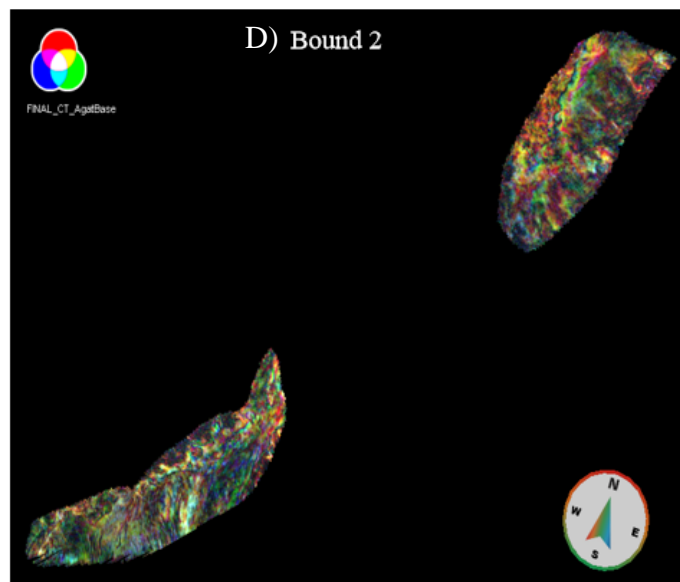


**Figure 47:** Iso-proportional slicing between Top and Base of Agat Formation. Constant Bandwidth Spectral decomposition with a RGB color blend (17Hz – 30Hz – 42Hz). d) Bound 2, e) Lower Bound, f) Base Agat. The same geometries as observed in Figure 46 are less evident in these three slices, where the color has dimmed significantly.

### *Interpretations*

The different frequency lines or color lines observed especially in the northern area can give indications of the reservoir properties of the formation. A study done by Weibull (2019) suggested a new method to make some inferences about the layering characteristics of reservoirs based on the analysis of frequency spectra of reflections. The inferences made are that the low frequencies (red) show reservoirs that are more homogeneous and showing a coarsening then fining upwards succession. The green and blue colors (medium and high frequencies) are indications of heterogeneous reservoirs. This could be used in the study area, as areas with red colors are observed, which could mean that these areas have the better and most homogeneous reservoirs. In addition, the lines interchanging frequency lines (changing from red to green to blue) might indicate that the reservoir is compartmentalized. This would correspond well with the idea of gravity mass flows, where the lobes would be deposited as different reservoir bodies that are not connected. However, this needs further investigation using the lithology, grain size, and the amplitude spectrum to do modeling of the reservoir as explained by Weibull (2019).

In addition, the alignments of different frequencies observed in the north might indicate that these are deposits such as submarine fans, while the circular features observed in the southern area are slump deposits. This explanation fits well with the results explained in all the previous chapters.

Lastly, from the iso-proportional slicing, the upper part of the formation seemed to be more influenced by the gravity flows, as the brightness dims towards the lower part.

## 5. DISCUSSION

### 5.1 Tectonic evolution

#### 5.1.1 Late Jurassic

The most important tectonic episode discussed in this study is the Late Jurassic rifting event. The extensional event during Late Jurassic to Early Cretaceous(?) is well covered and documented in several papers (Brekke & Riis, 1987; Blystad et al., 1995; Lundin & Dore, 1997; Brekke, 2000; Vergara et al., 2001; Osmundsen et al., 2002; Faleide et al., 2010), however, the timing of when the fault activity ended has been debated.

Several observations in the well and seismic data give good implications of tectonic activity during the Late Jurassic in the study area. These observations are growth strata or wedges in the hanging wall, thickness variations across faults, rotation of fault blocks, absence of Jurassic succession in the elevated areas and onlap surfaces.

It is worth mentioning that wells 6204/10-1 and 6204/10-R did not penetrate the Jurassic succession, however, these wells are drilled on the Selje High and the Måløy slope, while the two most northern wells are drilled in the Slørebotn Sub-basin. As a result, the Jurassic succession either has been removed by erosion on the high and the slope, while the lower areas in the basin have not been affected to the same extent or the Jurassic succession was never deposited in this area. Thus, the tectonic period during Late Jurassic evolved into large relief between the basins and the structural highs.

The growth strata together with the thickness variation and erosion across faults, especially the major ones from FF3, are good implications that the Late Jurassic rifting episode occurred around the Selje High, Slørebotn Sub-basin and the Måløy Slope as defined in several previous papers (Brekke & Riis, 1987; Blystad et al., 1995; Lundin & Dore, 1997; Brekke, 2000; Vergara et al., 2001; Osmundsen et al., 2002; Faleide et al., 2010). A typical expression for active rifting is rotated fault-blocks which are bounded by faults influencing the basement (Blystad et al., 1995; Færseth & Lien, 2002).

#### *Uplift and rotation of fault blocks*

The rotation of the fault blocks in the study area likely occurred during the Late Jurassic rifting events. The Pre-Cretaceous growth strata on the eastern side of Selje High show wedge geometries that onlap onto the basement in the hanging wall (Figure 16 and Figure 17). The

dipping wedge geometries are also observed along the entire eastern edge bounding the platform area (Figure 33, Figure 34, Figure 35, Figure 36 and Figure 37). These are good implications for the rotation happening before and during the deposition of these sediments. Furthermore, the steepness observed along the eastern Selje High in both basement surface (Figure 22) and the BCU surface (Figure 31), are good indications that the faults bounding this structural high were active and created the tilting during the Late Jurassic. Which is also suggested by Færseth and Lien (2002) and Jongepier and Rui (1996).

Furthermore, Jongepier and Rui (1996) did a reconstruction study on wells in the northern Slørebotn Sub-basin, using well 6205/3-1R to define the timing of rotation of the fault blocks in this basin from Kimmeridgian to Volgian.

- 1) Kimmeridgian: approximately 5 degrees.
- 2) Early Volgian: approximately 15-20 degrees.
- 3) Middle Volgian: approximately 20 degrees.

It is therefore believed that the fault blocks in the study area were subjected to the same rotational scheme.

The tilting of the Selje High and the faults bounding the platform area result in the highs being exposed to erosion at the tip of the footwall. Thus, the erosion leads to deposits of coarse grained material to the hanging wall. Furthermore, the drainage area of the basin are mainly the eastern platform area, which is a narrow shelf resulting in small area with limited sediments supply particularly during relative high sea level which is also discussed in Martinsen et al. (2005) and Bugge et al. (2001). The deposition of these sediments are highly dependent on the subsidence along the major fault along with the size of the drainage area. As high subsidence rate and small sediment supply would result in narrow fan structures, while a less subsidence and higher sediment supply would result in larger fans (Faleide et al., 2010).

Figure 48 shows a simplified illustration of the tilted fault blocks of the Selje High, and the deposition of the Pre-Cretaceous interval onlapping the basement to the east and is eroded away on top of the Selje High.



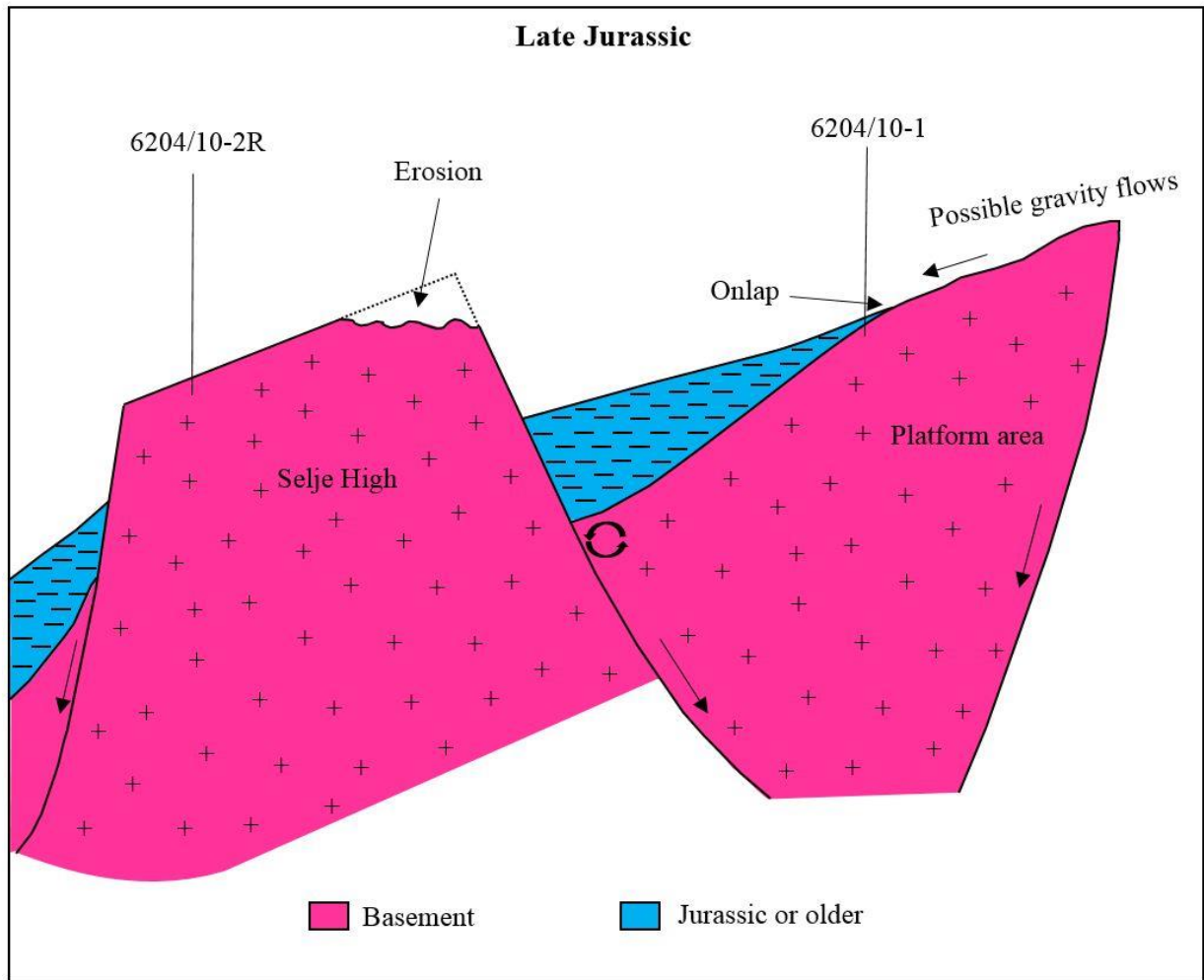


**Figure 48:** Structural model of the Late Jurassic highlighting the fault activity and rotation of the Selje High. The Jurassic or older interval are dominated by deep marine shales. Erosion in the foot wall is marked along with possible gravity flows in the hanging wall. The Jurassic or older onlaps the Basement in the hanging wall.

### 5.1.2 Early Cretaceous

As mentioned earlier, the debate around the tectonic activity during Early Cretaceous is still ongoing. One understanding is that the Early Cretaceous is part of the Late Jurassic rifting (Ziegler, 1975; Blystad et al., 1995; McCann et al., 1995; Brekke, 2000), however, several other models are proposed such as;

- 1) The rifting during Late Jurassic and Early Cretaceous are two separate tectonic events (Lundin & Dore, 1997; Doré et al., 1999).
- 2) The Early Cretaceous is a period of thermal subsidence and tectonic quiescence (Bertram & Milton, 1988; Gabrielsen et al., 2001; Færseth & Lien, 2002).

The Lower Cretaceous is in this study defined as syn-rift or immediate post-rift succession. The most prominent stratigraphic feature showing evidence of active rifting is wedge-shaped geometries close to the faults, indicating syn-rift strata. However, it is also important to be aware of the infilling of post-rift sediments may cause wedge-shaped bodies (Prosser, 1993). This is recognized in seismic as subparallel reflectors in relevance to the top surface of the wedge (Ravnås & Steel, 1998).

Two theories about the paleogeographic evolution of the area during Early Cretaceous Agat Formation will be presented in this discussion. This is mainly due to the study only considering the Agat Formation of Early Cretaceous and lacking detailed study of the entire Lower Cretaceous succession which could give better indications of the tectonic activity during this period.

#### 5.1.2.1 Theory 1: Tectonic quiescence – Thermal subsidence

Theory 1 favors the understanding of the Early Cretaceous as a period of tectonic quiescence with thermal subsidence leading to post-rift sediments infilling the topography caused by the Late Jurassic rifting.

##### *Immediate post-rift sediments*

The immediate post-rift stage is recognized by the infilling of the previous rifting topography, thus smoothing the bathymetry of the rift basin (Ravnås & Steel, 1998). Furthermore, the marine conditions during the Late Jurassic to Early Cretaceous would create an overall fine-grained succession, and only small intervals of interbedded coarse-grained sandstones likely

deposited as gravity flows from the structural highs occurred during regressive episodes (Bugge et al., 2001).

The Agat Formation onlaps the BCU in the southeast towards the margin as a relatively thin cover, which may indicate that the basin is starved of coarse-grained sediments due to increased accommodation space created during the Jurassic rifting and high eustatic sea level. This along with the lithology from the well reports and the climate indicate that the formation is likely underfilled of sand-rich sediments. The observations of thickness variation across faults are normally an indication of tectonic activity (Færseth & Lien, 2002), however, in this study, the Agat Formation show little indication of wedge-shaped geometries. Thus, the thickness variations across faults are likely a result of increased subsidence in the hanging-wall creating large accommodation space being infilled by the sediments of the Agat Formation, which creates thicker succession in the hanging-wall compared to the elevated areas. However, it is important to remember that the Agat Formation varies in thickness and has areas where it is below the seismic resolution, thus it may be difficult to identify wedge geometries.

#### *Problems with the theory*

However, the main problem with this theory is to understand the deposition of the Åsgard Formation in relevance to the Agat Formation. The Åsgard Formation is considered of Late Berriasian to Late Hauterivian age, yet, in areas lacking Tuxen and Sola formations, the Åsgard Formation can reach Late Aptian to Early Albian age (NPD, 2019). Moreover, the Agat Formation is of Albian age, meaning it was deposited either later than Åsgard Formation or approximately at the same time. It is, however, quite curious why the older Åsgard Formation is not present below the Agat Formation in well 6204/10-1 when it was deposited at the Selje High. Reversing this thought, another question arises, why did not Agat Formation deposit in well 6204/10-2R when it was deposited in the lower structural area of well 6204/10-1?

A possible answer is that even though the eustatic sea level was high during the Early Cretaceous, the Åsgard Formation may have only partially flooded the Selje High, as the highest points were still subaerially exposed. Hence, the Åsgard Formation did not deposit at the highest points of the Selje High. The deposition of the Agat Formation might be the result of erosion of the Selje High during a minor regression, resulting in coarse-grained deposition in the structural lows (Bugge et al., 2001). This might also explain that the sediments of the

Agat Formation bypassed the wells in Selje High and deposited to the west in the Sogn Graben and Slørebotn Sub-basin. Furthermore, if the Åsgard Formation was deposited during Albian (NPD, 2019), then likely the fine-grained Åsgard Formation was deposited on the structural highs, whereas the sandy Agat Formation was deposited in the lows due to the erosion of exposed footwall islands.

The second problem is the change in thickness of Cretaceous and Jurassic observed between the two wells 6204/11-1 and 6204/11-2. Based on the seismic section interpreted between the wells (Figure 43 and Figure 44), the elevated well 6204/11-1 seems to be located at small anticlinal shape likely caused by inversion of depocenters. This is normally a result of reactivation of older faults. However, this does not fit well with the theory of tectonic quiescence. Leading to the alternative theory.

Figure 49 is displaying a simplified structural model of the Selje High during the Early Cretaceous for Theory 1.

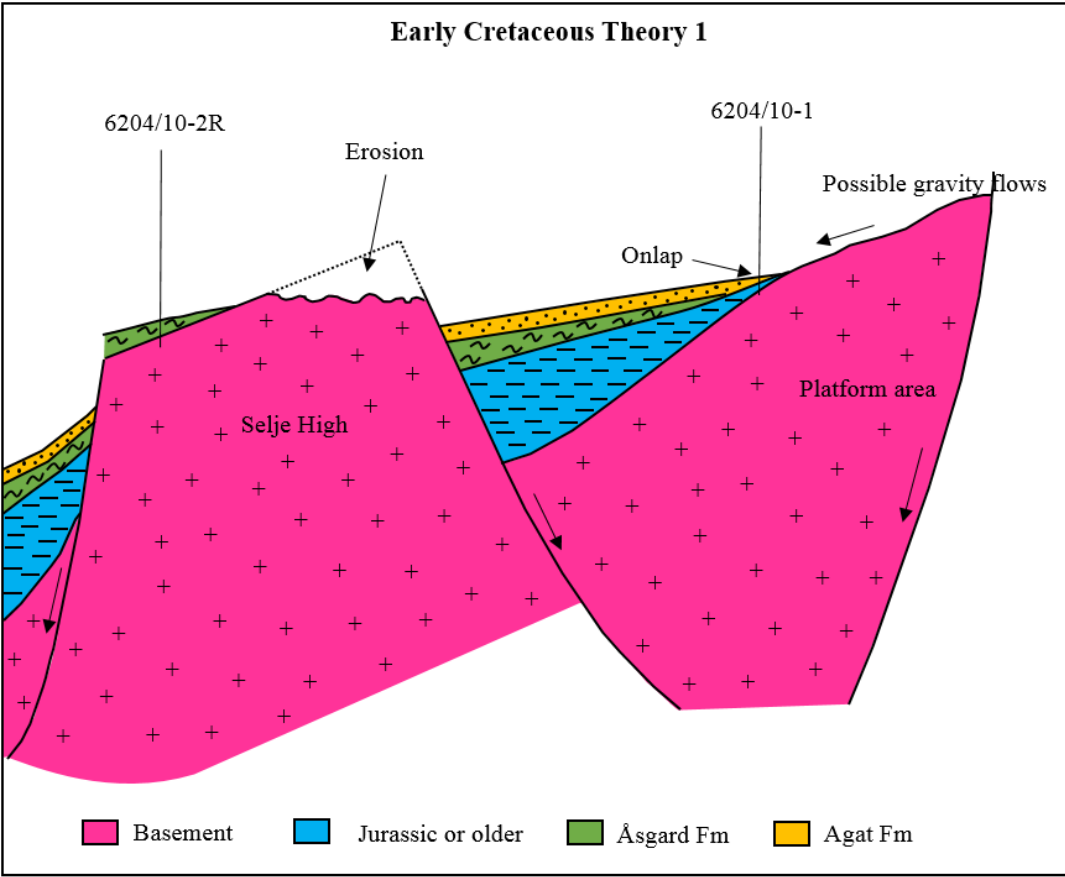


**Figure 49:** Structural model of the Early Cretaceous theory 1 highlighting the tectonic quiescence period around Selje High. Erosion in the foot wall is marked along with possible gravity flows in the hanging wall. The Agat Formation onlaps the Basement, while the Åsgard Formation is truncated. Åsgard Formation partially deposited on the Selje High.

### **5.1.2.2 Alternative theory: Tectonic activity – Fault reactivation**

The alternative theory favors the understanding of the Early Cretaceous as a period of minor tectonic activity leading to deposition of syn-rift sediments.

#### *Syn-rift sediments*

Based on the wedge geometries, the deposition of the lowest Cretaceous Åsgard Formation in part of the footwall areas, the lack of the Agat Formation, and the shift in depocenters observed in the well correlation (Figure 14, Figure 41, Figure 42, and Figure 44), it is interpreted that the Agat Formation was deposited during a period of fault activity.

The main observation favoring the alternative theory is the observed thickness variations across faults. The Agat Formation is only deposited in the structural lows and is missing at the Selje High (Figure 14). Either the formation did not deposit at the structural high or it was eroded away. The latter would likely implicate that the faults bounding the Selje High were active during this period. The upward dragging of the reflectors close to the fault plane can be used to justify both theory 1 and the alternative theory (Figure 16, Figure 17, Figure 18, Figure 19, Figure 20, and Figure 21). As can be seen in Figure 2, Prosser 1993 suggested that the syn-rift deposits contain upward dragging reflectors, however, this is also evident in the immediate post-rift succession, and hence both theories are possible. In addition, the upward dragging may indicate that the faults were reactivated during a later stage.

Furthermore, during the late syn-rift stage the hanging wall might receive sediments from footwall islands created by uplift during the rifting (Ravnås & Steel, 1998). These would likely deposit coarse-grained sediments. Like the conglomerates observed in the study area.

The alternative theory can be used to explain the change in thickness for Late Jurassic and Early Cretaceous between wells 6204/11-1 and 6204/11-2 (Figure 43). The change from Jurassic being thickest in well 6204/11-1 to Cretaceous being thickest in well 6204/11-2 can be explained by a minor fault in between these two wells which would be of Lower Cretaceous age. Thus, the Lower Cretaceous succession in well 6204/11-1 would be exposed to erosion and eroded away. In addition, the fault would increase the accommodation space in the hanging wall, thus increasing the thickness of the Cretaceous succession. Lastly, the anticlinal high in well 6204/11-1 could be explained by the reactivation of faults and inversion of depocenters.

### *Problems with the theory*

A small problem with the alternative theory is why Åsgard Formation is deposited at the Selje High and not eroded away. If the faults were active and eroded away the sediments of Early Cretaceous age on the Selje High, why are Åsgard still present? A possible explanation is that the Åsgard Formation is present in the hanging wall, however, it did not reach all the way up to the edge as shown in Figure 50. In addition, the Åsgard Formation might be deposited during a period of tectonic quiescence, and only partially eroded away. Furthermore, the Åsgard Formation was deposited during a transgression, while the Agat Formation was likely deposited during minor regressions as suggested in Bugge et al. (2001), thus the sediments of the Agat Formation have potentially been deposited only in the hanging wall and bypassed the Selje High traveling into the Sogn Graben and Slørebotn Sub-basin in the west.

Figure 50 displays the structural model for the alternative theory, which is similar to Figure 49, however, here one can observe the growth strata and an increase in the accommodation space in the hanging walls.

Based on the observations in the study area, and evaluating the two different theories, the alternative theory seems to be most likely. However, theory 1 is possible even though it has its problems that need further investigation before one can conclude that the Agat Formation is a result of a regressive event during the post-rift stage in Early Cretaceous and not an active rift event.

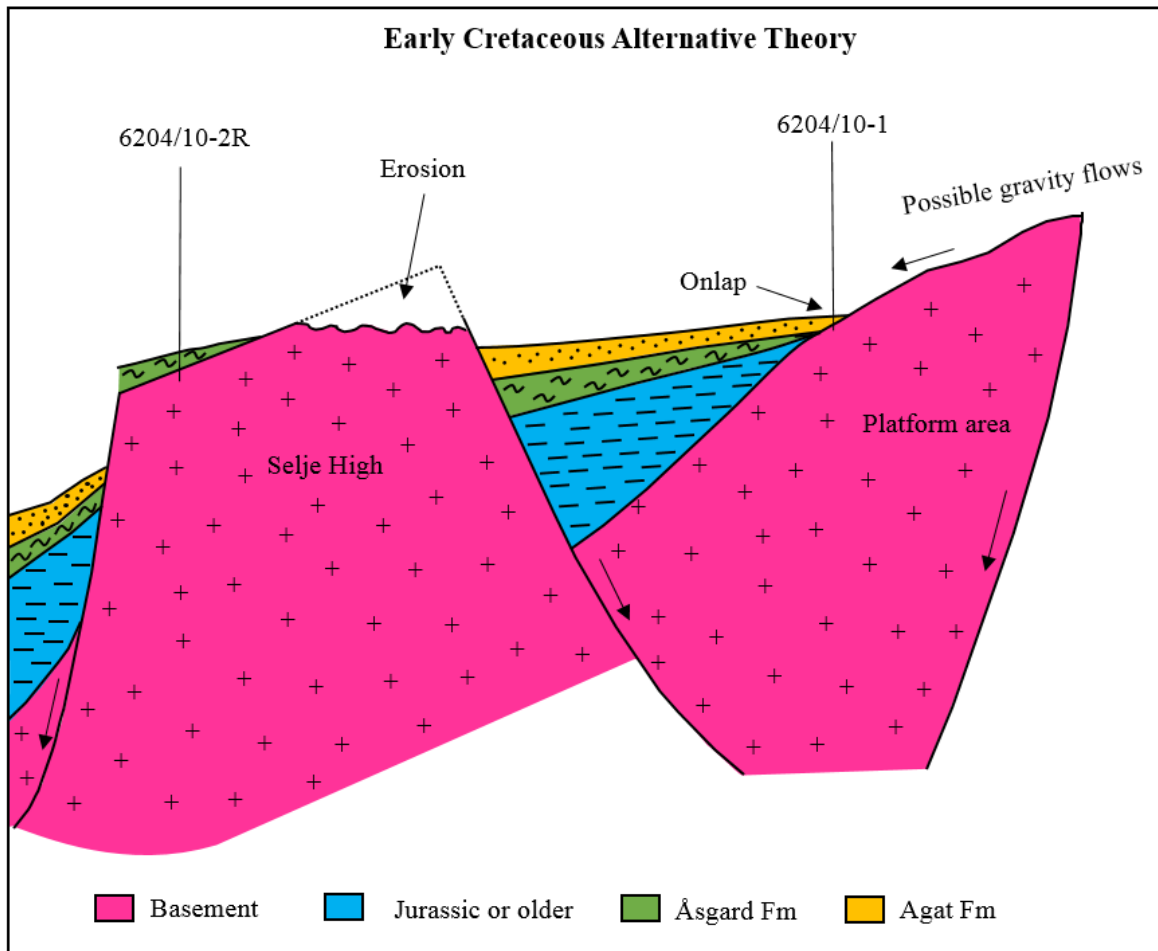


**Figure 50:** Structural model of the Early Cretaceous alternative theory highlighting the reactivation of the fault activity around Selje High. Erosion in the foot wall is marked along with possible gravity flows in the hanging wall. The Agat Formation onlaps the Basement, while the Åsgard Formation is truncated. Åsgard Formation partially deposited on the Selje High. Wedge geometries in the Åsgard and Agat Formation are observed.

## 5.2 Basement structure and implications for exploration

The basement in the study area consists of Pre-Devonian metamorphic sediments altered by extensional events and orogenic events during the tectonic evolution. Several observations are found in the data of the basement indicating it as an important interval for younger sediments, however, also for observations of the basement itself as a potential reservoir.

The basement structures in the northern North Sea are of great interest after the discovery of fractured basement in the Utsira High area, which worked as reservoirs (Riber, Dypvik, & Sorlie, 2015). Thus, the basement in the Selje High area would also be relevant for further investigation.

Although two wells that had the basement as a secondary target were dry, the conglomeratic material and the observations of possible fractures and incisions in the basement could indicate that the basement is weathered and has potential as a reservoir. The tilting of the fault blocks in the Late Jurassic caused erosion and subaerial exposure of the Selje High, which affected all the way down to the basement. The erosion caused large incisions in the basement resulting in fairways for sediments deposited later, but also caused fractures in the basement (Figure 25, Figure 26, Figure 27, Figure 28, and Figure 30). The minor alignments observed along the top of the Selje High interpreted as minor faults of FF3 or as fractures might suggest that the basement can bear potential as a reservoir. However, this would be further investigated by core data.

In Riber et al. (2015), a detailed study on core data of the basement in the Utsira High was executed giving a better understanding of the mineral composition and thus infer whether the basement was exposed to weathering or not. Well 16/1-15 in Utsira High bear resemblance to the stratigraphic situation in Selje High, where the basement is directly overlain by the Åsgard Formation. The first interval with sands, followed by marls. However, the sands show conglomeratic size on the sediments. In well 6204/10-2R in the study area, the well report suggested that the basement contained rock fragments of metamorphic rocks, however, it also contained traces of white opaque crystalline calcite in veins or fractures. This is a good indication that the basement was fractured. In addition, the conglomerates penetrated above the basement show some correspondence with the Utsira High, with sandy conglomerates found above the basement, which can imply that the basement was weathered.



The incisions, fractures or minor faults, and the conglomerates lying directly above the basement are all confirming that the basement was exposed to erosion and weathering during the Late Jurassic.

Introducing an analog to the submarine canyons observed in the seismic through the spectral decomposition (Figure 25, Figure 26, Figure 27, and Figure 28) might help to imply the depositional systems influencing these types of canyons. Submarine canyons interpreted on the African west coast of the Equatorial Guinean slope are shown in Figure 51 (Jobe et al., 2011). These canyons show similar appearance to the submarine canyons interpreted in the study area. However, the canyons in Africa show much more detail than what can be observed from the spectral decomposition. Nevertheless, the submarine canyons in Figure 51 show linear appearance from the shelf edge down to the basin, which is also observed in the study area (Figure 27 and Figure 28). Jobe et al. (2011) suggested to different canyon types. Type 1 was submarine canyons eroding into the shelf slope depositing sediments onto the basin floor as submarine fans due to high sediment supply. Type 2 canyons has low sediments supply, and therefore contain much hemipelagic sediments and not the typical submarine fans. The submarine canyons in the study area are likely more similar to Type 1, however, the sediment supply would only be high in certain periods caused by regression. This due to the high eustatic sea level resulting in periods with little sediment supply.

Nevertheless, the submarine canyons observed in the study area are good fairways for depositing sediments from the shelf down to the basinal areas, most likely caused by regressive periods with increased sediment supply.

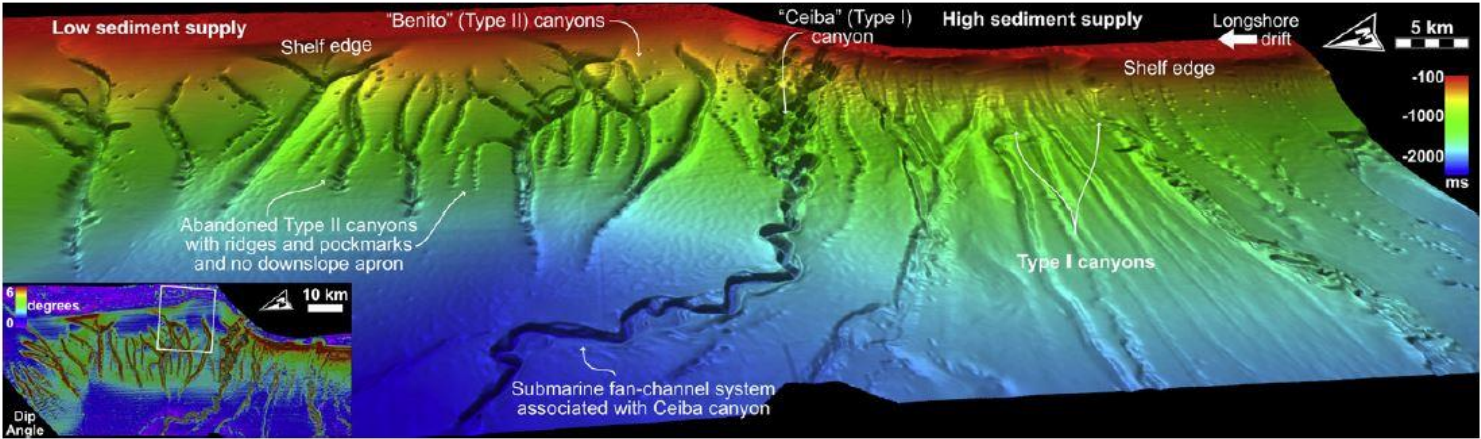


**Figure 51:** Submarine canyons observed downslope of the Equatorial Guinean seafloor. The figure displays to different canyons types. Type 1 favors submarine fans, while type 2 are more mud-rich and less carved into the slope (Jobe, Lowe, & Uchytel, 2011).

## 5.3 Paleogeography

### 5.3.1 Late Jurassic

During a rifting period, the basins are normally subjected to tectonic subsidence of fault blocks; however, the changing climate from the arid Triassic to more humid conditions along with a major transgression in the Late Jurassic further increased the subsidence. In addition, this period caused the tilting and rotation of the fault blocks, resulting in subaerial exposure of the footwall blocks and infilling the marine dominated fault blocks with coarse-grained sediments (Vergara et al., 2001). Evidence of this happening can be seen in the study area where several of the faults have been rotated resulting in large dipping wedge geometries in the hanging wall. Additionally, the onlapping of the Pre-Cretaceous interval on the basement in the hanging wall confirms the deposition of these sediments during the rotational event in the Late Jurassic.

Furthermore, the Late Jurassic rifting is associated with the formation of gullies along the eastern basin margin and the western side of the Selje High as it has been described before by Sømme and Jackson (2013). The increased water depth during the Late Jurassic transgression led to the first occurrence of deep-water settings in the study area. This is observed by the deep-marine shaly Heather Formation (Figure 14). In addition, the Heather SS Formation and the Sognefjord Formation are deposited, which are good indications of clastic sediment input from elevated areas likely as gravity flows.

Moreover, the canyons are interpreted in the basement at the structural highs. From the seismic (Figure 23 and Figure 24), it also looks like the BCU is affected by the gullies, however, this is only evident in the structural highs where it directly overlies the basement. Hence, the development of the canyons or gullies along both the Slørebotn Sub-basin, the Måløy slope and the western flank of Selje High most likely occurred at the end of the Late Jurassic rifting due to erosion.

Lastly, the observations done in this study indicate that these canyons are good transportation routes from the elevated platform area. The canyons observed along the eastern edge of the platform area in the spectral decomposition (Figure 22, Figure 25, Figure 26, Figure 27, Figure 28, and Figure 31), implicate that these canyons are a multiple source system, where the sediments can feed the basins from several different canyons. This also likely occurs on the western flank of the Selje High, showing similar canyons as observed in the platform area (Figure 25, Figure 26, Figure 27, and Figure 28). Whereas the eastern flank of the Selje High

has no observed canyons, however, more slump scarps at the upper slope (Figure 29), which imply that these slumps are deposited from a small source area at the top of the Selje High similar to a point source.

A conceptual sketch of the paleogeography during the Late Jurassic is suggested in Figure 52, with overall deep marine settings in the basins with occasional sandy sediment input from mass flows.

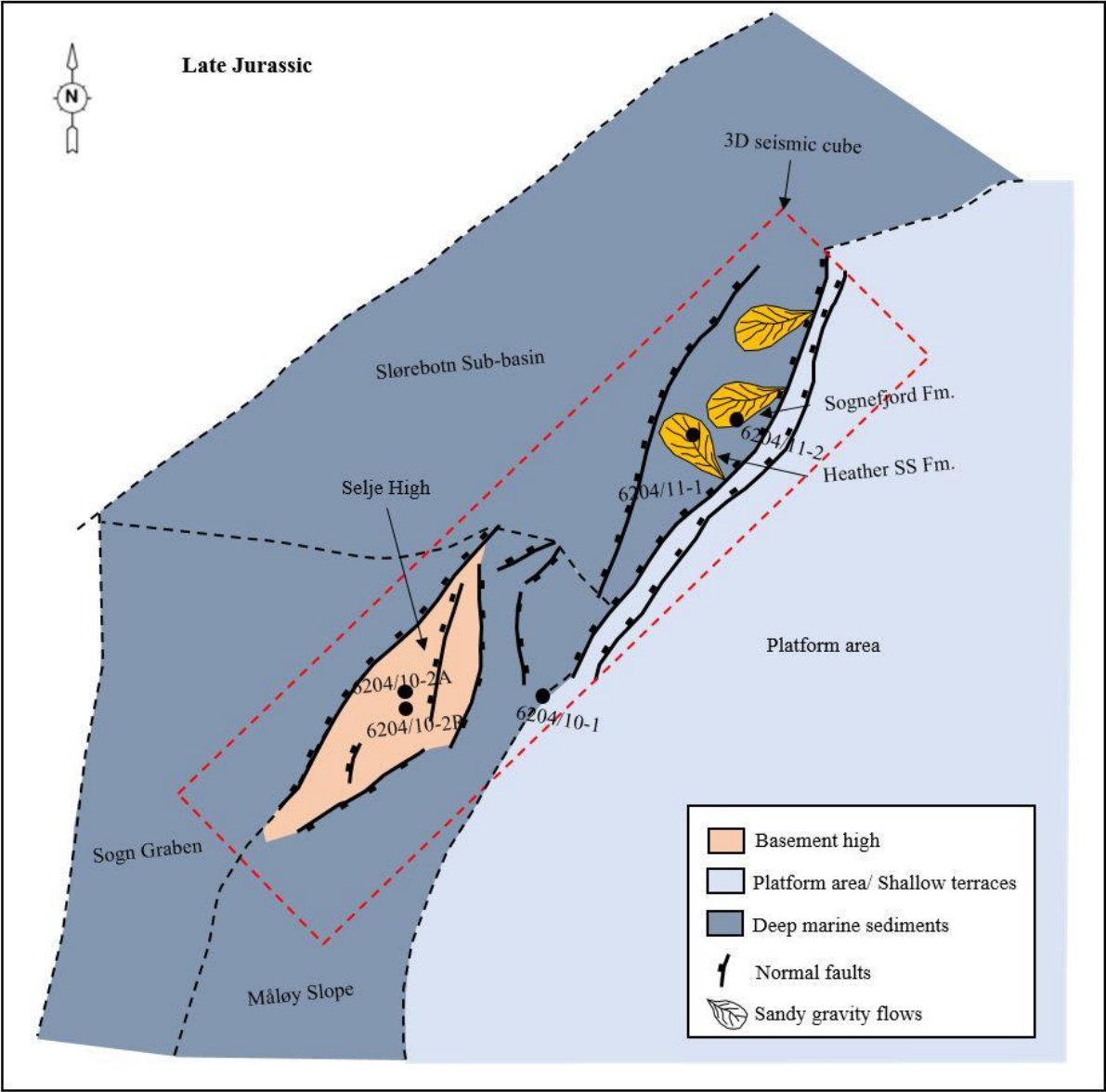


**Figure 52:** Conceptual sketch of the Late Jurassic. The Selje High is present during this period, and all the major faults in the study area are present in the Late Jurassic. Some sandy gravity flows are drawn in the northern area to imply that Sognefjord and Heather Sandstone Formation were also deposited during this period.

## **5.3.2 Early Cretaceous Agat Formation**

### **5.3.2.1 Depositional environment**

The overall depositional environment during the Early Cretaceous was still deep marine as in the Late Jurassic due to a transgression (Isaksen & Tonstad, 1989). This is evident in the study area by the cores from the Åsgard Formation in wells 6204/10-2R (Figure 7) showing dark shale. Thus, the coarse-grained deposits of the Agat Formation are likely caused by gravity flows down the slope from the platform area or the Selje High. Evidence of the gravity flows was difficult to detect in seismic, however, the spectral decomposition revealed the linear features interpreted as possible submarine fans, while the more circular features close to Selje High resembled slumps deposits (Figure 45). These gravity flows are either a result of the tectonic activity during the Albian (alternative theory) or due to minor regressive events (Theory 1) which has also been suggested by Bugge et al. (2001). The narrow platform area to the east was an important factor for the deposition of sandy sediments reaching the deep-water areas (Vergara et al., 2001).

### **5.3.2.2 Possible source areas**

As a result of the gullies observed in the basement and BCU being present along major parts of the study area (Figure 22, Figure 25, Figure 26, Figure 27, Figure 28, and Figure 31), the deposition of the Lower Cretaceous sediments can be deposited along the entire fault and structural high. This would imply that the Agat Formation could be sourced from both the Selje High and the platform area, which was also suggested in Vergara et al. (2001). Furthermore, the deposition of the Agat Formation would thus be deposited over a large lateral extent due to several source areas. Moreover, the thickest part of the Agat Formation in Figure 16 and Figure 17 is located towards the fault plane of Selje High with onlap features of the BCU to the east in the hanging wall. In addition, the mound feature observed close to the fault, further confirms that Selje High is a likely source area. Sømme et al. (2013) interpreted the source area for the Turonian mass flow sediments to be deposited from the shallow platform area; however, the Selje High was not discussed as a possible source area for that time period. Thus, the deposition of Agat Formation in the southern part of the study area was likely sourced from both the Selje High in the west and through the canyons from the platform area in the east, while the northern part of the Agat Formation was sourced from the canyons along the platform area as well. The source area in the east at the platform area was also suggested by Vergara et al. (2001), which also suggested that the conglomerates in well

6204/10-1 could be assigned to the same sequence and were deposits of proximal hyper-concentrated debris flows.

The well-developed confined submarine canyons of Late Jurassic age are found along the western edge of the Selje High and the eastern platform area (Figure 22, Figure 25, Figure 26, Figure 27, Figure 28, and Figure 31), thus the flow of Early Cretaceous sediments can be deposited through a number of canyons, thus it is regarded as a multiple source area.

However, the deposition might vary due to the activity of the different channels, as it is typical that some of the channels are inactive (Sømme et al., 2013). These canyons favor the deposition of submarine fans transported through the canyons down to the basins along the eastern platform area. Which corresponds well with the theory of Gulbrandsen (1987). Figure 53 displays an illustration of a possible drainage system in a rotated fault block system, which explains well the possible source areas and distribution of the Agat Formation (Faleide et al., 2010).

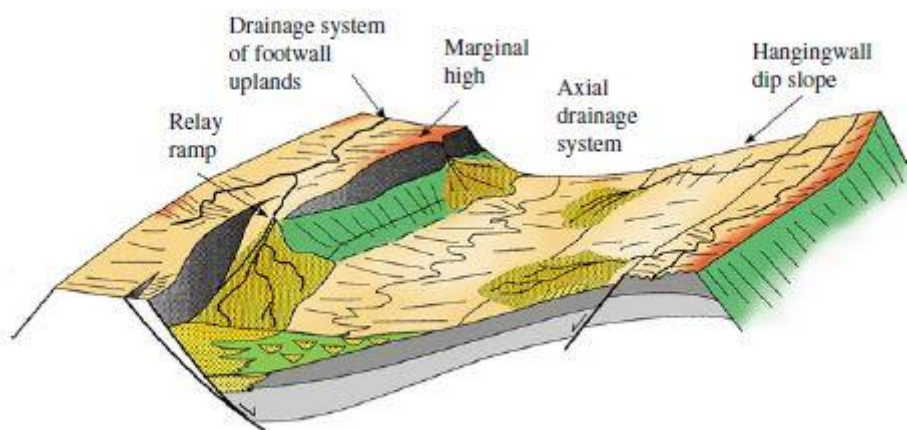


**Figure 53:** Drainage systems and source areas in a rotated fault block. A general illustration suggested by Faleide, Bjørlykke, and Gabrielsen (2010), which suits the deposition of the Agat Formation well.

Moreover, the eastern part of the Selje High with the larger scarps at the top of the fault plane (Figure 29) are indications of slumps which would result in more acute deposition of coarse-grained sediments, explaining the high amount of conglomerates found above the basement and within the Agat Formation, especially in well 6204/10-1. The Agat Formation found in the lower structural areas, showing a mix of coarse-grained sediments to fine to medium sediments, mixed with conglomeratic units are good indications that the Agat Formation

along with other sediments of the Lower Cretaceous interval is a result of the erosion of basement highs. The theory of slumps and debris flows were also suggested by Shanmugam et al. (1994) and Skibeli et al. (1995).

Figure 54 and Figure 55 summarize the interpretation of the Agat Formation in conceptual sketches highlighting the possible gravity flows for both the northern and southern areas for the two different theories explained in the tectonic evolution.

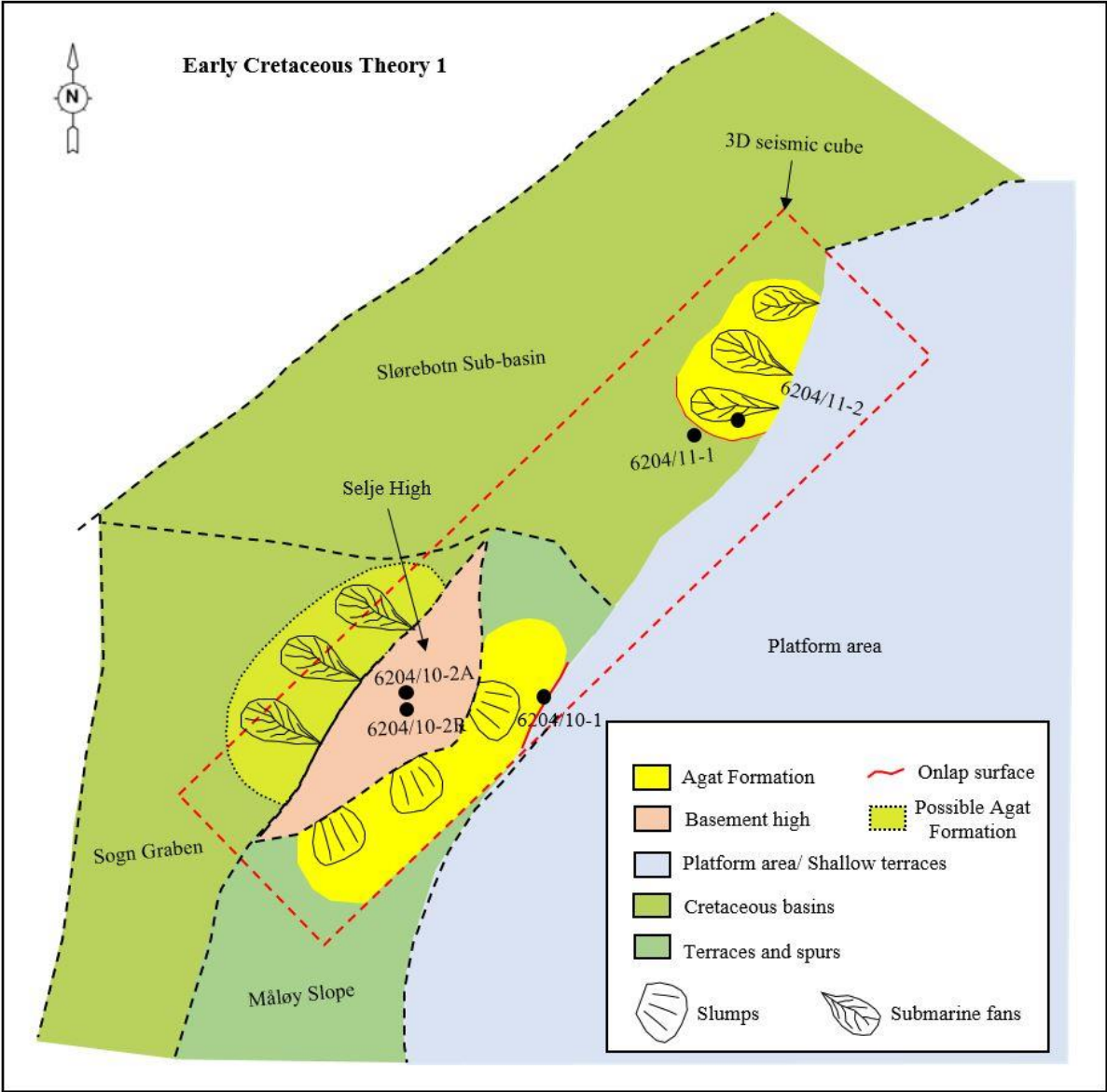


**Figure 54:** Conceptual sketch of the Early Cretaceous Theory 1. The Selje High is still a prominent structural high during this period, and for this theory none of the faults interpreted in the study area is present. Submarine fans are deposited in the northern area and possibly at the western flank of Selje High. Slump deposits are deposited on the eastern flank of the Selje High.

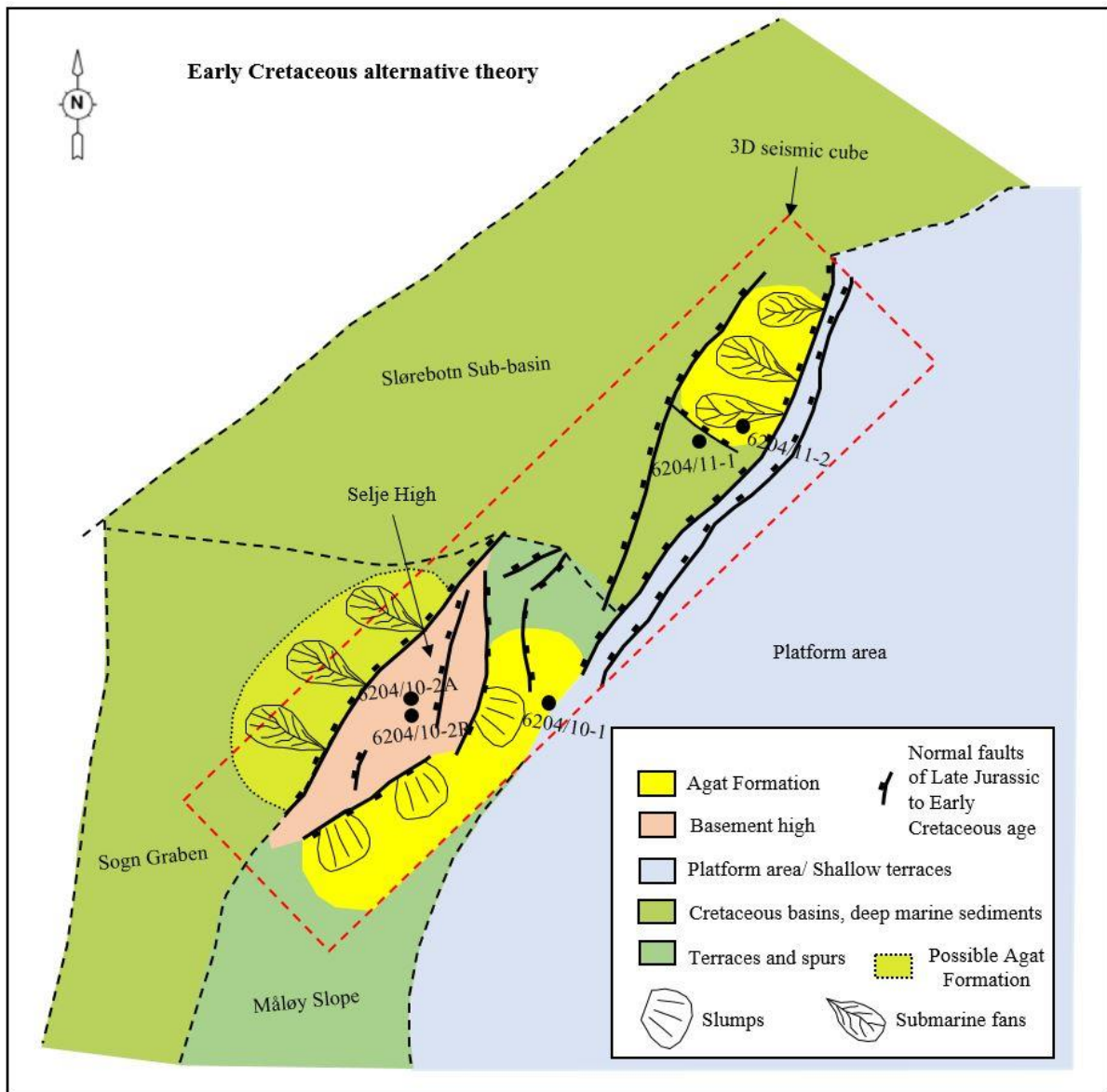


**Figure 55:** Conceptual sketch of the Early Cretaceous alternative theory. The Selje High is still a prominent structural high during this period, and for this theory the faults have been reactivated. Submarine fans are deposited in the northern area and possibly at the western flank of Selje High. Slump deposits are deposited on the eastern flank of the Selje High.

## 6. CONCLUSIONS

This study utilizes 3D and 2D seismic data and spectral decomposition to improve the knowledge of the Basement, Jurassic, and Early Cretaceous interval with respect to the timing of faults and sedimentation in the area around Selje High. The main conclusions from the study are as follows:

- The main faults in the Jurassic – Lower Cretaceous interval have been identified and divided into three fault families (FF1, FF2, and FF3). These have played a significant role in the structural evolution of the study area and influenced the sedimentation of the Lower Cretaceous Agat Formation. The main tectonic events recognized to have influenced the Selje High and surrounding areas are:
  - Late Jurassic rifting and rotation of fault blocks, causing the uplifting of the Selje High.
  - Tectonic quiescence during the deposition of Åsgard Formation.
  - Reactivation of faults during the Albian age.
- The submarine canyons or gullies are associated with the abrupt increase in water depth along the Møre – Trøndelag margin during the rifting in Late Jurassic and are caused by erosion.
- Submarine canyons or gullies facilitate for deposition of the Agat Formation as submarine fans (eastern basin margin and western Selje High) and slumps (eastern Selje High). The submarine fans are deposited from a multiple source area through several different canyons, while the slump scarps are from a smaller source area similar to a point source, however, deposited as separate events.
- The Agat Formation are likely syn-rift sedimentation from structural highs and narrow platform area in the east. However, a post-rift theory was also presented as an alternative.
- Both Selje High and the eastern basin margin were source areas for the sandy Agat Formation.
- The Basement showed evidence of weathering and fracturing, thus bearing the potential as a reservoir. However, further investigation is needed.



In conclusion, the Agat Formation represents a classic example of a deep-water sedimentary system in the North Sea and the Norwegian Sea, which is highly dependent on the local and regional tectonism.

## **6.1 Future work**

In this study, the timing of faults with respect to Pre-Devonian, Pre-Cretaceous, and Lower Jurassic are defined; however, a more detailed interpretation of the intervals, especially the Pre-Cretaceous, could further prove the syn-rift vs. post-rift sediments. Additionally, a more detailed study of the Pre-Cretaceous and Cretaceous interval could identify several minor rifting periods.

A more detailed investigation of the seismic facies and cores could reveal more information about the exact source area of the Agat Formation. Sømme et al. (2013), made inferences about which canyons were active during certain time intervals, which would be relevant for further interpretations and inferences about the study area.

Furthermore, modeling of the Agat Formation using the amplitude spectrum could highlight the reservoir properties, thus one can make better implications if the reservoir is homogeneous/heterogeneous and/or compartmentalized and thus be included in the discussion.

## REFERENCES

- Basset, M. G. (2003). Sub-Devonian geology. In D. Evans, C. Graham, A. Armour, & P. Bathurst (Eds.), *The Millennium Atlas: petroleum geology of the central and northern North Sea*. London: The Geological Society of London.
- Bertram, G. T., & Milton, N. J. (1988). Reconstructing basin evolution from sedimentary thickness; the importance of palaeobathymetric control, with reference to the North Sea Basin. . *Basin Research*, 1(4), 247-257.
- Blystad, P., Brekke, H., Færseth, R. B., Larsen, B. T., Skogseid, J., & Tørudbakken, B. (1995). *Structural elements of the Norwegian continental shelf. Part 2: The Norwegian Sea Region*. In NPD-bulletin, Vol. 8. *NPD-bulletin*.
- Brekke, H. (2000). The tectonic evolution of the Norwegian Sea Continental Margin with emphasis on the Vøring and Møre Basins. In A. Nøttvedt (Ed.), *Dynamics of the Norwegian Margin* (pp. 327-378). London: Geological Society Special Publications.
- Brekke, H., & Olausen, S. (2008). High seas and low horizons. In I. B. Ramberg, I. Bryhni, A. Nøttvedt, & K. Rangnes (Eds.), *The Making of Land: Geology of Norway* (pp. 418-441). Trondheim: Norsk Geologisk Forening.
- Brekke, H., & Riis, F. (1987). Tectonics and basin evolution of the Norwegian shelf between 62°N and 72°N. *Norsk Geologisk Tidsskrift*, 67, 295-322.
- Bugge, T., Tveiten, B., & Bäckström, S. (2001). The depositional history of the Cretaceous in the northeastern North Sea. In O. J. Martinsen & T. Dreyer (Eds.), *Sedimentary Environments Offshore Norway - Paleozoic to Recent* (Vol. 10, pp. 279-291): Norwegian Petroleum Society Special Publications.
- Cader, A. (2017). Why do Iso-Proportional Slicing (IPS) in GeoTeric? Retrieved from <https://www.geoteric.com/blog/wordpress/2017/01/19/iso-proportional-slicing-in-geoteric>
- Chopra, S., & Marfurt, K. J. (2016). Spectral decomposition and spectral balancing of seismic data. *Leading Edge*, 35(2), 176-179.
- Doré, A. G., Lundin, E. R., Jensen, L. N., Birkeland, Ø., Eliassen, P. E., & Fichler, C. (1999). Principal tectonic events in the evolution of the northwest European Atlantic margin. In *Petroleum Geology Conference series* (Vol. 5, pp. 41-61). London: Geological Society.

- Faleide, J. I., Bjørlykke, K., & Gabrielsen, R. H. (2010). Geology of the Norwegian Continental Shelf. In *Petroleum Geoscience* (pp. 603-635). Berlin, Heidelberg: Springer.
- Færseth, R. B., & Lien, T. (2002). Cretaceous evolution in the Norwegian Sea—a period characterized by tectonic quiescence. *Marine and Petroleum Geology*, *19*(8), 1005-1027.
- Gabrielsen, R. H., Kyrkjebo, R., Faleide, J. I., Fjeldskaar, W., & Kjennerud, T. (2001). The Cretaceous post-rift basin configuration of the northern North Sea. *Petroleum Geoscience*, *7*(2), 137-154. doi:10.1144/petgeo.7.2.137
- Gabrielsen, R. H., Odinsen, T., & Grunnaleite, I. (1999). Structuring of the Northern Viking Graben and the Møre Basin; the influence of basement structural grain, and the particular role of the Møre-Trøndelag Fault Complex. *Marine and Petroleum Geology*, *16*(5), 443-465.
- Gee, D. G., & Sturt, B. A. (1985). *The Caledonide orogen : Scandinavia and related areas* (Vol. 1). Chichester: Wiley.
- GeoTeric. (2017a). GeoTeric Frequency Decomposition. In. <https://www.youtube.com/watch?v=q7UF-7rHNAM>: GeoTeric.
- GeoTeric. (2017b). Reveal Overview. Retrieved from <https://www.geoteric.com/tutorials/reveal>
- Gulbrandsen, A. (1987). Agat Field. In M. A. Spencer (Ed.), *Geology of the Norwegian Oil and Gas Fields: An Atlas of Hydrocarbin Discoveries* (pp. 363-370). London: Graham and Trotman for the Norwegian Petroleum Society.
- Gulbrandsen, A., & Nyborkken, S. (1991). Agat Field - Norwegian North Sea, subplatform North Viking Graben. In (Vol. 75, pp. 586). Tulsa, OK: Tulsa, OK, United States: American Association of Petroleum Geologists.
- Isaksen, D., & Tonstad, K. (1989). *A Revised Cretaceous and Tertiary lithostratigraphic nomenclature for the Norwegian North Sea*. In Vol. 5. *NPD-bulletin*.
- Jobe, Z. R., Lowe, D. R., & Uchytel, S. J. (2011). Two fundamentally different types of submarine canyons along the continental margin of Equatorial Guinea. *Marine and Petroleum Geology*, *28*(3), 843-860. doi:10.1016/j.marpetgeo.2010.07.012
- Jongepier, K., & Rui, J. C. G., K. (1996). Triassic to Early Cretaceous stratigraphic and structural development of the northeastern Møre Basin margin, off Mid-Norway. *Norsk Geologisk Tidsskrift*, *76*, 199-214.

- Larsen, B. T., Olausen, S., Sundvoll, B., & Heeremans, M. (2007). Vulkaner, forkastninger og ørkenklima. In I. B. Ramberg, I. Bryhni, & A. Nøttvedt (Eds.), *Landet blir til: Norges geologi* (pp. 284-327). Trondheim: Norsk Geologisk Forening.
- Li, F., Qi, J., Marfurt, K. J., & Stark, T. J. (2015). Attribute mapping of variable-thickness incised valley-fill systems. *Leading Edge*, 34(1), 48-52. doi:10.1190/tle34010048.1
- Lundin, E. R., & Dore, A. G. (1997). A tectonic model for the Norwegian passive margin with implications for the NE Atlantic: Early Cretaceous to break-up. *Geological Society*, 154(3), 545-550.
- Martinsen, O. J., Lien, T., & Jackson, C. (2005). Cretaceous and Palaeogene turbidite systems in the North Sea and Norwegian Sea Basins: source, staging area and basin physiography controls on reservoir development. In A. G. Doré & B. A. Vining (Eds.), *Petroleum Geology: North-West Europe and Global Perspectives - Petroleum Geology Conference series* (Vol. 6, pp. 1147-1164). London: Geological Society.
- Martinsen, O. J., & Nøttvedt, A. (2007). Av hav stiger landet. In I. B. Ramberg, I. Bryhni, & A. Nøttvedt (Eds.), *Landet blir til: Norges Geologi* (pp. 440-477). Trondheim: Norsk Geologisk Forening.
- McCann, T., Shannon, P. M., & Moore, J. G. (1995). Fault styles in the Porcupine Basin, offshore Ireland: Tectonic and sedimentary controls. *Geological Society Special Publications*, 93, 371-383.
- Moore, R., & Smith, J. (2017). Multi-Volume Blending in GeoTeric. Retrieved from <https://geoteric.com/multi-volume-blending-in-geoteric/>
- Nasuti, A., Pascal, C., & Ebbing, J. (2012). Onshore-offshore potential field analysis of the More-Trondelag Fault Complex and adjacent structures of Mid Norway. *Tectonophysics*, 518, 17-28. doi:10.1016/j.tecto.2011.11.003
- NPD. (2014). Lithostratigraphic chart Norwegian North Sea. Retrieved from <https://www.npd.no/globalassets/1-npd/fakta/geologi-eng/ns-od1409001.pdf>
- NPD. (2019). Norwegian Petroleum Directorate fact pages. from Norwegian Petroleum Directorate <https://npdfactpages.npd.no/factpages/Default.aspx?culture=no>
- Nystuen, J. P. (1999). *Submarine sediment gravity flow seposits and associated facies: core examples from the Agat Member*. Paper presented at the Extended Abstract Bergen Conference.

- Nøttvedt, A., & Johannessen, E. P. (2008). The source of Norway's oil wealth. In I. B. Ramberg, I. Bryhni, A. Nøttvedt, & K. Rangnes (Eds.), *The Making of Land: Geology of Norway* (pp. 384-418). Trondheim: Norsk Geologisk Forening.
- Osmundsen, P. T., Sommaruga, A., Skilbrei, J. R., & Olesen, O. (2002). Deep structure of the Mid Norway rifted margin. *Norsk Geologisk Tidsskrift*, 82(4), 205-224.
- Partyka, G., Gridley, J., & Lopez, J. (1999). Interpretational applications of spectral decomposition in reservoir characterization. *Leading Edge*, 18(3), 353-354, 356-357, 360.
- Pickering, K. T., Bassett, M. G., & Siveter, D. J. (1988). Late Ordovician-early Silurian destruction of the Iapetus Ocean: Newfoundland, British Isles and Scandinavia - a discussion. *Earth and Environmental Science Transactions of the Royal Society of Edinburgh*, 79(4), 361-382.
- Posamentier, H. W., Davies, R. J., Cartwright, J. A., & Wood, L. J. (2007). Seismic geomorphology - An overview. *Geological Society Special Publications*, 277(1), 1-14. doi:10.1144/GSL.SP.2007.277.01.01
- Prosser, S. (1993). Rift-related linked depositional systems and their seismic expression. *Geological Society Special Publications*, 71(1), 35-66.
- Ramberg, I. B., Solli, A., Nordgulen, Ø., Binns, R., & Grogan, P. (2008). *The Making of a land : geology of Norway*. Trondheim: The Norwegian Geological Association.
- Ravnås, R., & Steel, R. J. (1998). Architecture of marine rift-basin successions. *AAPG Bulletin*, 82(1), 110-146. doi:10.1306/1D9BC3A9-172D-11D7-8645000102C1865D
- Riber, L., Dypvik, H., & Sorlie, R. (2015). Altered basement rocks on the Utsira High and its surroundings, Norwegian North Sea. *Norwegian Journal of Geology*, 95(1), 57-89.
- Shanmugam, G., Lehtonen, L. R., Straume, T., Syvertsen, S., Hodgkinson, R. J., & Skibeli, M. (1994). Slump and debris-flow dominated upper slope facies in the Cretaceous of the Norwegian and northern North seas (61-67 degrees N); implications for sand distribution. *AAPG Bulletin*, 78(6), 910-937.
- Skibeli, M., Barnes, K., Straume, T., Syvertsen, S. E., & Shanmugam, G. (1995). A sequence stratigraphic study of lower cretaceous deposits in the northernmost North Sea. *Norwegian Petroleum Society Special Publications*, 5, 389-400.
- Sømme, T. O., & Jackson, C. A. L. (2013). Source-to-sink analysis of ancient sedimentary systems using a subsurface case study from the Møre-Trøndelag area of southern

- Norway: Part 2 – sediment dispersal and forcing mechanisms. *Basin Research*, 25(5), 512-531.
- Sømme, T. O., Jackson, C. A. L., & Vaksdal, M. (2013). Source-to-sink analysis of ancient sedimentary systems using a subsurface case study from the Møre-Trøndelag area of southern Norway: Part 1 – depositional setting and fan evolution. *Basin Research*, 25(5), 489-511.
- Vergara, L., Brunstad, H., Nordlie, T., Chranock, M. A., & Gradstein, F. M. (2006). Agat Member. Retrieved from <http://www.nhm2.uio.no/norges/litho/agat.php>
- Vergara, L., Wreglesworth, I., Trayfoot, M., & Richardsen, G. (2001). The distribution of Cretaceous and Paleocene deep-water reservoirs in the Norwegian Sea basins. *Petroleum Geoscience*, 7(4), 395-408. doi:10.1144/petgeo.7.4.395
- Vollset, J., & Doré, A. G. (1984). *A Revised Triassic and Jurassic lithostratigraphic nomenclature for the Norwegian North Sea* (Vol. 3). Stavanger: Oljedirektoratet.
- Weibull, W. W. (2019). *A comparison of the effects of Layering and Attenuation on the Seismic Response of Gas Reservoirs*. Paper presented at the EAGE Annual, London.
- Ziegler, P. A. (1975). Geologic evolution of North Sea and its tectonic framework. *AAPG Bulletin*, 59(7), 1073-1097.